

NASA CONTRACTOR
REPORT

NASA CR-120518

CHARACTERIZATION OF EXOTHERMIC BRAZING COMPONENTS
SKYLAB EXPERIMENT M552

By H. E. Pattee and R. E. Monroe
Battelle Columbus Laboratories
Columbus, Ohio 43201

December 1973

Prepared for

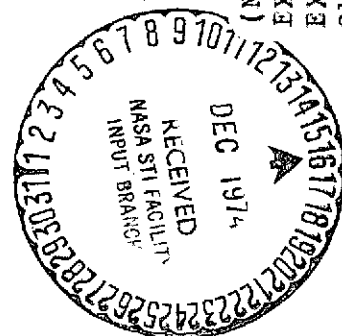
NASA-GEORGE C. MARSHALL SPACE FLIGHT CENTER
Marshall Space Flight Center, Alabama 35812

N75-12015

Unclas
03593

63/12

(NASA-CR-120518) CHARACTERIZATION OF
EXOTHERMIC BRAZING COMPONENTS SKYLAB
EXPERIMENT M552 (Battelle Columbus Labs.,
Ohio.) 98 p HC \$4.75 CSCI 13H



1. REPORT NO. NASA CR-120518		2. GOVERNMENT ACCESSION NO.		3. RECIPIENT'S CATALOG NO.	
4. TITLE AND SUBTITLE Characterization of Exothermic Brazing Components Skylab Experiment M552				5. REPORT DATE December 1973	
				6. PERFORMING ORGANIZATION CODE	
7. AUTHOR(S) H. E. Pattee and R. E. Monroe				8. PERFORMING ORGANIZATION REPORT #	
9. PERFORMING ORGANIZATION NAME AND ADDRESS Battelle Columbus Laboratories Columbus, Ohio 43201				10. WORK UNIT NO.	
				11. CONTRACT OR GRANT NO. NAS 8-28725	
12. SPONSORING AGENCY NAME AND ADDRESS National Aeronautics and Space Administration Washington, D. C. 20546				13. TYPE OF REPORT & PERIOD COVERED Contractor Report	
				14. SPONSORING AGENCY CODE	
15. SUPPLEMENTARY NOTES					
16. ABSTRACT Information developed to characterize flight and ground based samples from the Exothermic Brazing Experiment is detailed in this report. Included is information developed from metallographic observation, chemical analysis, and measurements of component dimensions. Comparisons of the flight and ground based specimens showed that good quality brazes were obtained. Effects of the zero gravity processing were noted on liquid metal flow and braze alloy-base metal reactions. Unusual metallurgical structures exhibited in the nickel brazes made in Skylab were the result of composition variations apparently related to the time-temperature cycle characteristic of this braze.					
17. KEY WORDS			18. DISTRIBUTION STATEMENT Unclassified - Unlimited <i>W K Vandorn</i>		
19. SECURITY CLASSIF. (of this report) Unclassified		20. SECURITY CLASSIF. (of this page) Unclassified		21. NO. OF PAGES 98	
				22. PRICE NTIS	

TABLE OF CONTENTS

	Page
SUMMARY	1
INTRODUCTION.	4
SECTION I - EVALUATION OF NICKEL GROUND CHARACTERIZATION SPECIMENS	6
SAMPLE DESCRIPTION	6
Sectioning.	6
VISUAL EXAMINATION	9
Sample MCN-2.	9
Sample MCN-3.	9
METALLOGRAPHIC EXAMINATION	9
Sample MCN-2.	10
Sample MCN-3.	17
MICROSTRUCTURAL STUDIES.	21
SECTION II - EVALUATION OF STAINLESS STEEL GROUND CHARACTERIZATION SAMPLES.	31
SAMPLE DESCRIPTION	31
SECTIONING	32
VISUAL EXAMINATION	32
Sample MCS-1.	34
Sample MCS-3.	34
METALLOGRAPHIC EXAMINATION	34
Sample MCS-1.	34
Sample MCS-2.	41
Sample MCS-3.	46
MICROSTRUCTURAL STUDIES.	55
SECTION III - EVALUATION OF SKYLAB SAMPLES.	59
MATERIAL TRANSFER.	59
SPECIMEN PROCESSING.	59
Specimen SLS-1.	60
Specimen SLN-2.	73
SECTION IV - CONCLUSIONS.	88

LIST OF ILLUSTRATIONS

Figure	Page
1. Effect of Zero Gravity on Braze Alloy Retention and Fillet Formation in Ring Groove Areas of Stainless Steel Brazes	2
2. Comparison of Microstructures in Skylab and Ground Based Nickel Braze Specimens.	3
3. Diffusion Bonded Area Formed in Skylab Stainless Steel Specimen.	5
I-1. Sectioning Plan for Ground Characterization Samples MCN-2 and MCN-3.	7
I-2. Surfaces Examined During Metallographic Evaluation (MCN-2)	11
I-3. Section MCN-2.1 (-4 to 4 mm) Showing Igniter End of Braze and Wedge	12
I-4. Section MCN-2.1 (0 mm) Microstructure.	12
I-5. Section MCN-2.1 (0 mm) Microstructure.	13
I-6. Section MCN-2.1 (0 mm) Microstructure.	13
I-9. Section MCN-2.3 (7 mm) Showing Braze Alloy in Ring Groove.	16
I-10. Microstructure of Braze Alloy in Ring Groove - Section MCN-2.3 (7 mm)	16
I-11. Appearance of Ring Groove Area Showing Alloy Flow to Low Point - Section MCN-2.9 (27 to 30mm)	18
I-12. Surfaces Examined During Metallographic Evaluation (MCN-3)	19
I-13. Macrograph of Ring Groove Area - Section MCN-3.2 (7 mm)	20
I-14. Microstructure of Ring Groove Area - Section MCN-3.2.	20
I-15. Macrograph of Section MCN-3.4 (15 mm).	22

LIST OF ILLUSTRATIONS (Continued)

Figure	Page
I-16. Section MCN-3.4 Showing Large Shrinkage Void Area.	22
I-17. Microstructure in Section MCN-3.4 (15 mm). . . .	23
I-18. Macrograph of Braze Between 15 and 17 mm Section MCN-3.5.	24
I-19. Phases Present in Section MCN-2.1.	26
I-20a. Nickel X-Ray Image	26
I-20b. Copper X-Ray Image	27
I-20c. Silver X-Ray Image	27
I-21a. Phases Present in Tee Joint Brazed at 1500 F . .	29
I-21b. Phases Present in Exothermic Braze - Section MCN-2.1.	29
II-1. Sectioning Plan for Ground Characterization Samples MCS-1, MCS-2, and MCS-3.	33
II-2. Surfaces Examined During Metallographic Evaluation (MCS-1)	35
II-3. Macrograph of Section MCS-1.1 (0 to 2.5 mm). . .	37
II-4. Microstructure in Section MCS-1.1 (1 mm)	38
II-5. Appearance of Gap and Ring Groove - Section MCS-1.2 (2.5 - 7 mm)	39
II-6. Microstructure of Bulk Braze Alloy on Inside Surface of Tube - Section MCS-1.2 (6 mm)	40
II-7. Macrograph of Section MCS-1.4 (15 mm).	42
II-8. Shrinkage Voids in Section MCS-1.4 (15 mm) . . .	42
II-9. Microstructure of Bulk Alloy in Section MCS-1.4 (15 mm).	43

LIST OF ILLUSTRATIONS (Continued)

Figure	Page
II-10. Thermocouple Wire Brazed into Section MCS-1.4 (15 mm)	43
II-11. Ring Groove Area in Section MCS-1.8 (29 mm) . . .	44
II-13. Cross Section MCS-2.5 (15 mm)	44
II-12. Surfaces Examined During Metallographic Evaluation (MCS-2)	45
II-14. Microstructure in Section MCS-2.4 (15 mm)	47
II-15. Microstructure of Bulk Filler Metal in Section MCS-2.4 (15 mm)	48
II-16. Cross Section MCS-2.7 (26 mm)	48
II-17. Radial Section MCS-2.9 at 180° (30 to 35 mm) . .	49
II-18b. Radial Section MCS-3.2 (2 to 6 mm)	49
II-18a. Surfaces Examined during Metallographic Evaluation (MCS-3)	50
II-19a. Cross Section MCS-3.3.	52
II-19b. Microstructure of Bulk Filler Metal in Section MCS-3.3 (11 mm)	52
II-20. Radial Section MCS-3.5 (15-18 mm)	53
II-21. Radial Sections MCS-3.9 (30-35 mm)	54
II-22. Phases Present in Section MCS-2.4.	56
II-23a. Section MCS-2.4 - Silver X-Ray Image	56
II-23b. Section MCS-2.4 - Copper X-Ray Image	57
II-23b. Section MCS-2.4 - Nickel X-Ray Image	57
II-23d. Section MCS-2.4 - Chromium X-Ray Image	58
II-23e. Section MCS-2.4 - Iron X-Ray Image	58

LIST OF ILLUSTRATIONS (Continued)

Figure	Page
III-1. Cross Section SLS-1.2 (3 mm)	62
III-2. Cross Section SLS-1.4 (14 mm)	63
III-3. Radial Sections Through Igniter Ring Groove SLS-1.3 (3.5 to 10 mm)	64
III-4. Radial Section of Ring Groove Area - SLS-1.7.1 (23.5 to 31 mm and 210°)	66
III-5. Typical Microstructure in SLS-1.4 (14 mm and 300°)	67
III-6. Microstructure of Bulk Braze Alloy - Section SLS-1.4 (14 mm and 300°)	68
III-7. Solid-State Bond Area - Section SLS-1.4 (14 mm and 0°)	69
III-8. Shrinkage Voids in Section SLS-1.7.1 (24 mm and 210°)	70
III-9. Plot of Joint Gap Measurements	72
III-10. Section SLN 2.4 (5 mm) and 2.7 (20 mm)	74
III-11. Section SLN-2.5.1 (5.5 to 10 mm and 90 and 270°) Showing Meniscus Shape and Void Areas Around Igniter End Ring Groove.	75
III-12. Section SLN-2.9.1 (25.5 to 31 mm and 90 and 270°) Showing Fillets in Ring Groove Opposite Ignited End.	76
III-13. Variation in Microstructure in Section SLN-2.7 (20 mm)	77
III-14. Microstructure of Braze in Ring Groove Showing Coarse Copper-Nickel Phase and Wide Diffusion Zone (SLN-2.4 - 5 mm)	79
III-15. Section SLN-2.10 (35 mm) Showing Variation in Braze Microstructures.	80

LIST OF ILLUSTRATIONS (Continued)

Figure		Page
III-16.	Comparison of Optical and Electron Microprobe Images - Section SLN-2.7 (20 mm - 0°)	81
III-17.	Comparison of Optical and Electron Microprobe Images - Section SLN-2.7 (20 mm - 90°)	82
III-18.	Comparison of Optical and Electron Microprobe Images - Section SLN-2.7 (20 mm - 180°)	83
III-19.	Comparison of Optical and Electron Microprobe Images - Section SLN-2.7 (20 mm - 270°)	84
III-20.	Limits of Magnetic Region Indicating High Nickel Content	86

LIST OF TABLES

Table		Page
III-1.	Location of Sectioning Planes Skylab Specimens-M552	61
III-2.	Measurements of Joint Gap - Specimen SLS-1. . .	71
III-3.	Volume Fraction of Second Phase in Braze Gap. .	85

Contractor Report

CHARACTERIZATION OF EXOTHERMIC BRAZING COMPONENTS SKYLAB EXPERIMENT M552

SUMMARY

Exothermic braze specimens from both ground-based characterization and Skylab were examined to determine any differences and similarities. Good quality brazes were produced in both environments, with both stainless steel and nickel assemblies brazed with a Ag-28Cu-0.4Li alloy. At the brazing temperatures used, reaction between the braze alloy and base metal constituents (predominately nickel) resulted in a shift in the final braze alloy composition.

Significant findings were as follows:

- (1) Specimen SLS-1 (Skylab-stainless steel-0.005 inch gap) was an essentially void-free braze. The microstructure and many other characteristics of this braze were similar to comparable ground-based specimens. Retention of braze alloy in corners of the oversize ring groove and fillet formation in this region was significantly better on the Skylab specimen as shown in Figure 1. This observation clearly supports the enhancement of surface tension forces in a zero gravity field. The tendency for excess braze alloy to collect at low points in the ground-based specimens was completely absent in the Skylab sample. This confirms expectations that braze assembly orientation will have no effect on braze distribution in zero gravity.
- (2) Specimen SLN-2 (Skylab-nickel-0.010 inch gap) contained minor voids comparable to the ground-based specimens. The microstructure of the braze alloy in this specimen varied with location and was frequently different from the structure exhibited by ground-based specimens as shown in Figure 2. The resulting microstructures clearly indicate variations in the braze alloy composition and perhaps some variation in the cooling rate. However, there is no obvious relation to an effect of the zero gravity environment. Observations of braze alloy retention and fillets in the ring groove area and the location of excess alloy in the nickel specimens further supports the conclusions given above about surface tension forces and orientation effects.

a. Ground Specimens

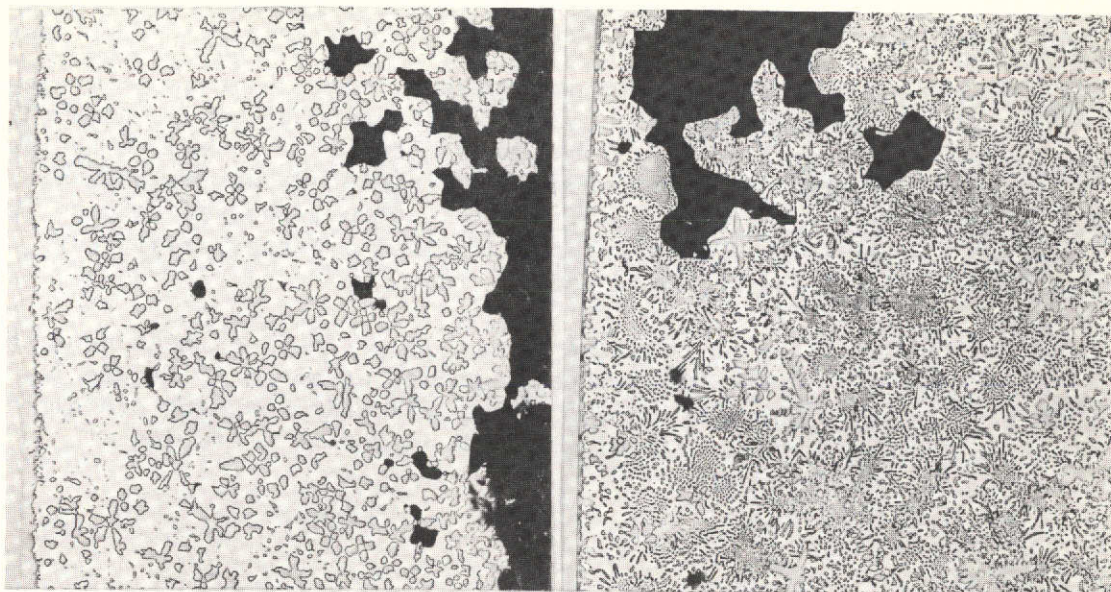
FIGURE NOT AVAILABLE AT TIME OF PUBLICATION

All 20X

Dark Area is
Ring Groove

b. Skylab Specimens

FIGURE 1. EFFECT OF ZERO GRAVITY ON BRAZE ALLOY RETENTION AND
FILLET FORMATION IN RING GROOVE AREAS OF STAINLESS
STEEL BRAZES

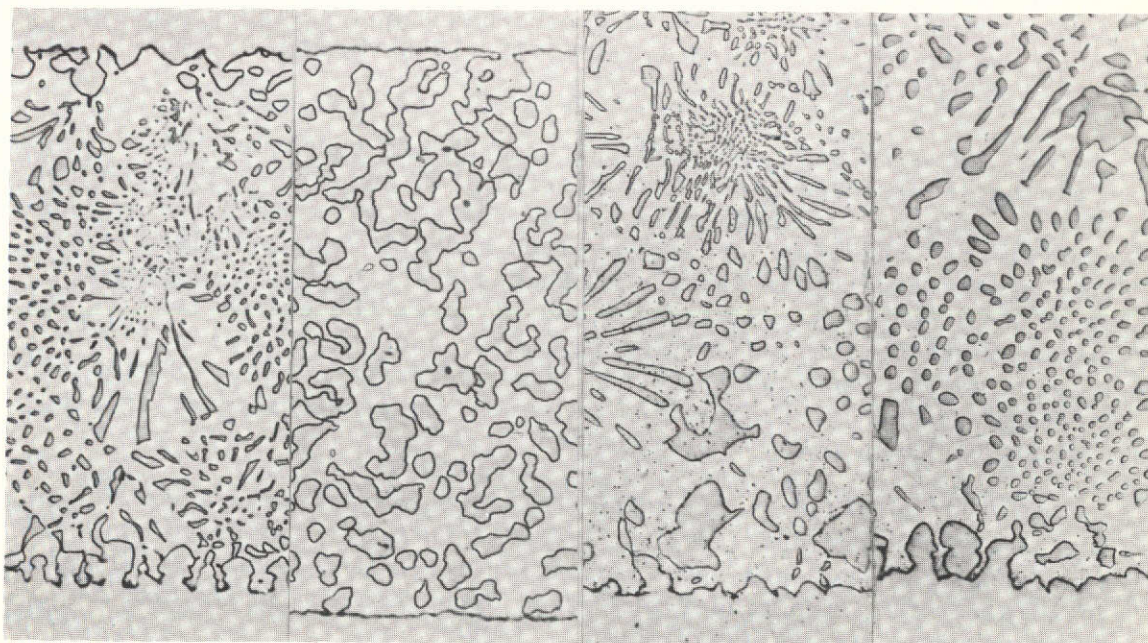


Skylab

Ground

Microstructure Ring Groove

100X



Skylab

Ground

Microstructure in Braze Gap-500X

FIGURE 2. COMPARISON OF MICROSTRUCTURES IN SKYLAP AND GROUND BASED NICKEL BRAZE SPECIMENS

- (3) Both Skylab specimens exhibited smaller braze alloy gaps than intended or observed in the ground-based specimens. The smaller gap probably resulted from an end restraint condition that prevented unrestricted thermal expansion of the assembly. If this did occur, the restraining members would also have provided a better axial heat sink and a faster cooling rate.
- (4) A diffusion bond was formed in a tight gap region of the Skylab stainless steel specimen as shown in Figure 3. This observation shows that diffusion bonding can also be used as a joining method in the zero gravity environment.

INTRODUCTION

This report covers the work conducted at Battelle-Columbus in support of Skylab experiment M552 - Exothermic Brazing. The report covers characterization of both ground-based and Skylab processed specimens during the period from May 15, 1972 through December 4, 1973.

The work was conducted in three phases concerned with: A - Planning, B - Ground-Based Characterization, and C - Skylab Specimen Characterization. Inputs made during Phase A were reflected in the experimental details that have evolved and are reported elsewhere. This report covers the details of Phases B and C and is organized into three sections. Sections I and II cover the evaluation of ground characterization samples of nickel and stainless steel, respectively. Section III covers characterization of the Skylab specimens examined at Battelle. Finally, conclusions covering all aspects of the program are presented in Section IV.

The Battelle effort under this program was only a portion of the total effort conducted both by NASA and other contractors. For completeness, some data and information for other sources is included in this report. The reader will find much related information in other reports on this experiment.

500X

As Polished

7G851

FIGURE NOT AVAILABLE AT TIME OF PUBLICATION

500X

97HCL, 3HNO₃, 0.5gCuCl₂

7G852

FIGURE 3. DIFFUSION BONDED AREA FORMED IN SKYLAB STAINLESS
STEEL SPECIMEN

SECTION I

EVALUATION OF NICKEL GROUND CHARACTERIZATION SPECIMEN

A detailed metallurgical evaluation of two exothermically-brazed nickel ground characterization samples was conducted at Battelle-Columbus. Samples MCN-2 and MCN-3 were among six samples that were brazed as part of Exothermic Brazing Experiment M552 at the Marshall Space Flight Center in November, 1972.* They were made to obtain base-line data for use in determining the effect of weightlessness on (1) the wetting and flow behavior of brazing filler metals and (2) the metallurgical characteristics of the brazed joints.

SAMPLE DESCRIPTION

Each sample consisted of a nickel** sleeve into which a thin-wall nickel tube was brazed with the self-fluxing silver-copper filler metal Ag-28 Cu-0.2 Li (BAg-8a). The filler metal strip (0.035 inch thick by 0.145 inch wide) was formed into rings; one ring was placed in each of two grooves that were located near each end of the sleeve. The brazing clearance, i.e., the spacing between the tube and the sleeve, was 0.010 inch; the clearance was uniform for the full joint length. Spacers or inserts were used to provide this clearance and maintain the concentricity of the tube within the sleeve.

Sectioning

Samples MCN-2 and MCN-3 were sectioned perpendicular to the longitudinal axis of the tube assembly to produce a series of circular sections. Sectioning was done with a water-cooled silicon carbide cut-off wheel, 0.5 mm wide. The use of a narrower cut-off wheel to minimize the width of the kerf was considered. However, cutting tests conducted with a 0.25 mm wide wheel indicated that equipment modifications would be needed to produce parallel cuts and avoid wheel breakage; also, cutting rates with this wheel were very slow.

Both samples were sectioned as shown in Figure I-1. Sectioning was done in general conformance with the plan adopted during a meeting that was held at Battelle-Columbus in August, 1972. However, instead of sectioning to produce circular specimens with a uniform width of 0.100 inch (2.5 mm), the samples were sectioned in areas that appeared to be more informative, i.e., through the filler metal ring grooves, through porosity areas, etc. Ten sections were cut from Sample MCN-2 and nine sections were cut from Sample MCN-3. Each section was

* The other samples were also sent to Battelle-Columbus. After preliminary examination and sectioning, two samples were sent to the Oak Ridge National Laboratory for isotope mapping and two samples were sent to the University of Wisconsin for metallurgical study.

** The composition of the bar stock from which the tube and sleeve were machined was essentially pure nickel with traces of copper and iron.

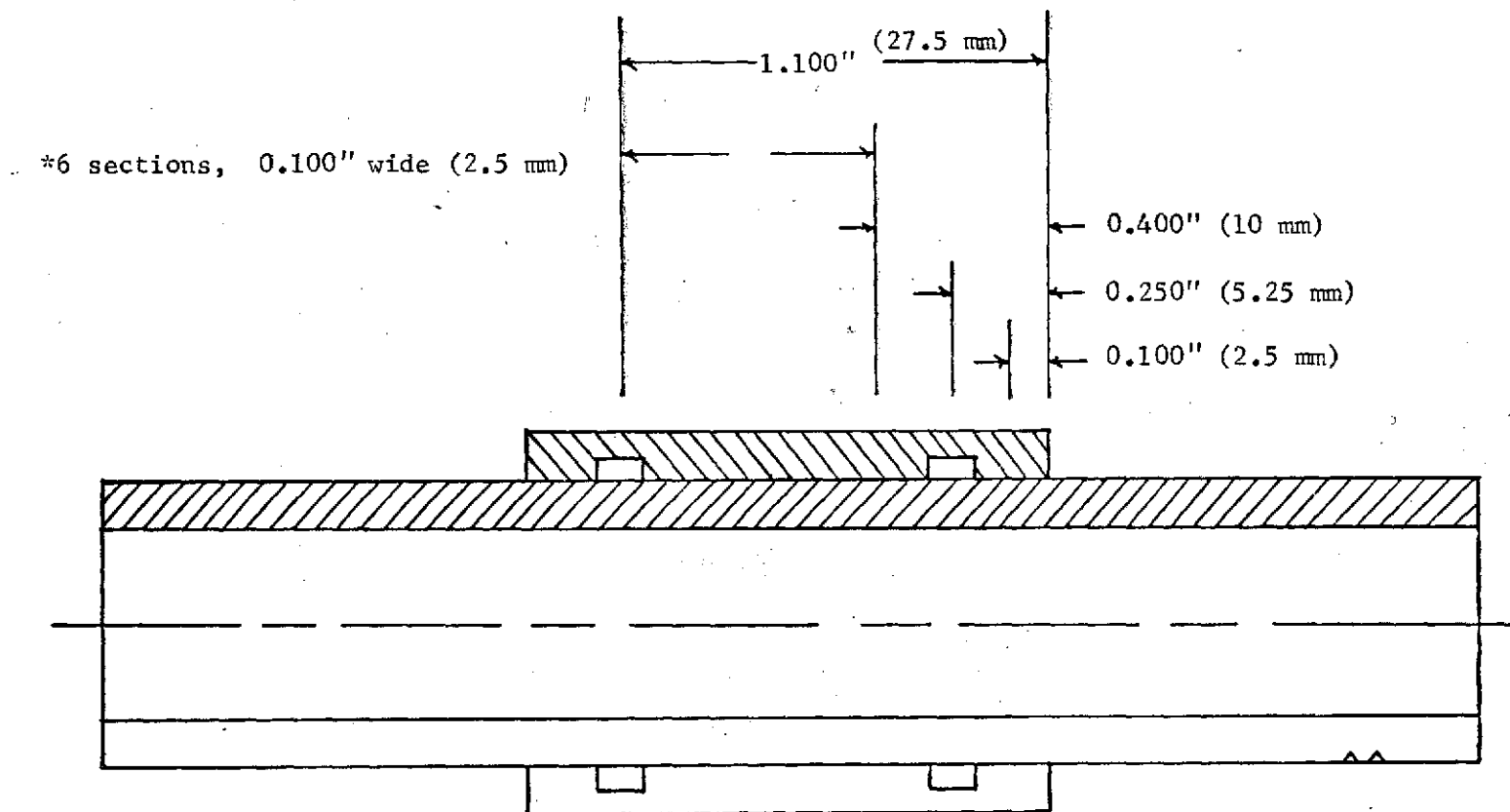


FIGURE I-1. SECTIONING PLAN FOR GROUND CHARACTERIZATION
SAMPLES MCN-2 AND MCN-3

Sections to be cut at indicated distances
from right end of sample.

identified to indicate its location along the longitudinal axis of the sample.

To aid in studying the flow characteristics of the filler metal, a short section of one filler metal ring in each sample was removed, irradiated with neutrons to produce radioisotope Ag^{110} , and replaced in the groove. The isotope was located in register with axial lines that were machined on the outer surface of the sleeve to fix the isotope position with respect to the sample orientation during brazing. The isotope activity level of Samples MCN-2 and MCN-3 was slightly less than 50 microcuries.

Samples MCN-2 and MCN-3 were almost identical. Both samples were brazed in the horizontal position; however, the samples were oriented during brazing to locate the isotope tracers in MCN-2 and MCN-3 at 3 o'clock and 6 o'clock, respectively. The samples were brazed in a vacuum furnace with exotherms that weighed 60 grams; the pressure within the furnace was 8.5×10^{-5} torr for MCN-2 and 9.8×10^{-5} torr for MCN-3. The brazing temperature was monitored with a thermocouple attached to the center ID of the tube. The maximum temperature was monitored with a thermocouple attached to the center ID of the tube. The maximum temperature to which the samples were heated during brazing was 1930 F (1054.4 C) for MCN-2 and 1915 F (1046.1 C) for MCN-3.

After brazing, the samples were radiographed at the Marshall Space Flight Center. The following comments are based on the interpretation of the radiographs.

Sample MCN-2: Excess filler metal puddled in the bottom, i.e. 6 o'clock position, of the ring grooves -- excellent joint quality -- no porosity.

Sample MCN-3: Excess filler metal puddled in the bottom of one ring groove -- some porosity in one location.

VISUAL EXAMINATION

The sections from Samples MCN-2 and MCN-3 were examined under low-power magnification to (1) study the visual appearance of the brazed tube assembly, (2) confirm the radiographic findings, and (3) select sections for metallographic examination. The results of these studies are discussed below.

Sample MCN-2

As indicated by radiography, this tube assembly was well brazed from one end to the other. Filler metal was present around the entire joint circumference in each section (except those that were cut through the filler metal ring grooves). The joint quality was excellent, and there were no visible defects in any of the sections. Excess filler metal was accumulated at the bottom of each ring groove; i.e., at the 6 o'clock position of the sample during brazing. However, excellent flow was indicated by the presence of a thin layer of filler metal over the entire surface of the ring grooves. Five sections were selected for more detailed metallographic study.

Sample MCN-3

This tube assembly was also well brazed for its entire length, and the circumferential joints in all sections (excluding sections cut through the ring grooves) were filled with brazing filler metal. While the joint quality was generally excellent, there was evidence of porosity or voids in the joint contained in one section. The porous area was located to the left of the right-hand ring groove in the 1 or 2 o'clock position during brazing. The existence of porosity in this location was also indicated by radiography. Excess filler metal was accumulated at the bottom of each ring groove; there was considerably more filler metal in the right-hand groove than in the left-hand groove. The surfaces of each ring groove were coated with a thin layer of filler metal. Five of these sections were also selected for further study.

METALLOGRAPHIC EXAMINATION

Sections from Sample MCN-2 and MCN-3 were examined metallographically to study (1) the wetting and flow characteristics of the filler

metal, (2) the quality of brazing, (3) defects and their frequency of occurrence, (4) metallurgical reactions between the base metal and filler metal, and (5) joint microstructures. These studies are discussed below.

Sample MCN-2

Five sections representing areas where differences in the joint characteristics might be evident were examined. The designation and approximate location of each section are shown in Figure I-2. Sections MCN-2-1 and MCN-2-9 were cut and mounted to permit examination of the joint surfaces parallel to the longitudinal axis of the sample. The remaining sections were mounted to show the entire circumferential joint between the tube and sleeve, i.e., the surface perpendicular to the longitudinal axis of the sample. After polishing, the metallographic specimens were examined in the unetched and etched condition; the metallurgical features of the joints were generally most evident in the unetched condition.

Section MCN-2-1

One side of the joint in this section is shown at a magnification of 20X in Figure I-3. The joint quality is excellent; the filler metal wet the base metal well and flowed to completely fill the joint between the tube and sleeve. The insert used to maintain the spacing between the tube and sleeve was brazed to the remainder of the assembly. A few isolated voids were present in the joint area. The other side of the joint had an appearance similar to that shown in Figure I-3.

Selected areas of this joint are shown in the as-polished condition at 250X and 500X in Figures I-4 and I-5, respectively; the area covered by Figures I-4 is also shown in the etched condition at the same magnification in Figure I-6. The microstructure between the joint interfaces is largely comprised of a second phase in a high silver matrix. A phase produced by the reaction of the filler metal with the base metal is also present. Etching appeared to have the same effect on this phase as it did on the phase along the joint interface. The reaction of the base metal with the molten filler metal is clearly evident in the attached photomicrographs. The width of the zone resulting from this reaction was about 0.001 inch.

The microstructure of the brazed joints is discussed in more detail later in this report.

Section MCN-2-2

The full circumferential joint between the nickel tube and sleeve is shown at 4X in Figure I-7. The quality of this joint was generally excellent except for an accumulation of voids that are evident at the

↓ Denotes surface perpendicular
to axis of sample

+ Denotes surface parallel
to axis of sample

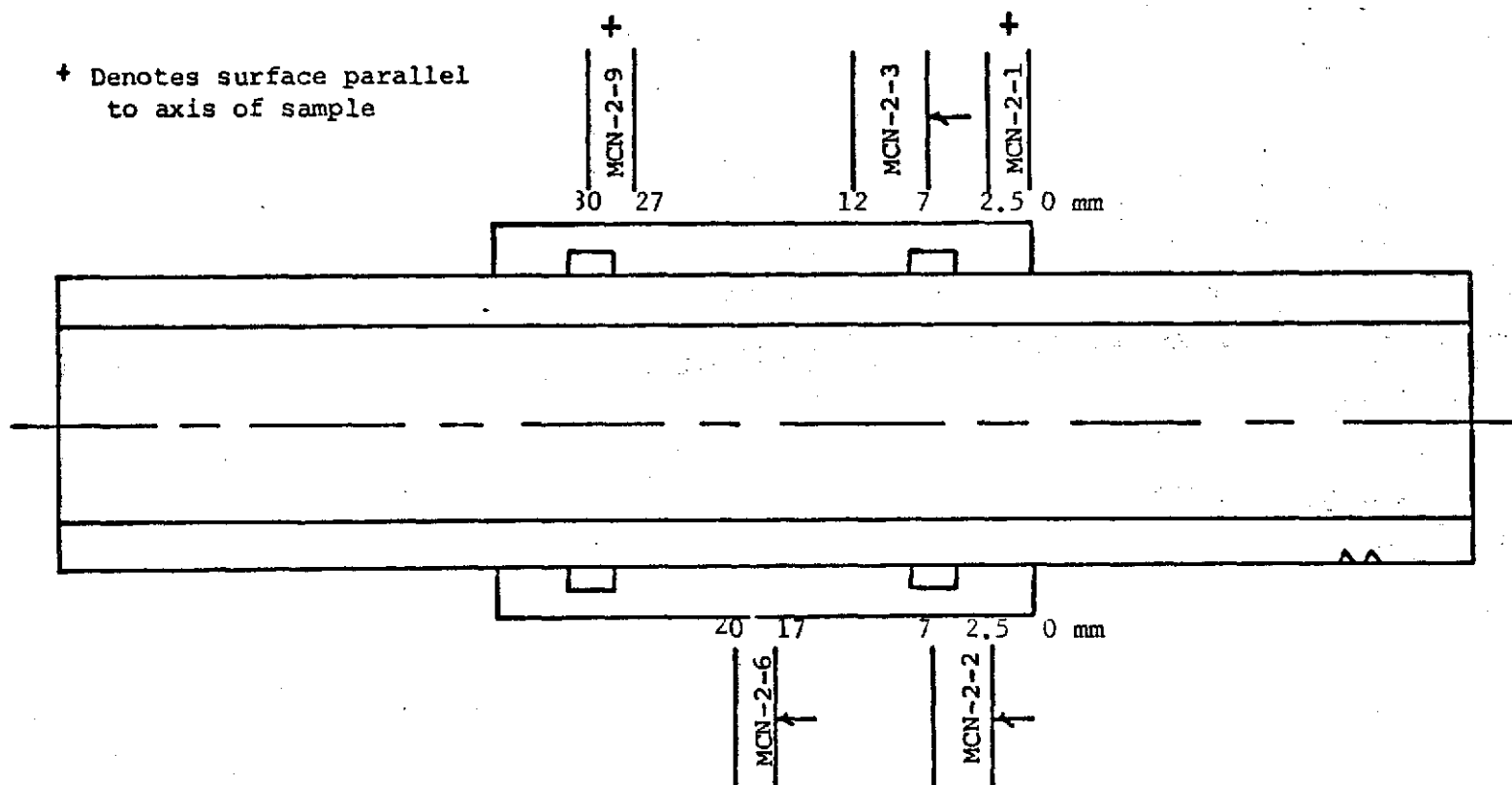
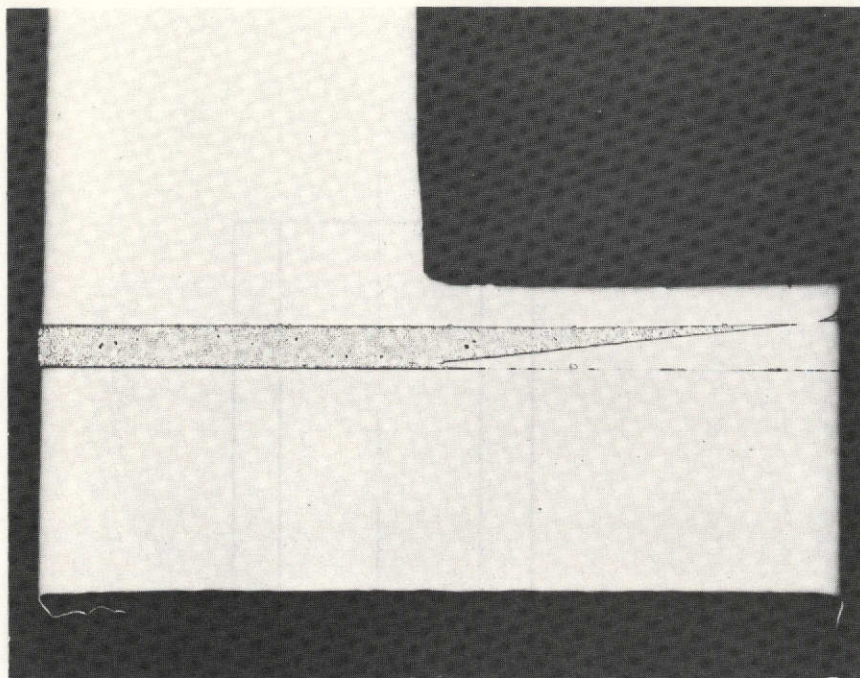


FIGURE I-2. SURFACES EXAMINED DURING METALLOGRAPHIC EVALUATION (MCN-2)

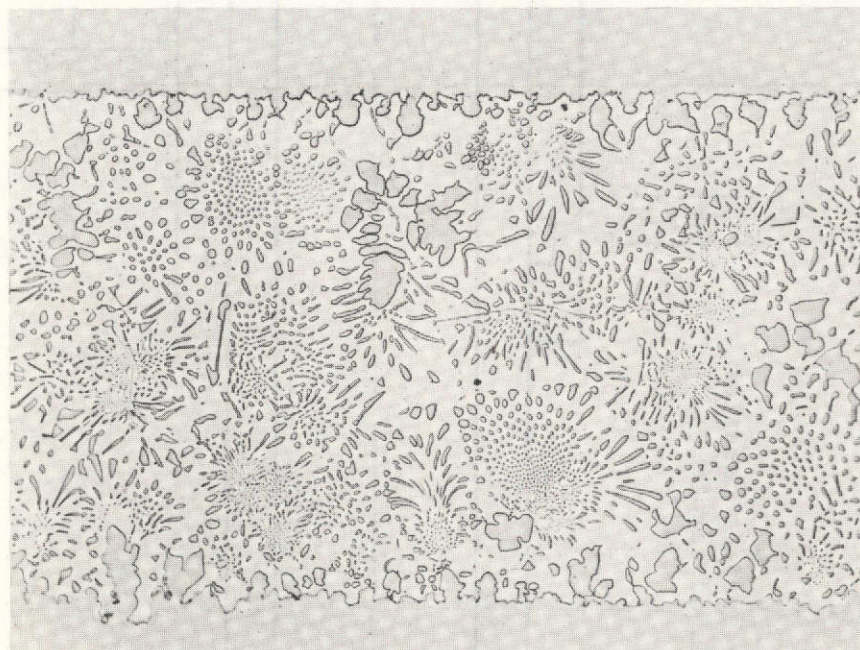


20X

As Polished

5G282

FIGURE I-3. SECTION MCN-2.1 (-4 to 4 mm) SHOWING
IGNITER END OF BRAZE AND WEDGE



180°

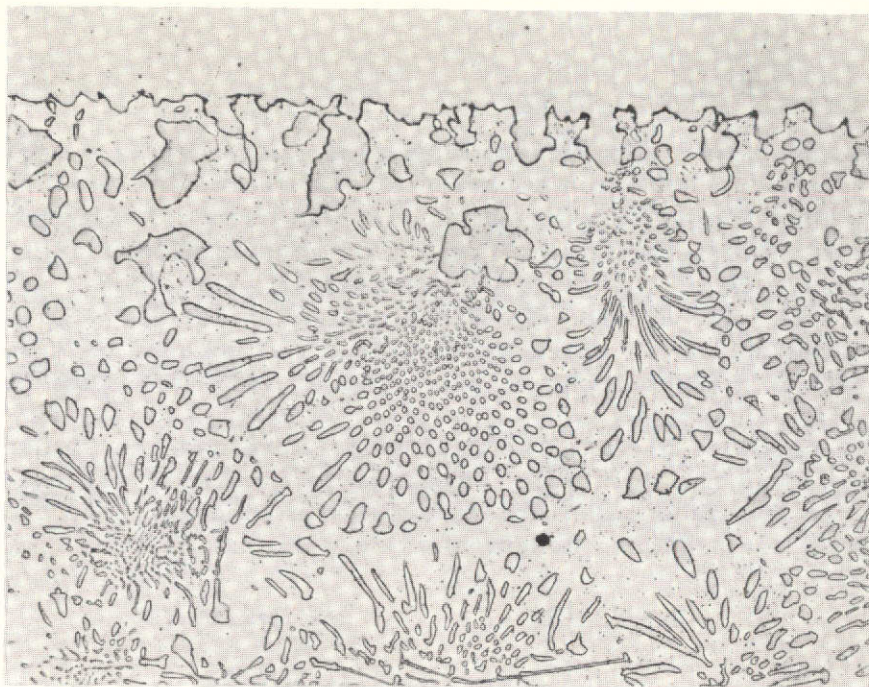
250X

As Polished

5G273

FIGURE I-4. SECTION MCN-2.1 (0 mm) MICROSTRUCTURE

REPRODUCIBILITY OF THE
ORIGINAL PAGE IS POOR

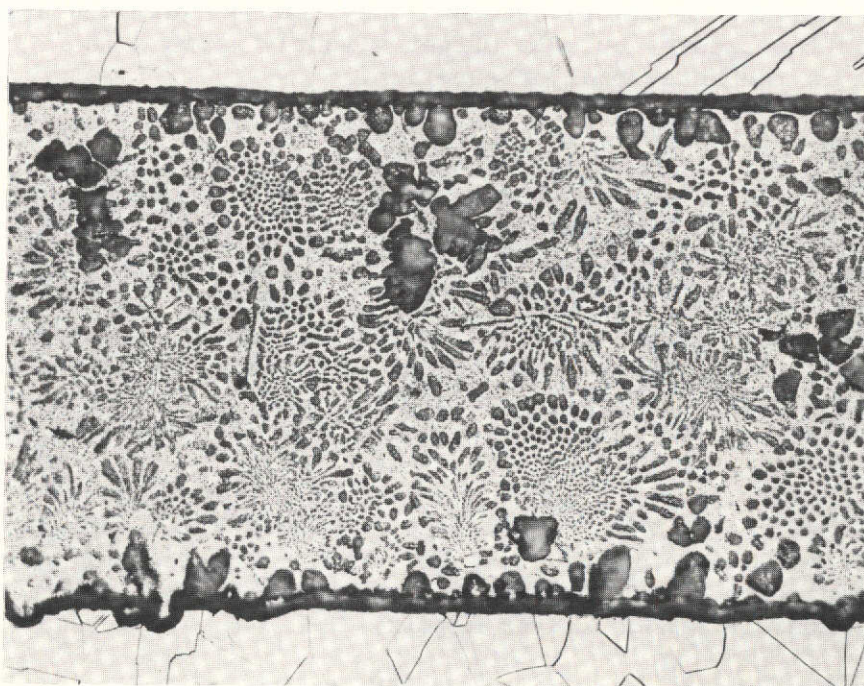


500X

As Polished

5G274

FIGURE I-5. SECTION MCN-2.1 (0 mm) MICROSTRUCTURE



250X

Etched

5G434

FIGURE I-6. SECTION MCN-2.1 (0 mm) MICROSTRUCTURE

REPRODUCIBILITY OF THE
ORIGINAL PAGE IS POOR

12 o'clock and 3 o'clock locations in Figure I-7. (The 3 o'clock position corresponds to the location of the isotope tracer in this sample.) These voids, one of which extended across 70 percent of the joint, could have formed as the result of insufficient filler metal in this area. They could have also formed if filler metal drained from this area into an area deficient in filler metal. Their presence was not noted in the interpretation of the radiographs of this sample. Voids at the 3 o'clock location are shown at 250X in Figure I-8.

Interface-to-interface measurements were made at 90 degree intervals around the joint circumference to determine (1) the clearance between the tube and sleeve and (2) the concentricity of the tube within the sleeve. These measurements are listed below.

<u>Location</u>	<u>Clearance, in.</u>
12 o'clock	0.0093
3 o'clock	0.0078
6 o'clock	0.0099
9 o'clock	0.0109

The average joint clearance, 0.0095 inch, was just slightly less than the design clearance of 0.010 inch. The tube was well-centered vertically in the sleeve, but was offset slightly (toward the 3 o'clock location) in the horizontal orientation.

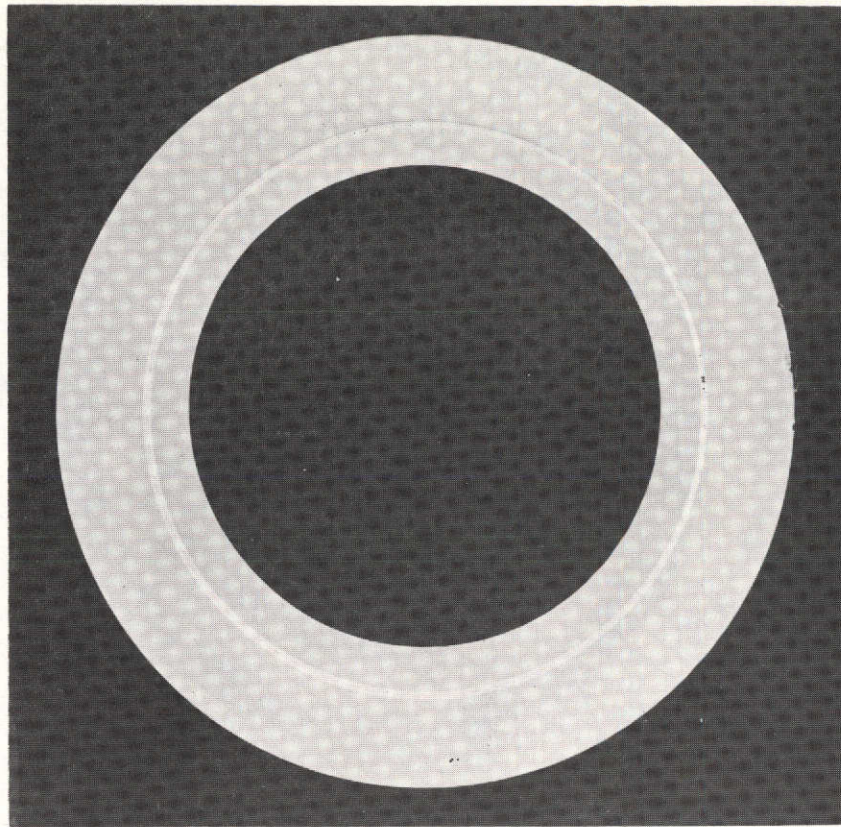
Section MCN-2-3

A section of the right-hand filler metal ring groove is shown at 4X in Figure I-9. The accumulation of filler metal at the bottom of the ring groove indicates that the tube assembly was brazed in the orientation shown in this figure. Capillary forces were ineffective because the ring groove was too wide (0.055 inch). As a result, the filler metal collected in a puddle due to gravity and it did not form a smooth meniscus. Nevertheless, sufficient flow occurred to coat the entire surface of the ring groove with a thin film of filler metal.

A section near the left-hand edge of the accumulated filler metal is shown at 100X in Figure I-10. There are some isolated voids in this area. The microstructure is largely comprised of a second phase and a phase resulting from the reaction of the filler metal with the base metal in a high silver matrix.

Section MCN-2-6

The entire circumferential joint in a section midway between the ring grooves was examined; its appearance is similar to that of the joint shown in Figure I-7. The joint quality was generally excellent; the filler metal wet the base metal and filled the joint almost completely. There were a few isolated voids in the joint; they increased

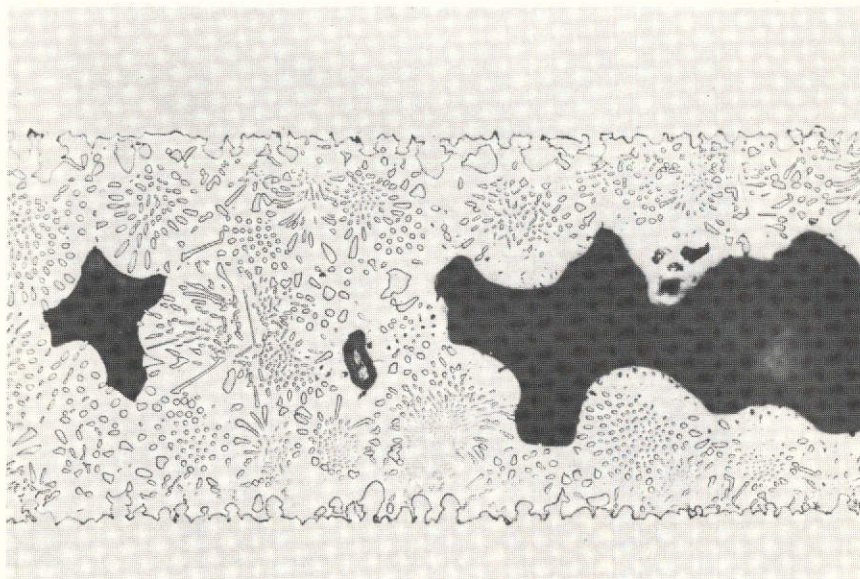


4X

As Polished

5G287

FIGURE I-7. MACROGRAPH OF SECTION MCN-2.2 (2.5 mm)

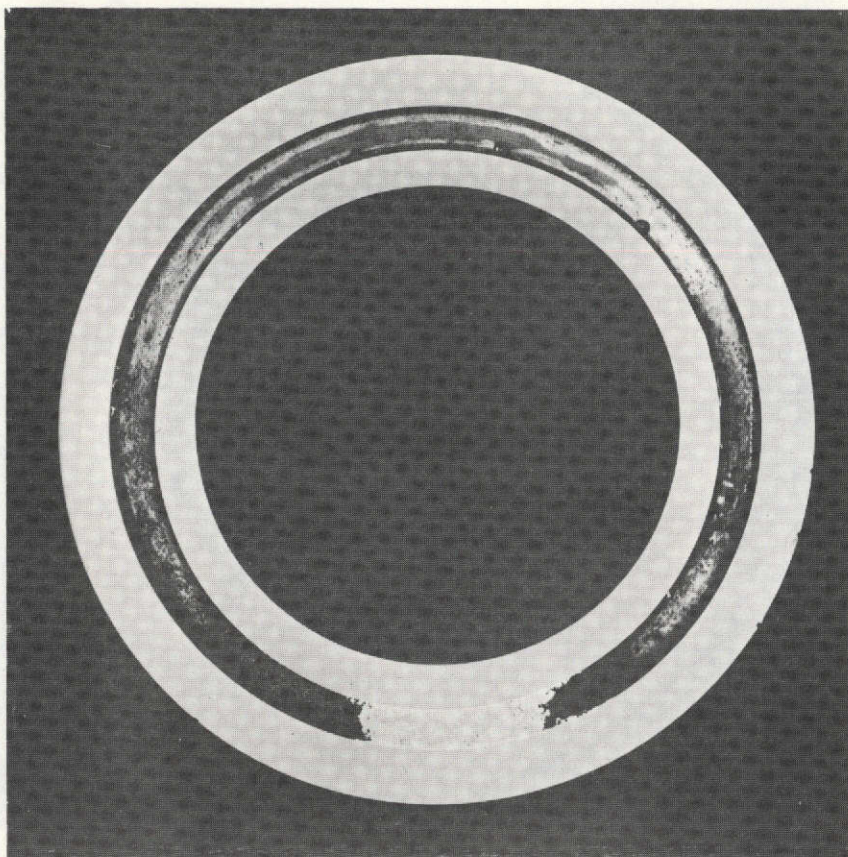


250X

As Polished

5G276

FIGURE I-8. SECTION MCN-2.2 MICROSTRUCTURE

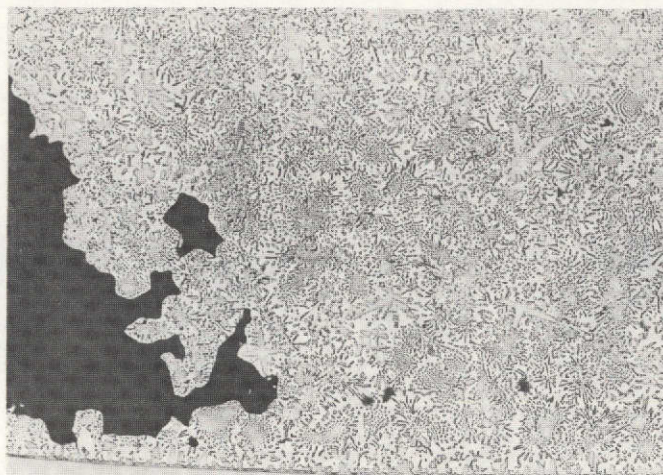


4X

As Polished

5G288

FIGURE I-9. SECTION MCN-2.3 (7 mm) SHOWING
BRAZE ALLOY IN RING GROOVE



100X

As Polished

5G277

FIGURE I-10. MICROSTRUCTURE OF BRAZE ALLOY IN RING
GROOVE - SECTION MCN-2.3 (7 mm)

in size and number in the 3 to 6 o'clock quadrant. The joint microstructure was similar to that of the section discussed above.

Section MCN-2-9

A complete cross section of the left-hand ring groove is shown at 20X in Figure I-11. In the section of the joint that was located at the 12 o'clock position during brazing (Figure I-11a), there was a fillet of filler metal in the corners of the ring groove, but the groove itself was empty. However, the surfaces of the groove were coated with a thin film of filler metal as it flowed into the joint between the tube and sleeve. In the section that was located at 6 o'clock during brazing (Figure I-11), the ring groove was completely filled with accumulated filler metal as indicated by the radiograph of this area.

Sample MCN-3

Five representative sections from Sample MCN-3 were examined metallographically. The designation and approximate location of each section are shown in Figure I-12. Three sections (MCN-3-3, MCN-3-5, and MCN-3-9) were cut and mounted to permit examination of the joint surfaces parallel to the longitudinal axis of the sample. The remaining sections were mounted to show the full circumferential joint between the tube and sleeve.

Section MCN-3-2

A circumferential section through the right-hand ring groove of this sample is shown at 4X in Figure I-13. The location of the accumulated filler metal indicates that the tube assembly was brazed in the orientation shown in Figure I-13. Considerably more filler metal remained in the ring groove of this sample after brazing than in the corresponding ring groove of Sample MCN-2 (Figure I-9). Apparently, the filler metal did not flow as well as it did in the previous sample. As observed previously, however, the surfaces of the ring groove were coated with a thin film of filler metal.

The microstructure of the accumulated filler metal is shown at 100X in Figure I-14. It is similar in appearance to microstructures examined previously.

Section MCN-3-3

The cross section of the right-hand ring groove was also examined. In appearance, this cross section was essentially identical to that shown in Figures I-11a and I-11b. The lower portion of the ring groove was filled with filler metal; the upper portion was empty. However, filler metal had flowed from the ring groove to fill the joint between the tube and sleeve.

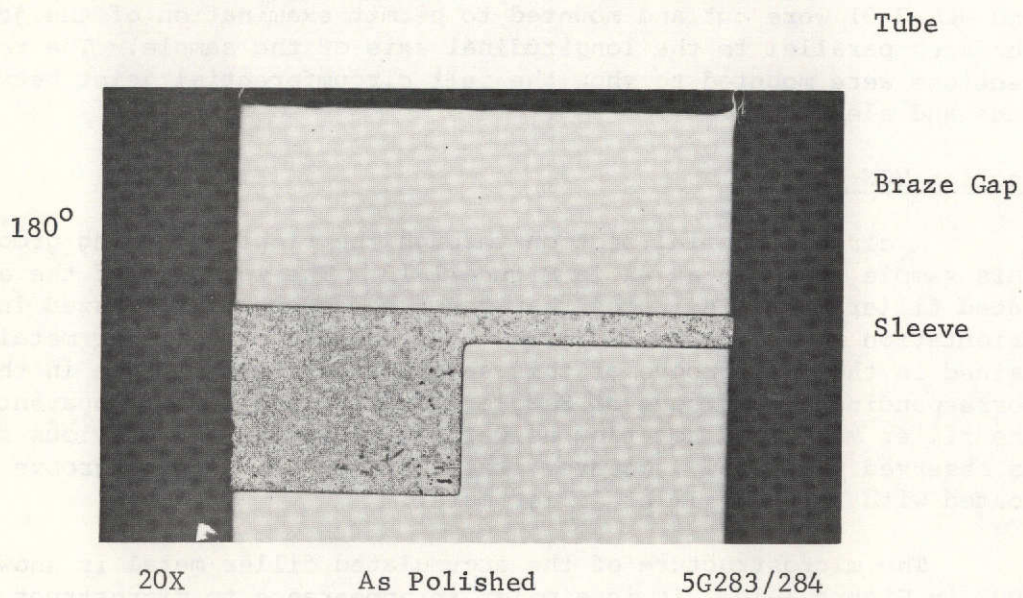
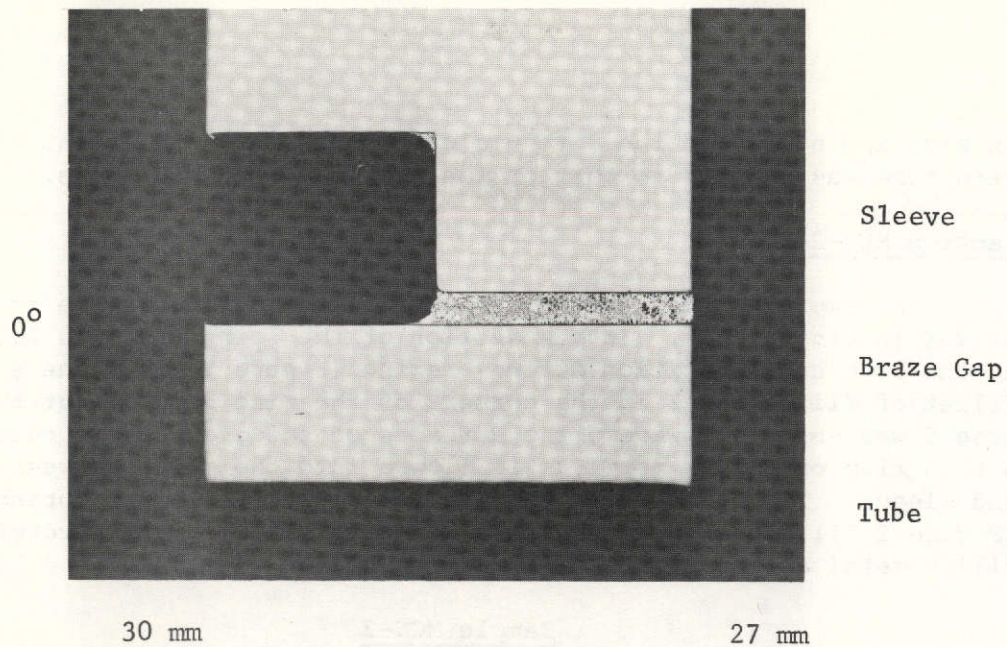


FIGURE I-11. APPEARANCE OF RING GROOVE AREA SHOWING ALLOY FLOW TO LOW POINT - SECTION MCN-2.9 (27 to 30 mm)

↓ Denotes surface perpendicular
to axis of sample

+ Denotes surface parallel
to axis of sample

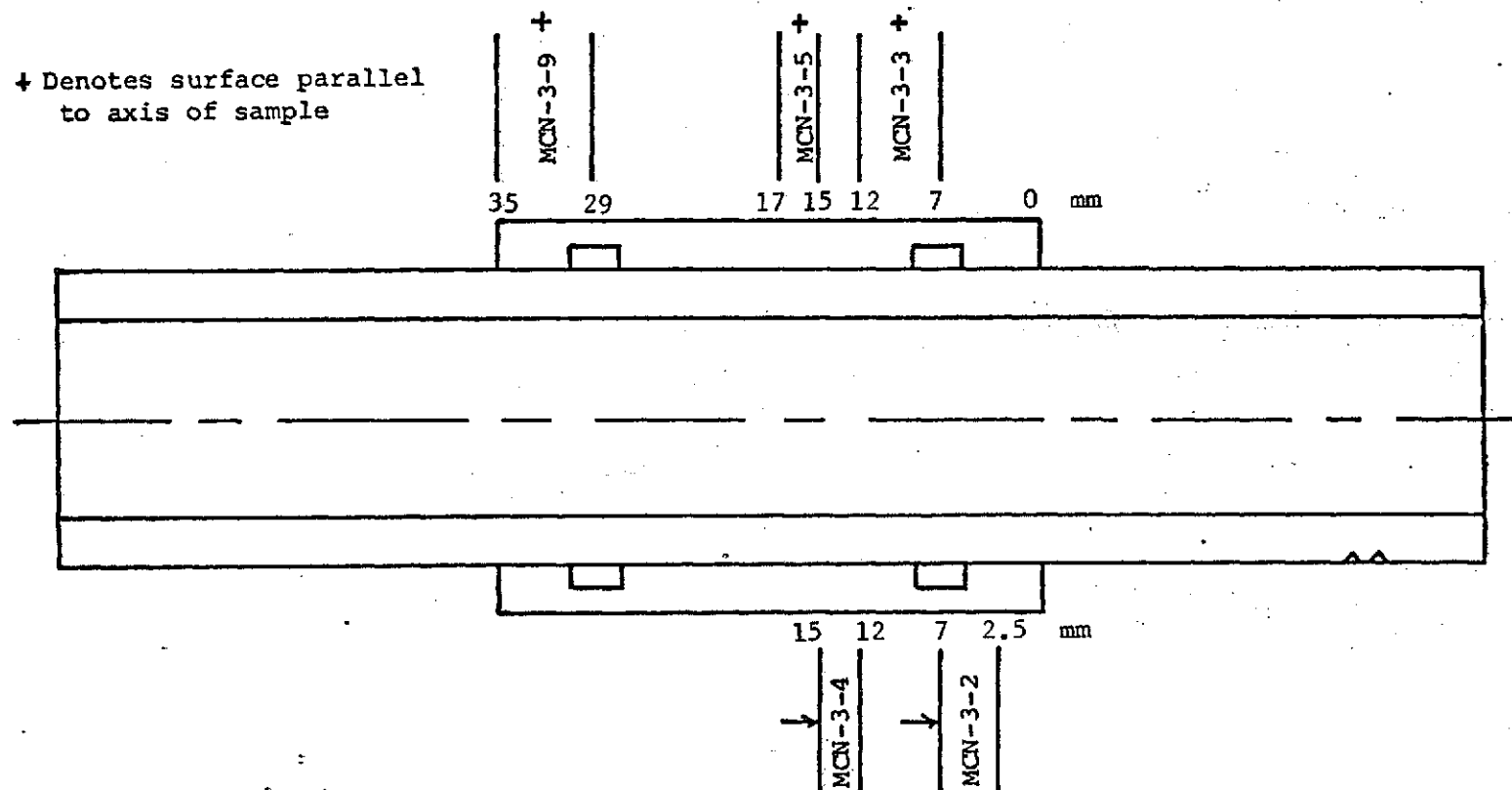
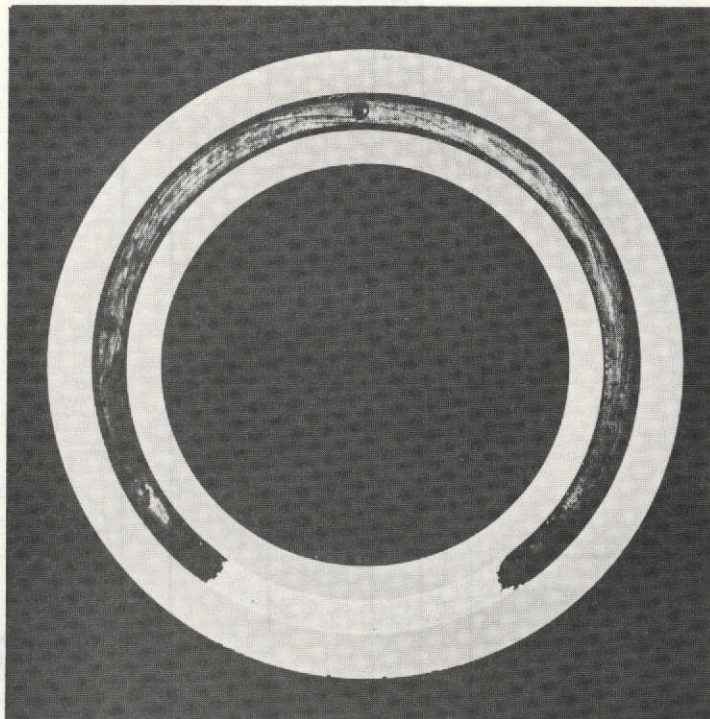


FIGURE I-12. SURFACES EXAMINED DURING METALLOGRAPHIC EVALUATION (MCN-3)

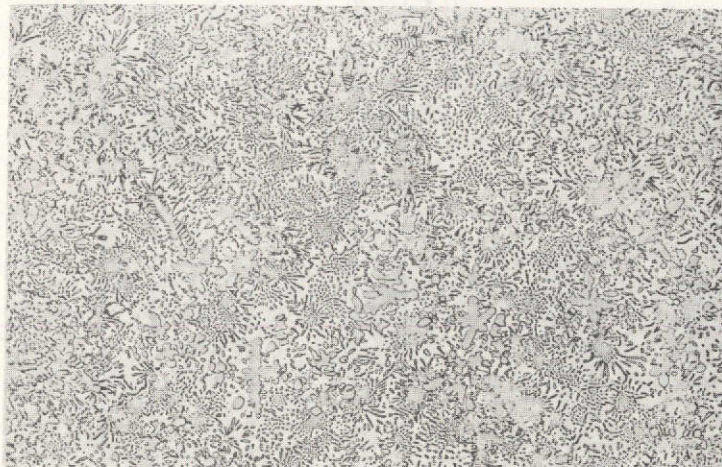


4X

As Polished

5G289

FIGURE I-13. MACROGRAPH OF RING GROOVE AREA -
SECTION MCN-3.2 (7 mm)



100X

As Polished

5G278

FIGURE I-14. MICROSTRUCTURE OF RING GROOVE AREA -
SECTION MCN-3.2

Section MCN-3-4

A circumferential section between the ring grooves is shown at 4X in Figure I-15. The joint between the tube and the sleeve is essentially void for about 40 degrees of its circumference, and there are numerous voids on either side of this area. The void area was located at the top of the sample during the brazing cycle. In the radiographs of this joint, it was interpreted as an area of porosity. The remainder of this joint was largely defect-free.

A section of the void area is shown at 250X in Figure I-16. The presence of some filler metal and some material in a zone where the molten filler reacted with the base metal implies that filler metal was present in this area during the brazing cycle. However, much of it (presumably of the eutectic composition) drained into areas deficient in filler metal before solidification was completed. There is one area along the lower interface where the filler metal appears to have penetrated the boundaries of a grain in the base metal.

A defect-free area of this joint is shown at 250X and 500X in Figure I-17. The joint microstructure is similar to that observed in various sections of Sample MCN-2. However, the length of the particles along the interface indicates that more reaction between the molten filler metal and the base metal occurred in this sample than in Sample MCN-2.

Section MCN-3-5

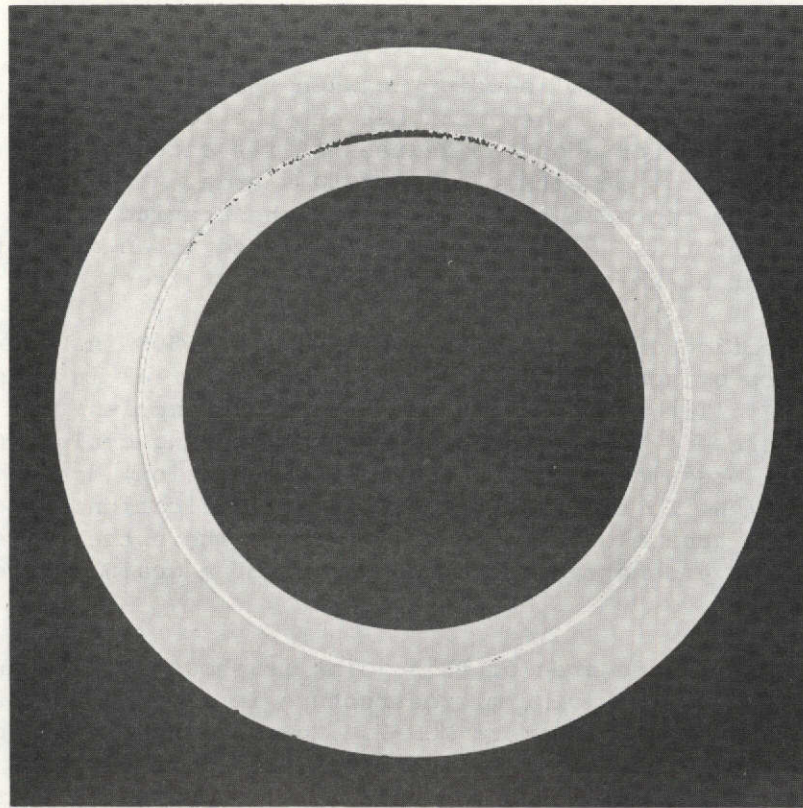
The section adjacent to MCN-3-4 was examined in cross section. The continuation of the area that is essentially void can be seen in the upper section of this joint (Figure I-18a). This area has the appearance of being once filled with filler metal during the brazing cycle. The lower section of this joint, i.e., the section located at 6 o'clock during brazing, is completely filled with filler metal (Figure I-18b). Numerous isolated voids are present in the joint.

Section MCN-3-9

This section was mounted to permit examination of the cross section of the left-hand ring groove. The ring groove in the area located at 12 o'clock during brazing was empty; the bottom of the ring groove was partially filled with filler metal. The joint microstructure was similar to that observed in other sections of this sample.

MICROSTRUCTURAL STUDIES

An investigation was conducted to study the base metal-filler metal reactions that occurred during brazing and their

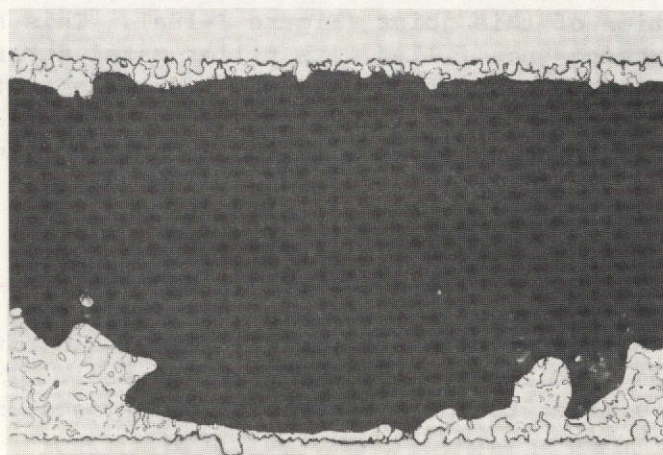


4X

As Polished

5G290

FIGURE I-15. MACROGRAPH OF SECTION MCN-3.4 (15 mm)

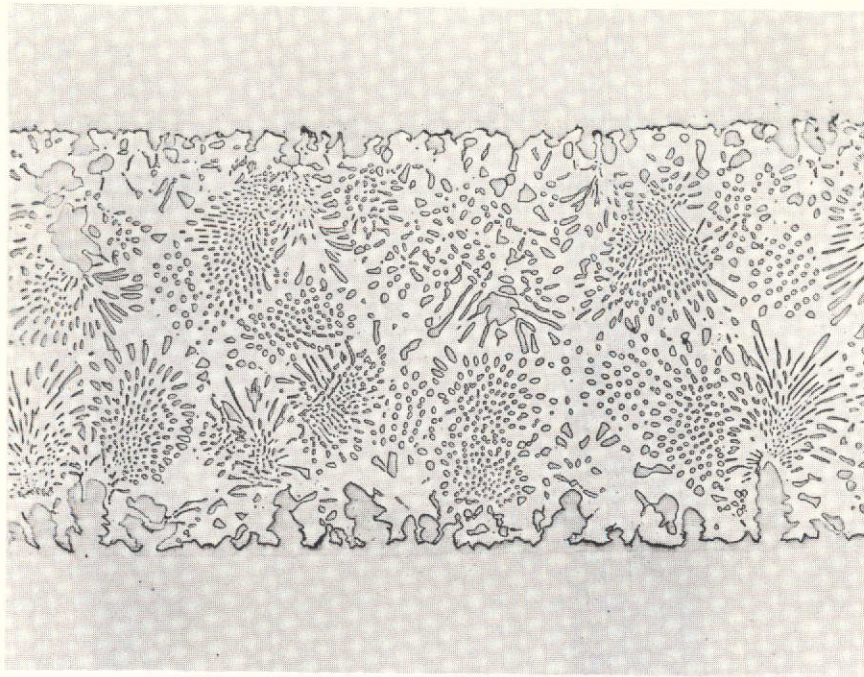


250X

As Polished

5G279

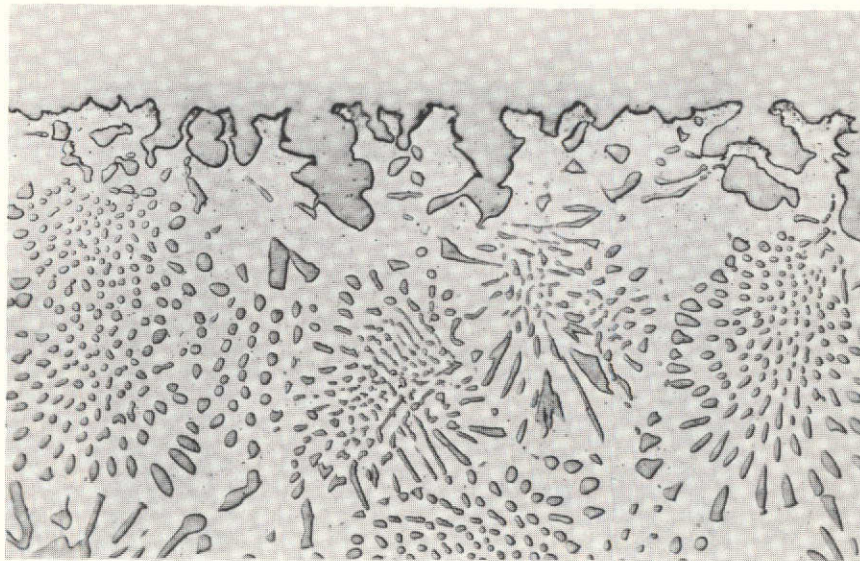
FIGURE I-16. SECTION MCN-3.4 SHOWING LARGE SHRINKAGE VOID AREA



250X

As Polished

5G280



500X

As Polished

5G281

FIGURE I-17. MICROSTRUCTURE IN SECTION MCN-3.4 (15 mm)

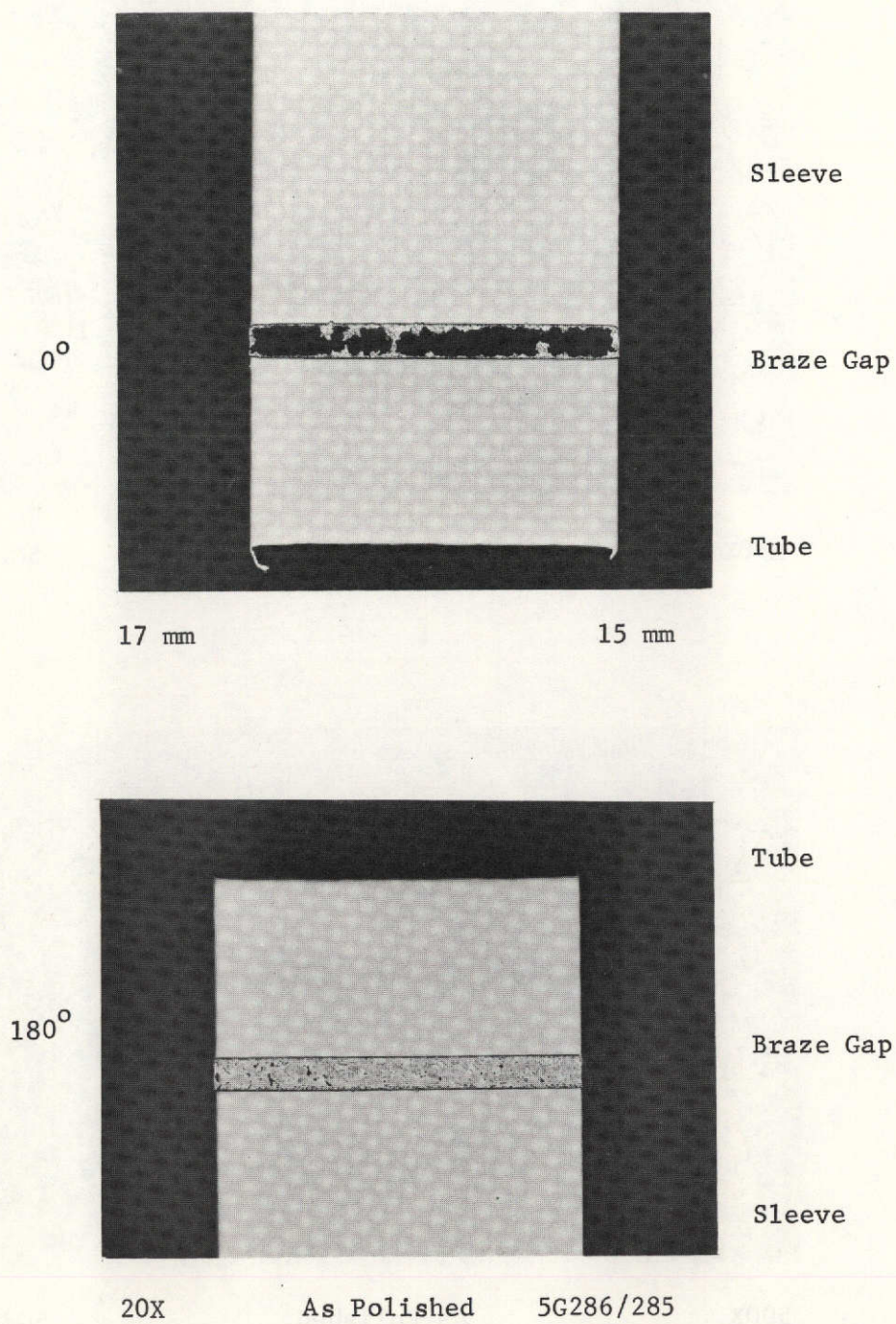


FIGURE I-18. MACROGRAPH OF BRAZE BETWEEN 15 AND 17 mm -
SECTION MCN-3.5

effects on the microstructure of the brazed joint. Also, the approximate composition of some of the phase constituents was determined.

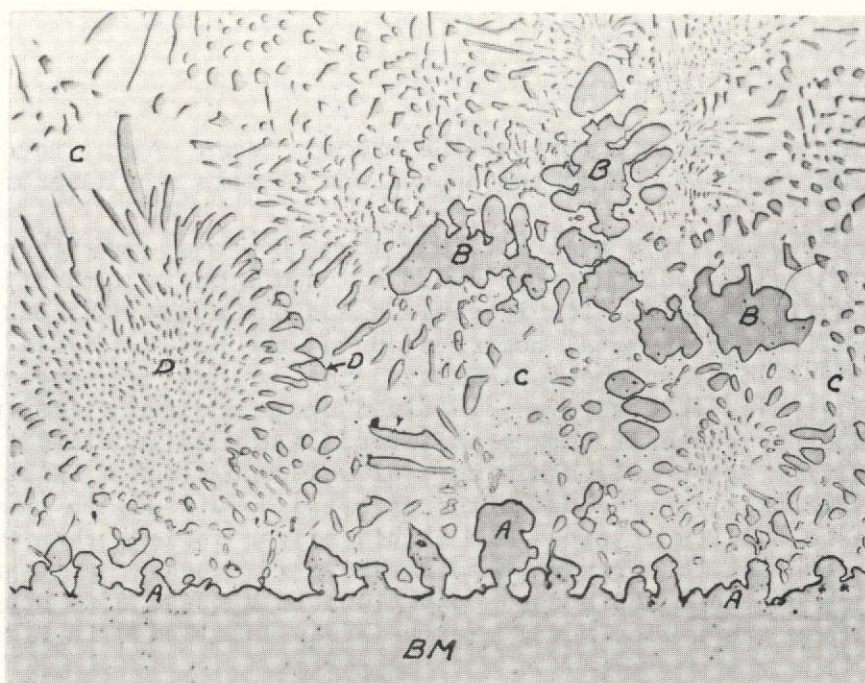
The microstructure of a typical area along the joint interface of Section MCN-2-1 is shown in the unetched condition at a magnification of X500 in Figure I-19. Considerable reaction between the base metal and the molten filler metal occurred during the brazing cycle. In Section MCN-2-1, measurements indicated that a layer of base metal, 0.0005 inch thick or less, was dissolved by the molten filler metal to form another phase at the joint interface (areas labelled A in Figure I-19). Presumably, this is a nickel-copper phase because nickel and copper form a continuous series of solid solutions; on the other hand, the solubility of nickel in liquid silver is less than 0.5 weight percent at the brazing temperature.^(1,2) Based on its appearance in the unetched and etched condition, this phase also appears to be present in the filler metal matrix (areas labelled B in Figure I-19).

The microstructure of the brazed joint was further studied by electron microprobe analysis. An area* similar to that indicated in Figure I-19 was scanned with the electron beam to determine the distribution of the following elements: nickel, copper, and silver. The resulting X-ray images for these elements are shown in Figures I-20a, I-20b, and I-20c. By examining the variations in intensity that indicate the approximate concentration distribution of each element in the area being scanned, it was possible to estimate the composition of phase constituents in areas of interest. The results of electron microprobe analysis are discussed below.

- (1) The approximate composition of the phase (A in Figure I-19) at the joint interface that resulted from reaction of the base metal with the molten filler metal is 95Cu-5Ni.
- (2) The composition of the phase (B in Figure I-19) in the filler metal matrix is identical to that of the phase at the joint interface. This copper-rich reaction product formed along the interface and became detached.

-
1. Hansen, M., Constitution of Binary Alloys, McGraw-Hill Book Company, New York, N. Y. (1958).
 2. Elliot, R. P., Ed., Constitution of Binary Alloys, First Supplement, McGraw-Hill Book Company, New York, N. Y. (1965).

* The area scanned by the electron beam differed slightly from that shown in Figure I-19 because the specimen was repolished before examination. However, the area scanned contained the features shown in Figure I-19.

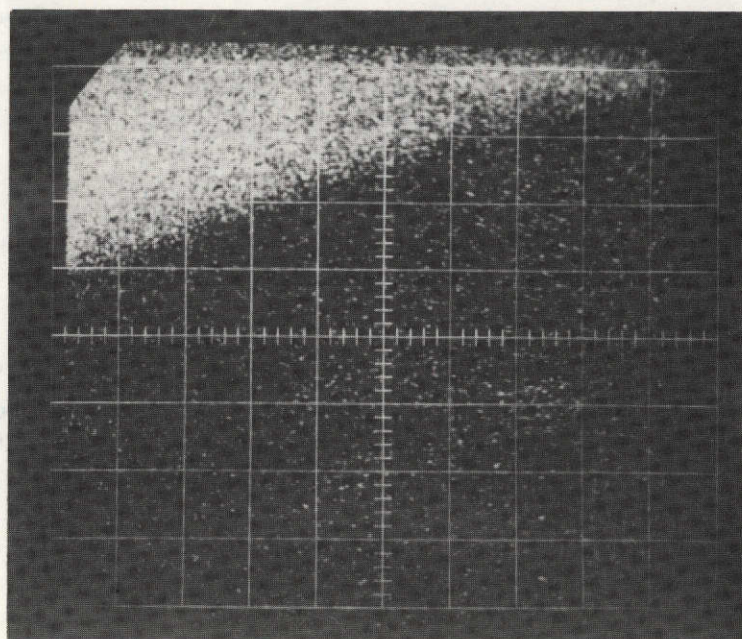


500X

As Polished

5G275

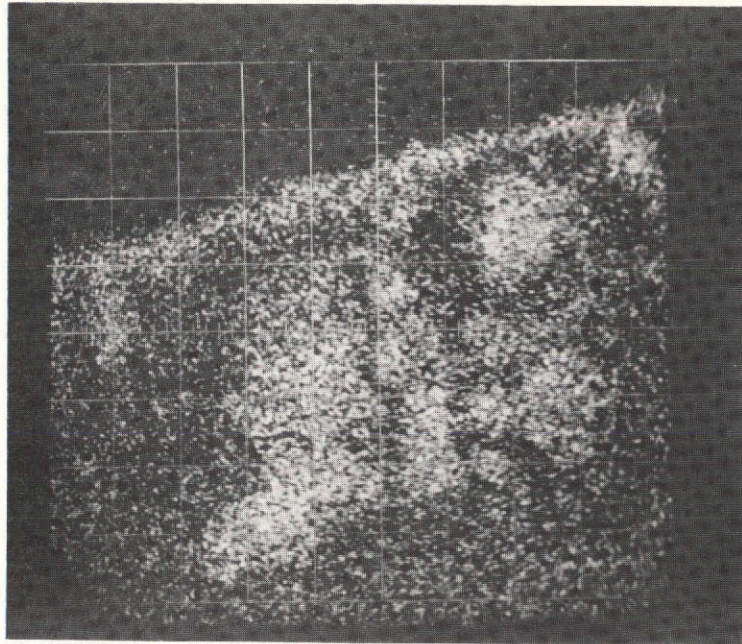
FIGURE I-19. PHASES PRESENT IN SECTION MCN-2.1



300X

11305

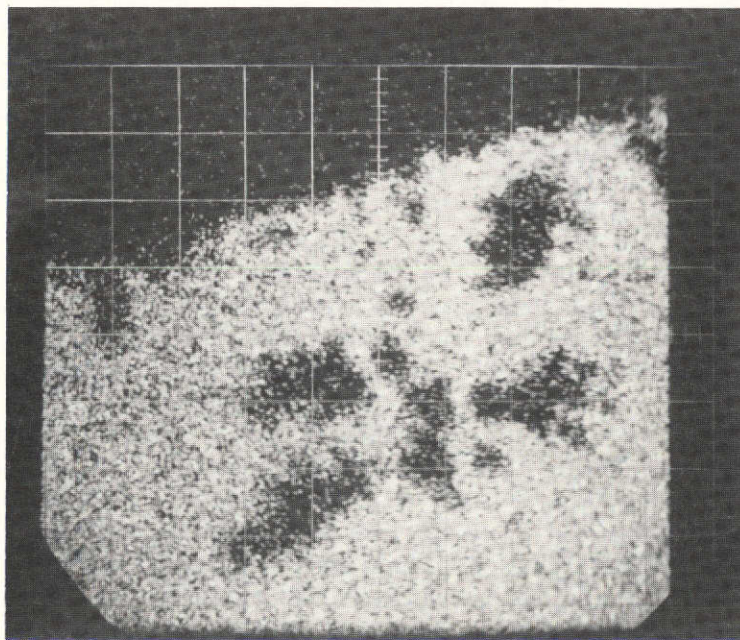
FIGURE I-20a. NICKEL X-RAY IMAGE



300X

11304

FIGURE I-20b. COPPER X-RAY IMAGE



300X

11303

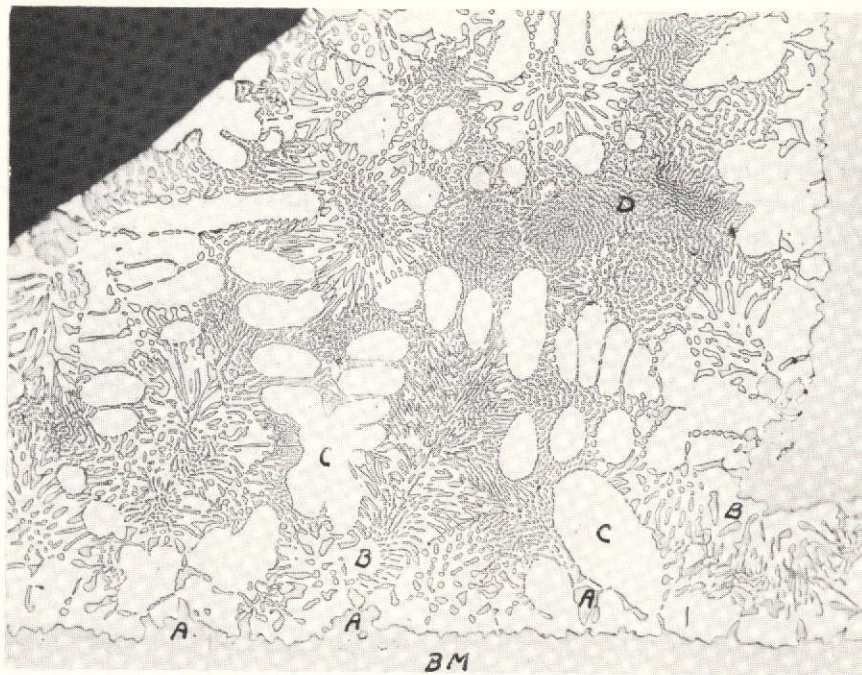
FIGURE I-20c. SILVER X-RAY IMAGE

- (3) The light areas of the filler metal matrix (C in Figure I-19) are composed of essentially pure silver. These areas are low in copper because of the reaction of the molten filler metal with the base metal.
- (4) Attempts were made to identify other constituents of the microstructure, e.g., areas labelled D. However, the composition of these areas could not be determined because they were too small. Presumably, they represent a copper-rich phase similar to areas A and B.

The exothermic brazing cycle differs substantially from that used for conventional brazing operations with Ag-28Cu-0.2Li filler metal. Ground characterization samples MCN-2 and MCN-3 were brazed at temperatures above 1900 F (1037.8 C); that is, at temperatures much higher than the liquidus temperature of Ag-28Cu-0.2Li filler metal, 1400 F (760.0 C). The time required to heat these samples to the brazing temperature was very short (one minute) and the total time during which the filler metal was molten was correspondingly short also. In contrast, most assemblies made with this filler metal are brazed at 1450 to 1500 F (787.7 to 815.5 C). While the time required to braze the assembly depends on its mass and the capabilities of the furnace, it is relatively long in comparison with the time required for exothermic brazing. Since the amount of reaction between the base metal and filler metal is largely dependent on the brazing temperature and the time during which the filler metal is molten, the microstructure of exothermically brazed joint could differ appreciably from those of joints brazed conventionally. To study this possibility, a nickel-tee joint was brazed with Ag-28Cu-0.2Li filler metal in a vacuum (2.8×10^{-5} torr) at 1500 F for 5 minutes.*

An unetched section of the nickel tee-joint is shown at 250X in Figure I-21a; for direct comparison, a section from MCN-2 is shown at the same magnification in Figure I-21b (this figure is identical to I-4). The microstructures of these joints reflect differences attributable to the brazing conditions. The amount and distribution of the copper-rich phase (A in Figure I-21a and I-21b) indicates that more reaction between the base metal and filler metal occurred in the exothermically brazed joint than in the furnace brazed joint. However, the width of the reaction zone at the interface was comparable for both joints. The microstructure of areas at some distance from the joint interface differs considerably. In the furnace-brazed joint (Figure I-21a), there is a silver-rich dendritic phase (C) dispersed in a matrix of the silver-copper eutectic (D). In the exothermic-brazed joint (Figure I-21b), the following phases are present: a copper-rich phase (a), a phase that is essentially pure silver (B), and a phase that was not identified (C).

* The material for the tee joint was obtained from excess stock on Sample MCN-2; the filler metal was obtained from MSFC.

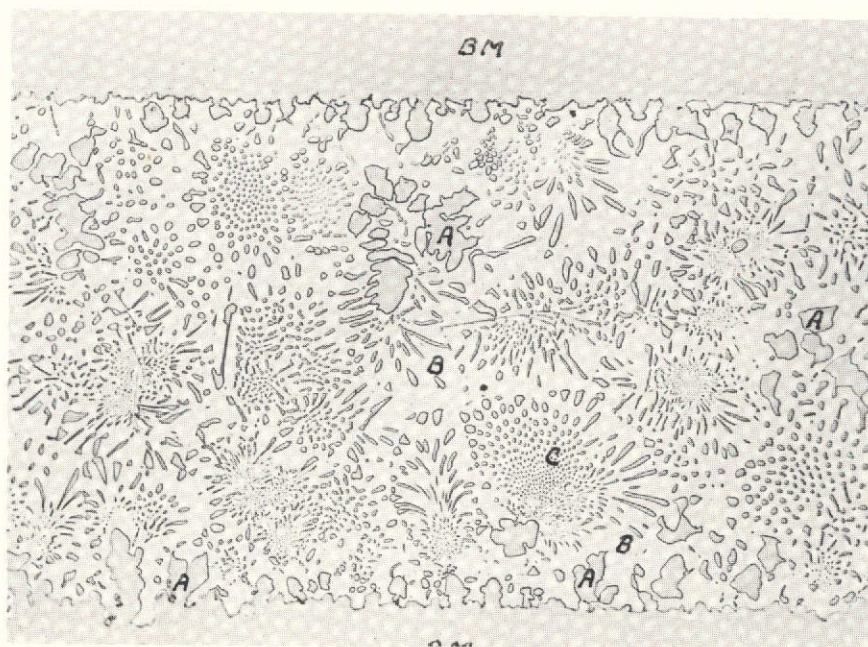


250X

As Polished

5G647

FIGURE I-21a. PHASES PRESENT IN TEE JOINT BRAZED AT 1500 F



250X

As Polished

5G273

FIGURE I-21b. PHASES PRESENT IN EXOTHERMIC BRAZE -
SECTION MCN-2.1

REPRODUCIBILITY OF THE
ORIGINAL PAGE IS POOR

The differences in the microstructures of exothermically brazed and furnace-brazed joints appear to be primarily attributable to the difference in the brazing thermal cycle.

SECTION II

EVALUATION OF STAINLESS STEEL GROUND CHARACTERIZATION SAMPLES

A detailed metallurgical evaluation of three exothermically brazed stainless steel ground characterization samples was conducted at Battelle-Columbus. Samples MCS-1, MCS-2, and MCS-3 were among six samples that were brazed as part of Exothermic Brazing Experiment M552 at the Marshall Space Flight Center in January, 1973.* They were made to obtain base-line data for use in determining the effect of weightlessness on (1) the wetting and flow behavior of brazing filler metals and (2) the metallurgical characteristics of the brazed joints. The samples were evaluated by metallographic examination and electron microprobe analysis.

SAMPLE DESCRIPTION

Each sample consisted of a 304L S.S.** sleeve into which a thin-wall 304L S.S. tube was brazed with the self-fluxing silver-copper filler metal Ag-28Cu-0.2Li (BAg-8a). The filler metal strip (0.035 inch thick by 0.145 inch wide) was formed into rings; one ring was placed in each of two grooves that were located near each end of the sleeve. The brazing clearance, i.e., the spacing between the tube and the sleeve, was 0.005 inch; the clearance was uniform for the full joint length. Spacers or inserts were used to provide this clearance and maintain the concentricity of the tube within the sleeve. The tube was slit at its center.

Samples MCS-1 and MCS-2 were almost identical. Both samples were brazed in the horizontal position in a vacuum furnace with exotherms that weighed 60 grams. The sample temperature was monitored by thermocouples attached in the following locations: (1) inside the tube at the center of the sample, (2) inside the tube at the end of the sleeve, and (3) outside and at the end of the tube. The pressure within the vacuum furnace and maximum temperature (measured at the center ID of the tube) are indicated below.

MCS-1: 3.5×10^{-5} torr and 1915 F (1046.1 C)
MCS-2: 2.6×10^{-5} torr and 1910 F (1043.3 C)

* The other samples were also sent to Battelle-Columbus. After preliminary examination and sectioning, three samples were sent to the University of Wisconsin for metallurgical study.

** The composition of the bar stock from which the tube and sleeve were machined was 11.46Ni-18.70Cr-1.8Mn-0.44Si-0.014S-0.030P-0.036C-Fe (rest).

Sample MCS-3 was brazed under the same conditions as Samples MCS-1 and MCS-2. However, as indicated below, the pressure and temperature at which brazing occurred varied from the planned schedule because of an equipment malfunction.

MCS-3: 1.5×10^{-4} torr and 1810 F (987.7 C)

After brazing, the samples were radiographed at the Marshall Space Flight Center. The following comments are based on the interpretation of the radiographs.

Sample MCS-1: Voids at center and both ends of sleeve; excess filler metal in bottom tube; no filler metal in ring grooves.

Sample MCS-2: Voids at center and both ends of sleeve; excess filler metal in bottom of tube; no filler metal in ring grooves.

Sample MCS-3: Voids at both ends of sleeve; excess filler metal in bottom of tube; no filler metal in ring grooves.

SECTIONING

Samples MCS-1, MCS-2, and MCS-3 were sectioned perpendicular to the longitudinal axis of the tube assembly to produce a series of circular sections. Sectioning was done with a water-cooled silicon carbide cutoff wheel, 0.5 mm wide. The use of a narrower cutoff wheel to minimize the width of the kerf was considered. However, cutting tests conducted with a 0.25 mm wide wheel indicated that equipment modifications would be needed to produce parallel cuts and avoid wheel breakage; also, cutting rates with this wheel were very slow.

Both samples were sectioned as shown in Figure II-1. Sectioning was done in general conformance with the plan adopted during a meeting that was held at Battelle-Columbus in August, 1972. However, instead of sectioning to produce circular specimens with a uniform width of 0.100 inch (2.5 mm), the samples were sectioned in areas that appeared to be more informative, i.e., through the filler metal ring grooves, through porosity areas, etc. Nine sections were cut from each sample. Each section was identified to indicate its location along the longitudinal axis of the sample.

VISUAL EXAMINATION

The sections from Samples MCS-1, MCS-2, and MCS-3 were examined under low-power magnification to (1) study the visual appearance of

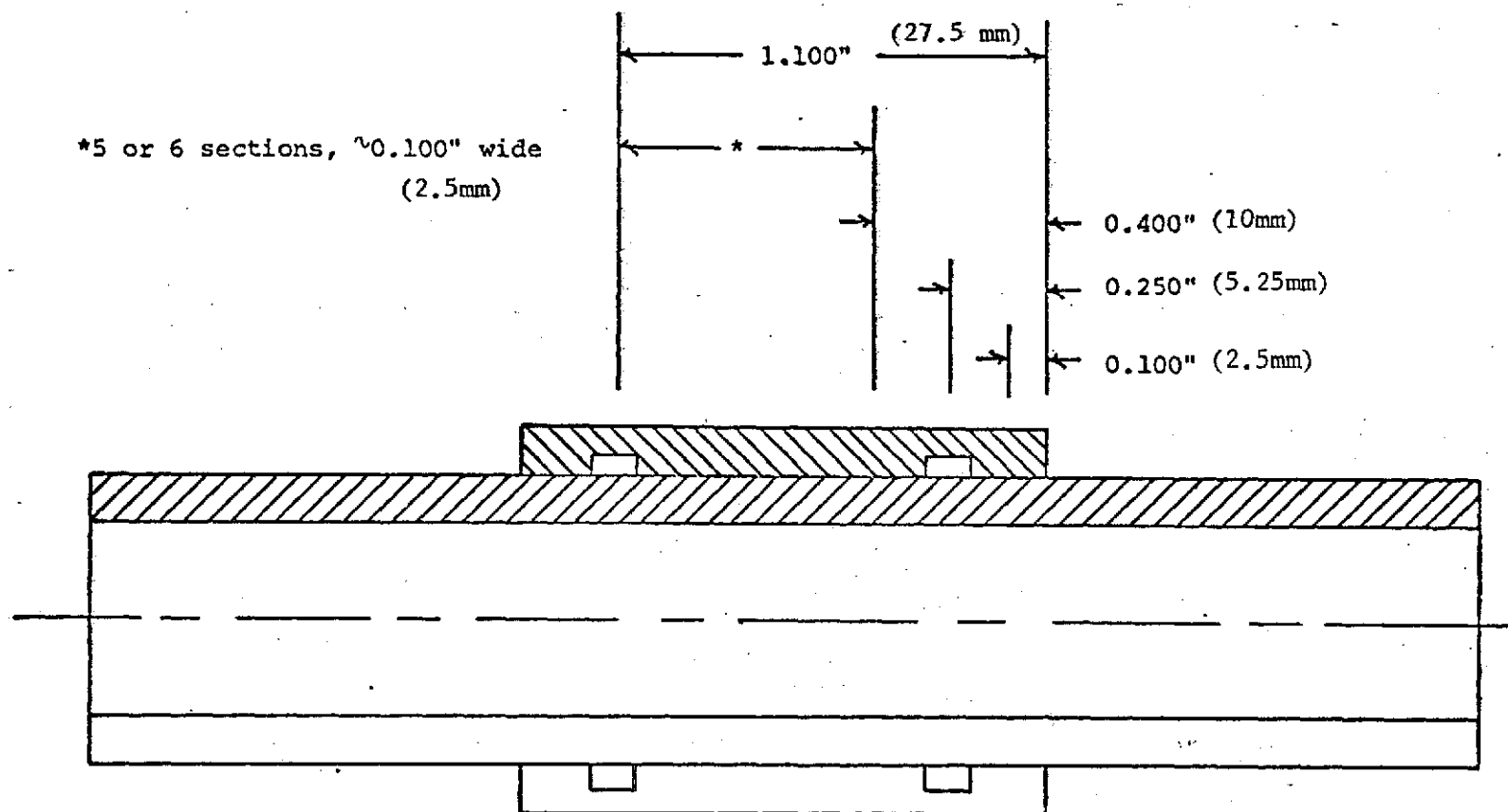


FIGURE II-1. SECTIONING PLAN FOR GROUND CHARACTERIZATION
SAMPLES MCS-1, MCS-2, AND MCS-3

Sections to be cut at indicated distances
from right end of sample.

the brazed tube assembly, (2) confirm the radiographic findings, and (3) select sections for metallographic examination. The results of these studies are discussed below.

Sample MCS-1

This tube-sleeve assembly appeared to be well brazed from one end to the other. Filler metal was present around the entire joint circumference in each section (except sections that were cut through the filler metal ring grooves). The joint quality was visually excellent; there was one void near the center of the sample at the 12 o'clock position during brazing. Excess filler metal was accumulated inside the tube at the 6 o'clock position. The ring grooves were empty; however, excellent flow was indicated by the presence of a very thin film of filler metal over the ring groove surface. One thermocouple was brazed on the inside of the tube. Four sections were selected for metallographic study.

Sample MCS-3

This assembly was well brazed for its entire length, and the circumferential joints in all sections (excluding those cut through the ring grooves) were filled with brazing filler metal. The joint quality was generally good; there were some voids between the tube and sleeve in a section near the left-hand end of the sleeve. Both ring grooves were essentially empty; there appeared to be a very small fillet in the ring grooves and the surfaces of both were coated with a film of filler metal. Filler metal was accumulated in the bottom of the tube. The surface of the accumulated filler metal was extremely rough and there were numerous areas of porosity. The surface of the accumulated filler metal in Samples MCS-1 and MCS-2 was smooth and there was no evidence of porosity. Four samples were selected for metallographic examination.

METALLOGRAPHIC EXAMINATION

Sections from Samples MCS-1, MCS-2, and MCS-3 were examined metallographically to study (1) the wetting and flow characteristics of the filler metal, (2) the quality of brazing, (3) defects and their frequency of occurrence, (4) metallurgical reactions between the base metal and filler metal, and (5) joint microstructures. These studies are discussed below.

Sample MCS-1

Four sections representing areas where significant joint features might be evident were examined. The designation and approximate location of each section are shown in Figure II-2. Sections MCS-1-1 and

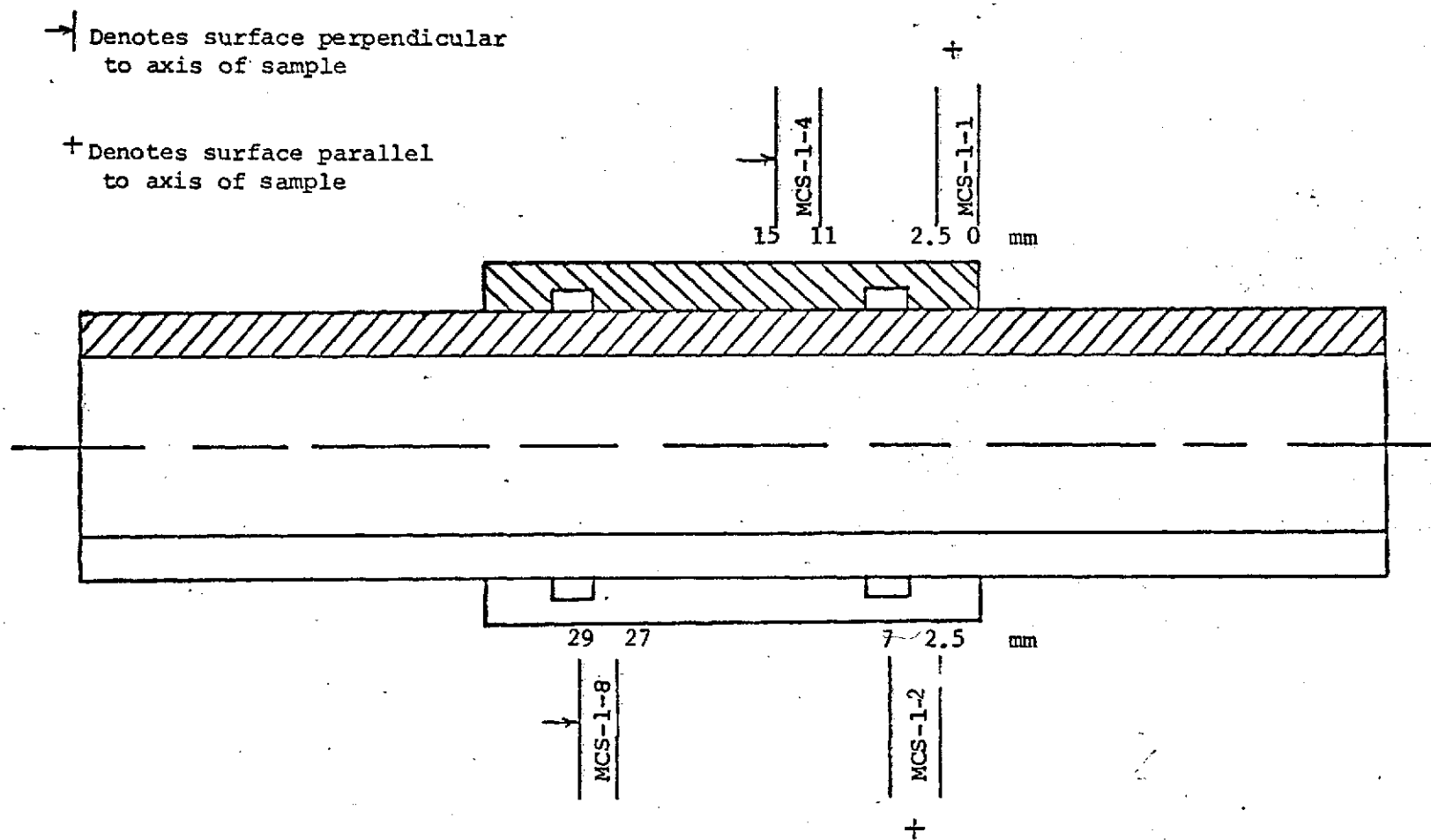


FIGURE II-2. SURFACES EXAMINED DURING METALLOGRAPHIC EVALUATION (MCS-1)

MCS-1-2 were cut and mounted to permit examination of the joint surfaces parallel to the longitudinal axis of the sample. Sections MCS-1-4 and MCS-1-8 were mounted to show the entire circumferential joint between the tube and the sleeve, i.e., the surface perpendicular to the longitudinal axis of the sample. The metallographic specimens were examined in the unetched and etched condition.

Section MCS-1-1

The upper and lower sides of this joint are shown at 20X in Figure II-3. The upper side of this joint is completely filled and the joint quality is excellent. Excellent flow of the filler metal is also indicated in the bottom section of this joint; however, as indicated by radiography, the joint was partially void. The insert that is used to insure the concentricity of the tube within the sleeve is well brazed also.

Selected areas of this joint are shown in the unetched condition at magnifications of 250X and 500X in Figure II-4. The microstructure between the joint interfaces appears to consist of a three-phase structure. The reaction of the base metal with the molten filler metal is clearly evident. The width of the joint between interfaces is 0.0044 inch; some products of the base metal-filler metal reaction extend about 0.001 inch from the interface.

The joint microstructure and the phases contained therein are discussed in more detail later in this section.

Section MCS-1-2

The upper and lower portions of the section adjacent to the one discussed above (MCS-1-1) are shown at 20X in Figures II-5; this section contains the filler metal ring groove and a short length of tube-to-sleeve joint. The ring groove is devoid of filler metal; however, there was evidence of a very thin film of filler metal on the ring groove surfaces at high magnification. As in the previous section (and as indicated by radiography), the upper section of the joint was filled with filler metal; the lower section was void. Filler metal is puddled at the bottom inside of the tube. This filler flowed from the ring groove to the center of the sample, through the slits in the tube, and back along the inside of the tube.

The microstructure of an area of accumulated filler metal is shown in the unetched condition at 250X and 500X in Figure II-6. Reaction between the base metal and molten filler metal at the interface is clearly evident. The microstructure of the bulk filler metal is quite complex, consisting of products from the base metal-filler metal reaction and possibly some silver-copper eutectic.

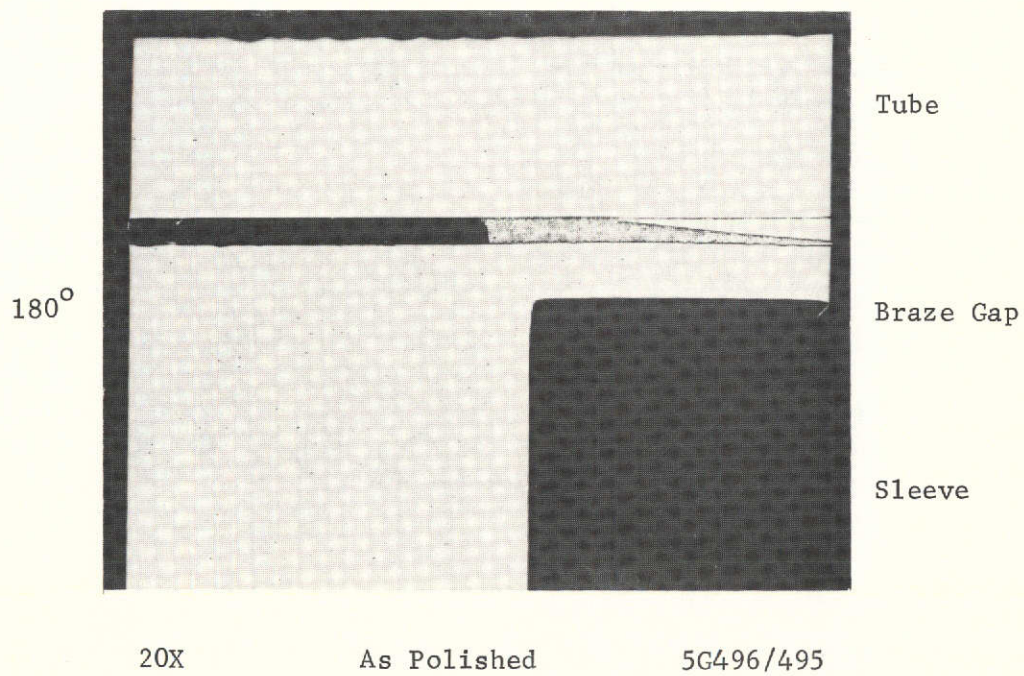
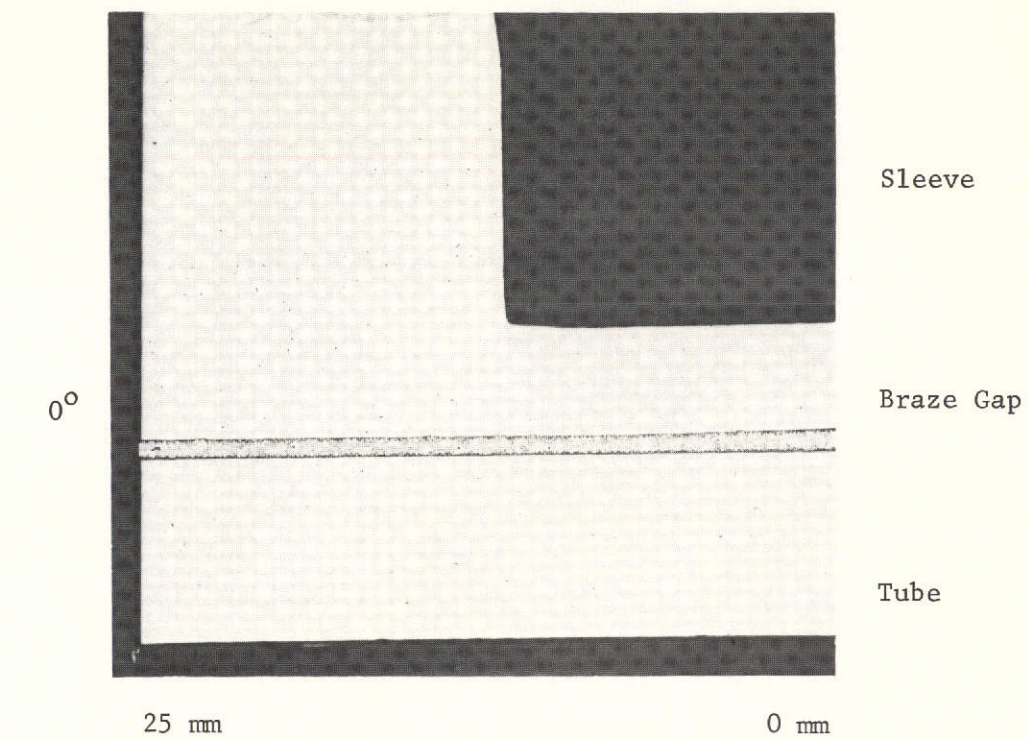
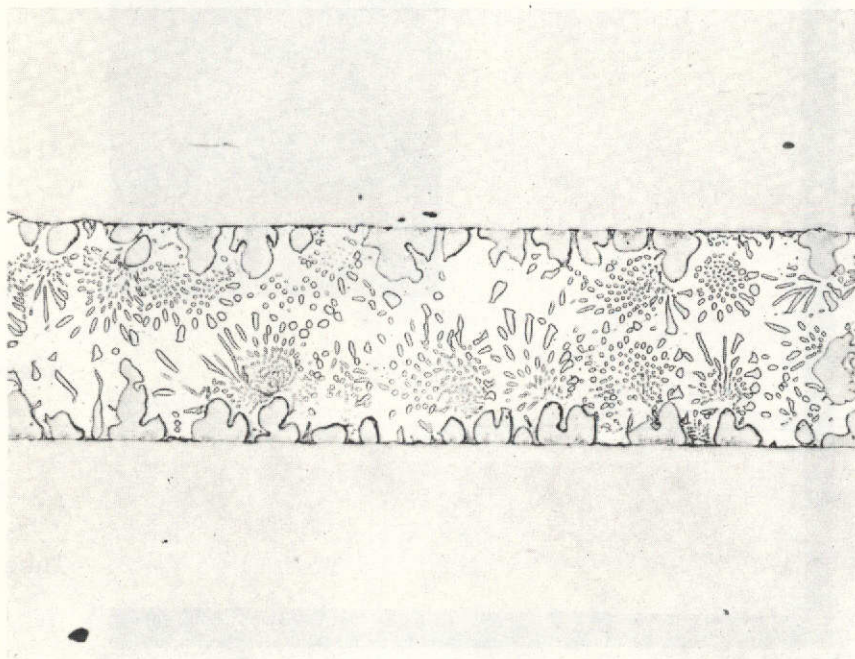


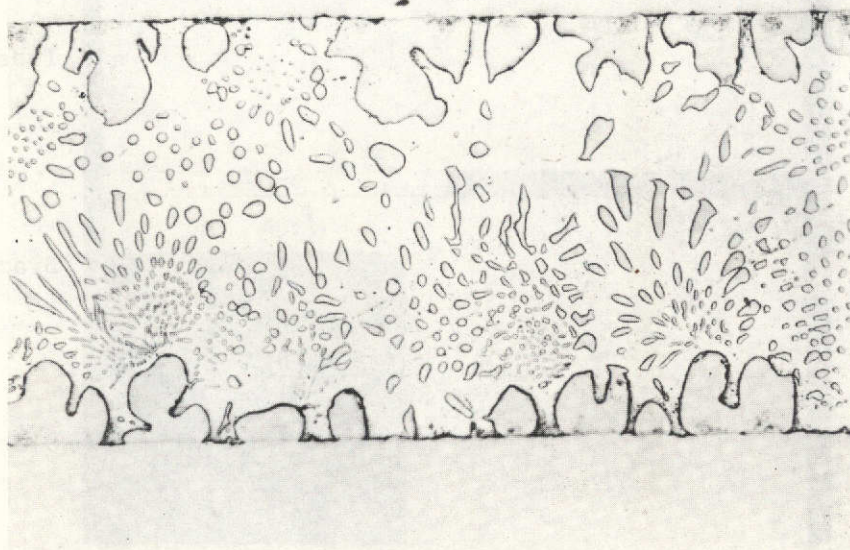
FIGURE II-3. MACROGRAPH OF SECTION MCS-1.1 (0 to 2.5 mm)



250X

As Polished

5G483

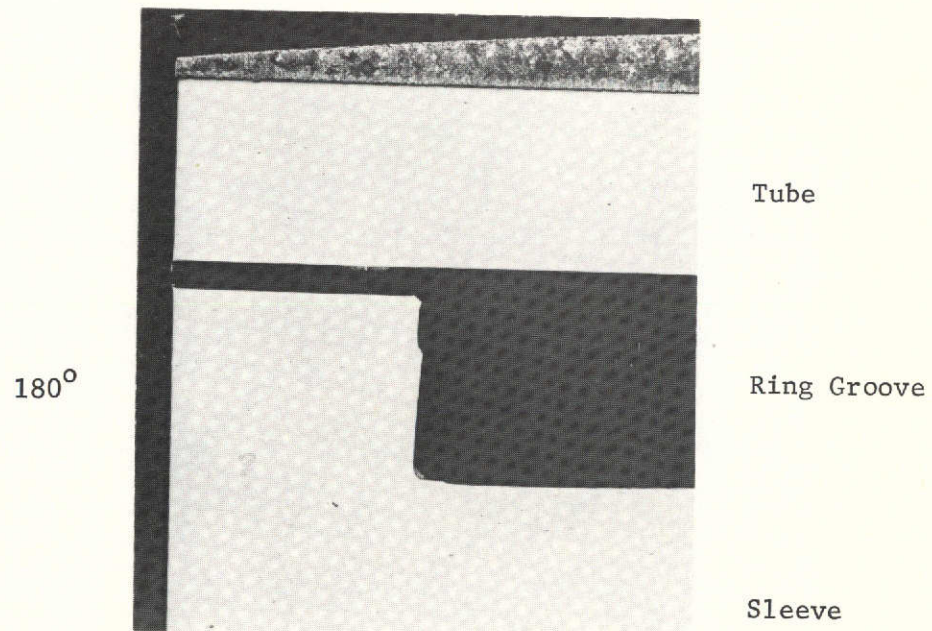
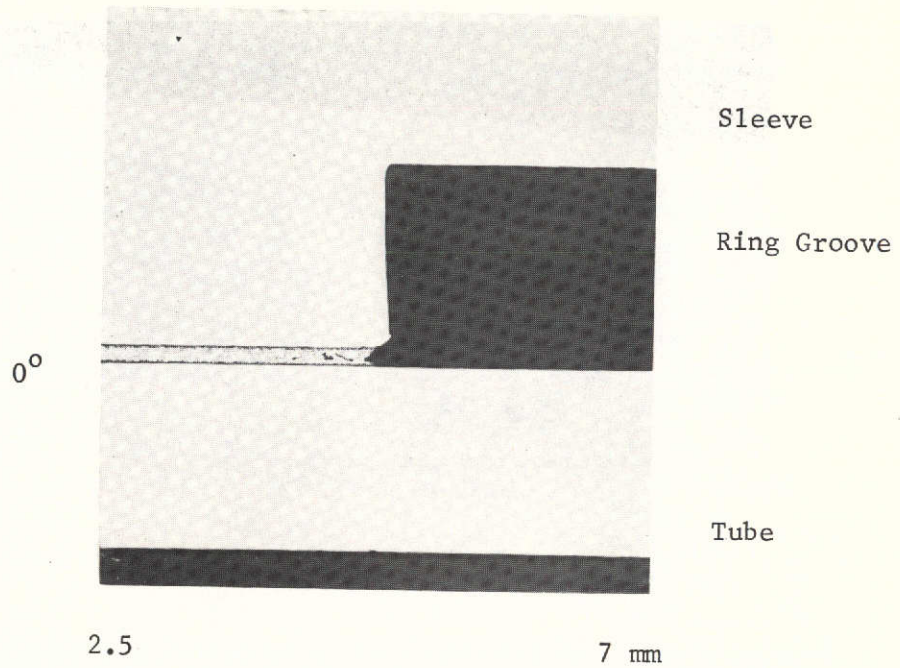


500X

As Polished

5G484

FIGURE II-4. MICROSTRUCTURE IN SECTION MCS-1.1 (1 mm)

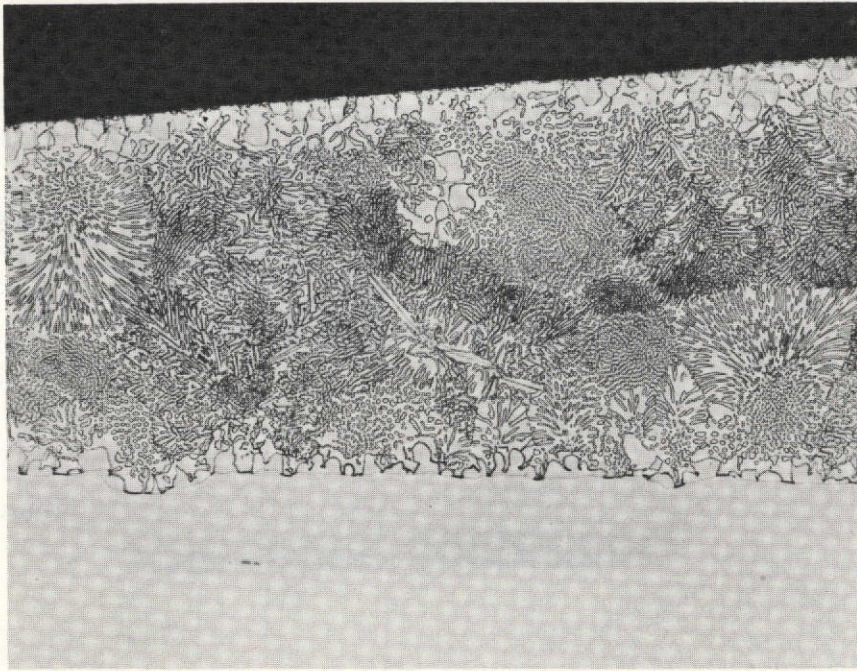


20X

As Polished

5G498

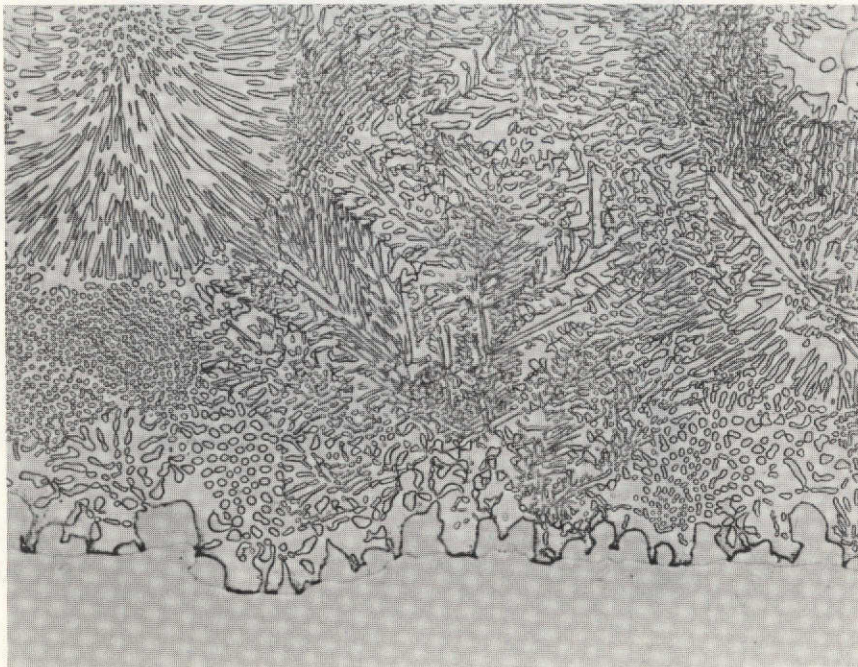
FIGURE II-5. APPEARANCE OF GAP AND RING GROOVE -
SECTION MCS-1.2 (2.5 - 7 mm)



250X

As Polished

5G485



500X

As Polished

5G486

FIGURE II-6. MICROSTRUCTURE OF BULK BRAZE ALLOY ON INSIDE SURFACE OF TUBE - SECTION MCS-1.2 (6 mm)

Section MCS-1-4

The full circumferential joint between the tube and the sleeve is shown at 4X in Figure II-7. The joint quality is generally excellent except for two void areas in the upper right-hand quadrant. Filler metal has accumulated at the bottom inside of the tube (the macrograph is slightly out of the orientation in which brazing occurred) and it has flowed to envelop the thermocouple.

A section of void area is shown at 100X in Figure II-8. The entire area between the joint interface appears to have been once filled with filler metal; the void occurred when filler metal drained from this area into others that were deficient in filler metal.

An area of the filler metal accumulated inside the tube is shown at 250X in Figure II-9. The microstructure of this area is somewhat different than that shown in Figure II-6; a dendritic phase is present in a matrix of filler metal. The amount of reaction between the base metal and molten filler metal is comparable in both areas.

One of the thermocouple wires is shown at 250X in Figure II-10. As indicated, filler metal flowed around the inside of the tube to encase these wires. Considerable reaction between the molten filler metal and the thermocouple wire occurred; the maximum depth of reaction is about 0.0008 inch.

Section MCS-1-8

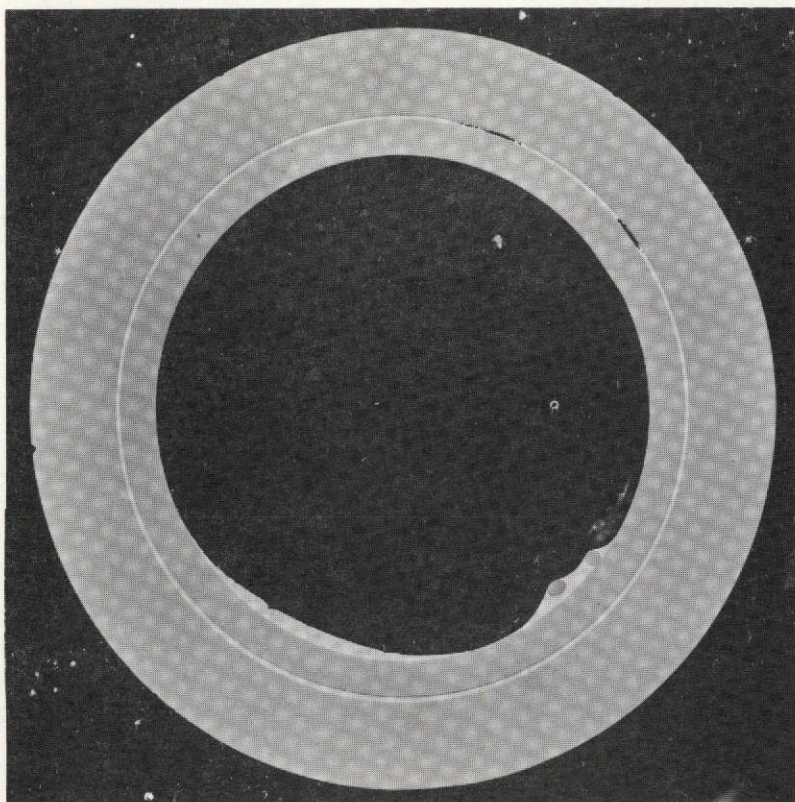
A section through the left-hand filler metal ring groove is shown at 4X in Figure II-11. The ring groove is empty; however, its surfaces are covered with a very thin film of filler metal. Filler metal has accumulated at the bottom inside of the tube. The microstructure of the accumulated filler metal is similar to that observed in other sections of this joint.

Sample MCS-2

Three representative sections from this sample were examined; their location and designation are indicated in Figure II-12. Two sections (MCS-2-4 and MCN-2-7) were cut and mounted to permit examination of the entire circumferential joint between the tube and sleeve, i.e., the surface perpendicular to the longitudinal axis of the sample. The other section (MCS-2-9) was cut and mounted so that the joint surfaces parallel to the longitudinal axis of the sample could be examined.

Section MCS-2-4

The full circumferential joint between the tube and sleeve is shown at 4X in Figure II-13. The joint quality was excellent and there

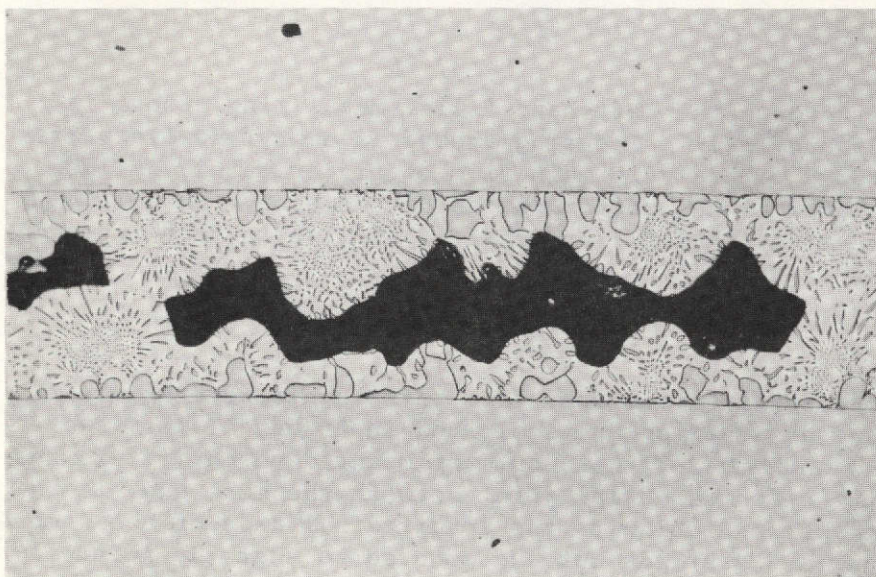


4X

As Polished

5G507

FIGURE II-7. MACROGRAPH OF SECTION MCS-1.4 (15 mm)

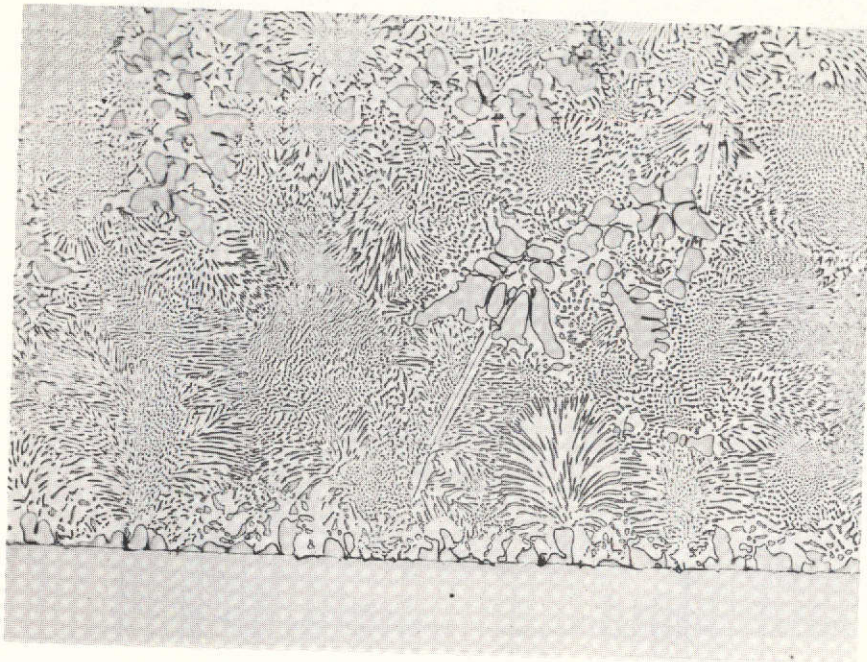


100X

As Polished

5G489

FIGURE II-8. SHRINKAGE VOIDS IN SECTION MCS-1.4 (15 mm)

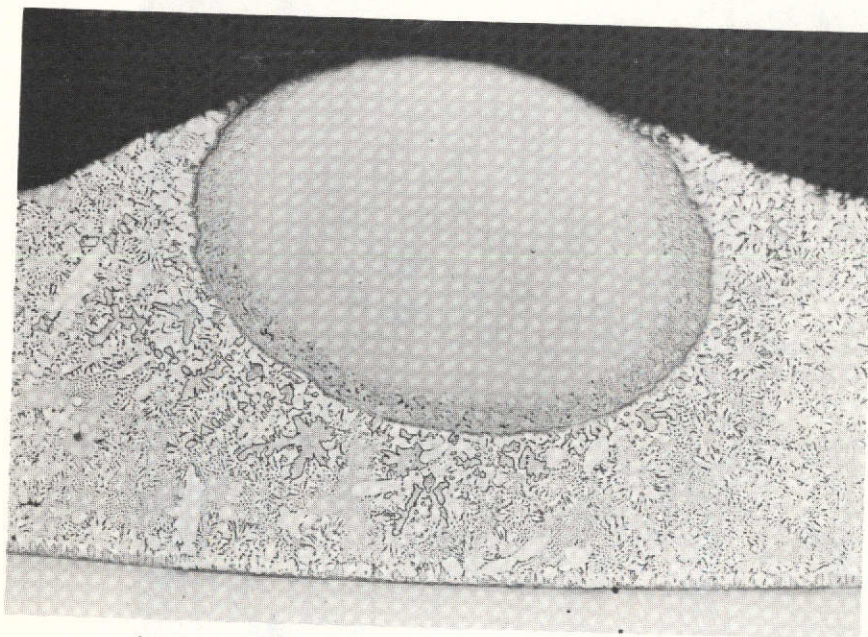


250X

As Polished

5G488

FIGURE II-9. MICROSTRUCTURE OF BULK ALLOY IN SECTION MCS-1.4 (15 mm)

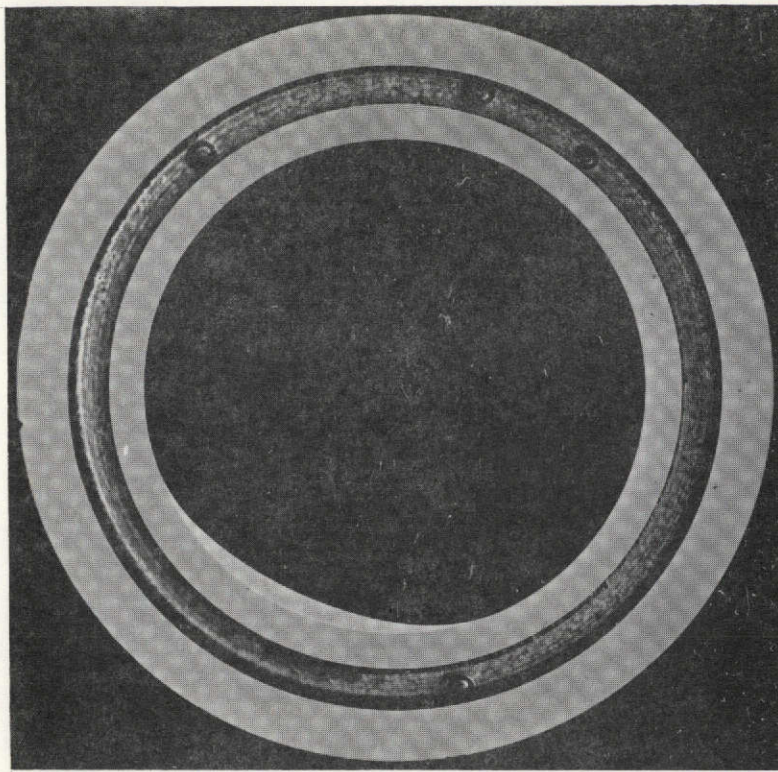


250X

As Polished

5G487

FIGURE II-10. THERMOCOUPLE WIRE BRAZED INTO SECTION MCS-1.4 (15 mm)

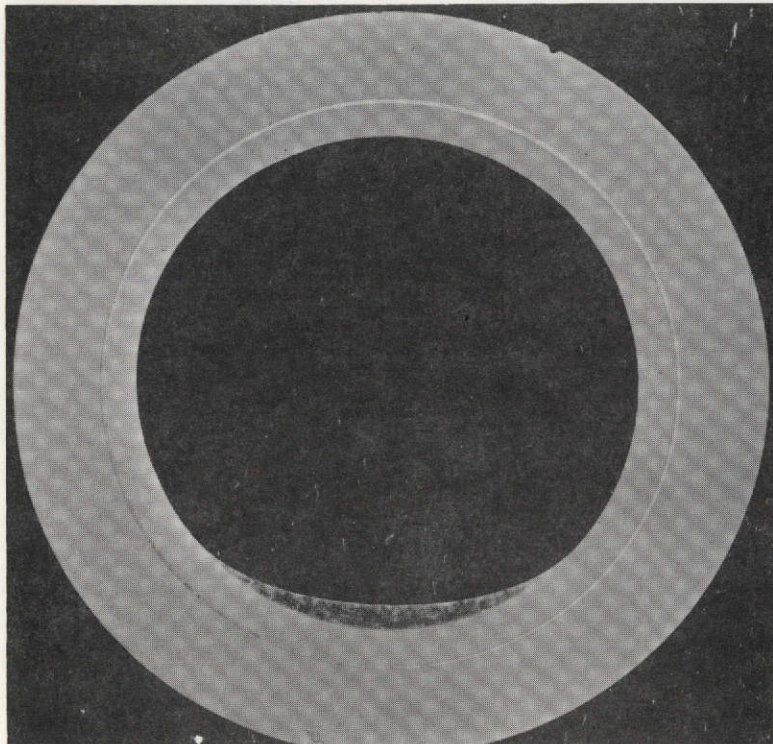


4X

As Polished

5G508

FIGURE II-11. RING GROOVE AREA IN SECTION MCS-1.8 (29 mm)



4X

As Polished

5G509

FIGURE II-13. CROSS SECTION MCS-2.5 (15 mm)

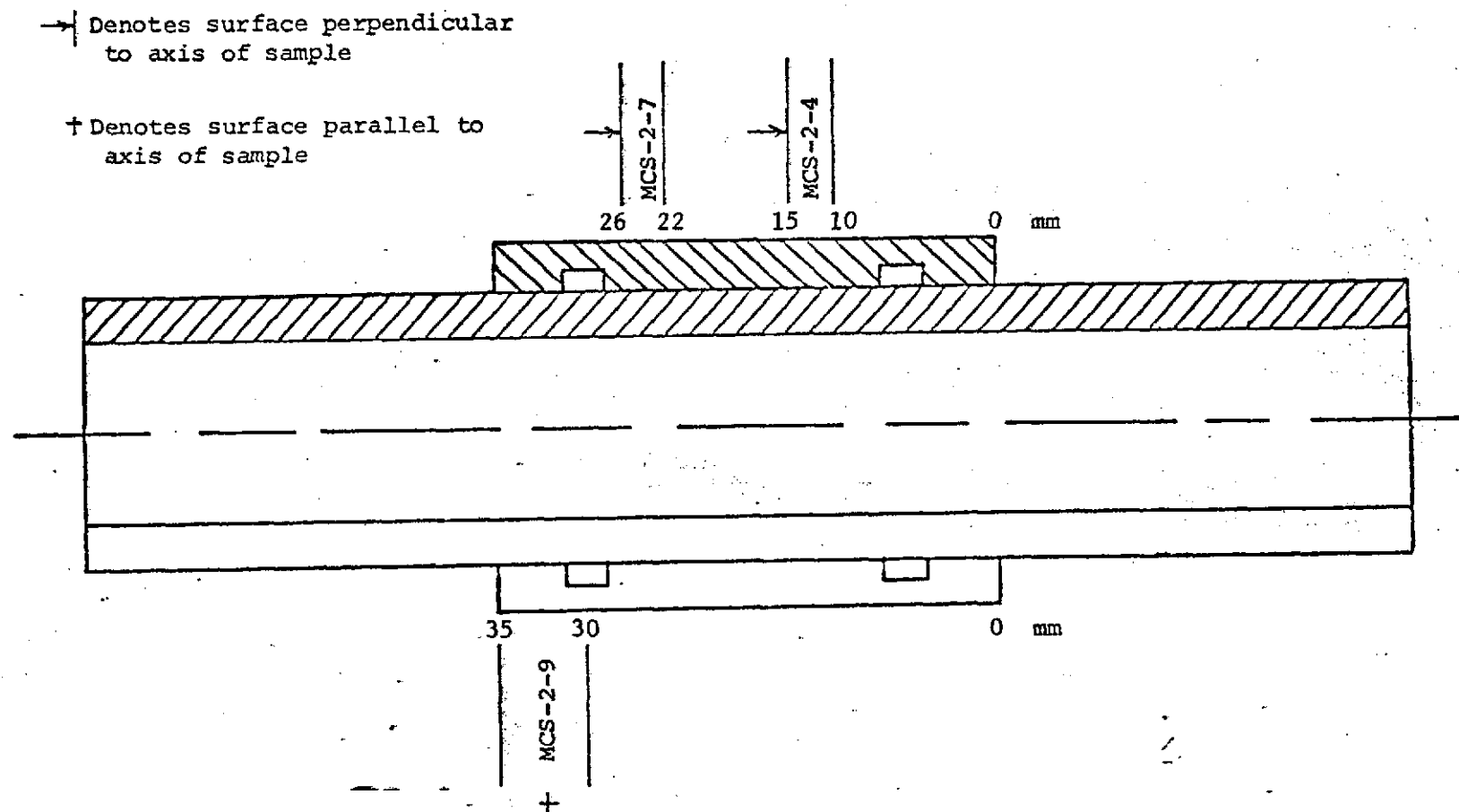


FIGURE II-12. SURFACES EXAMINED DURING METALLOGRAPHIC EVALUATION (MCS-2)

were no void areas of significance. A section of this joint is shown in the unetched condition at 250X in Figure II-14a; the same section is shown etched in Figure II-14b. The joint microstructure appears similar to those observed in sections from Sample MCS-1.

Filler metal has accumulated on the inside bottom of the tube. The microstructure of an area of accumulated filler metal is shown in Figure II-15 at 250X. There appears to be little reaction at the interface between the filler metal and base metal; the microstructure is comprised primarily of the silver-copper eutectic.

Section MCS-2-7

The circumferential joint between the tube and sleeve is shown at 4X in Figure II-16. Excellent flow of the filler metal during brazing occurred. The joint is completely filled; there were a few small isolated voids of little significance. Filler metal flowed through the slits in the center of the tube and accumulated in the bottom inside of the tube. As it did so, it brazed the thermocouple to the inside of the tube. The joint microstructure and the microstructure of the accumulated filler metal is similar to those observed previously.

Section MCS-2-9

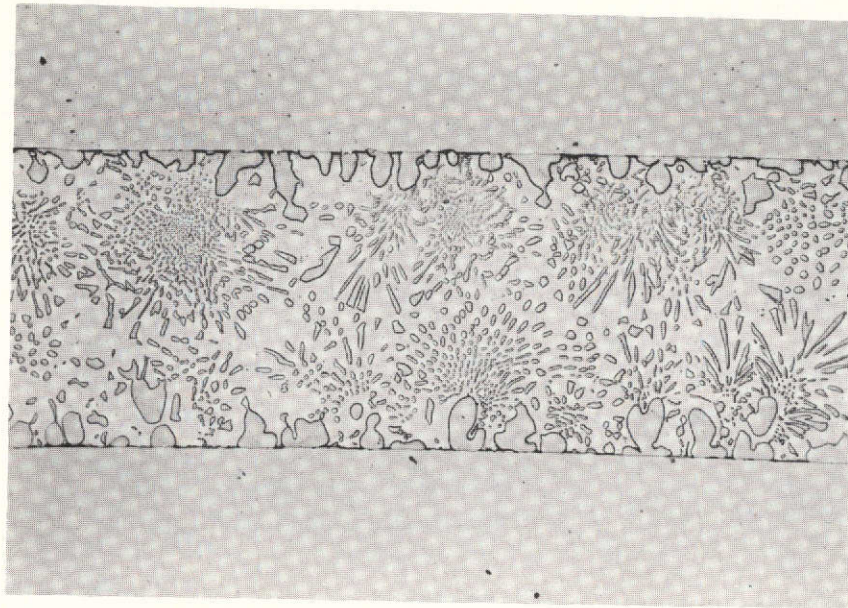
The lower half of the joint in this section is shown at 4X in Figure II-17. Excellent flow of the filler metal occurred during brazing; the joint between the tube and sleeve is completely filled and the insert is brazed into the remainder of the assembly. The filler metal ring groove is essentially empty. A few isolated voids are visible in the joint. The appearance of the upper section of this joint is similar to that shown in Figure II-17.

Sample MCS-3

Four sections representing typical joint areas in this tube assembly were examined metallographically; the location and designation of each section are shown in Figure II-18a. Three sections were cut and mounted to permit examination of the joint surfaces parallel to the longitudinal axis of the sample. The remaining section was mounted to permit examination of the entire circumferential joint.

Section MCS-3-2

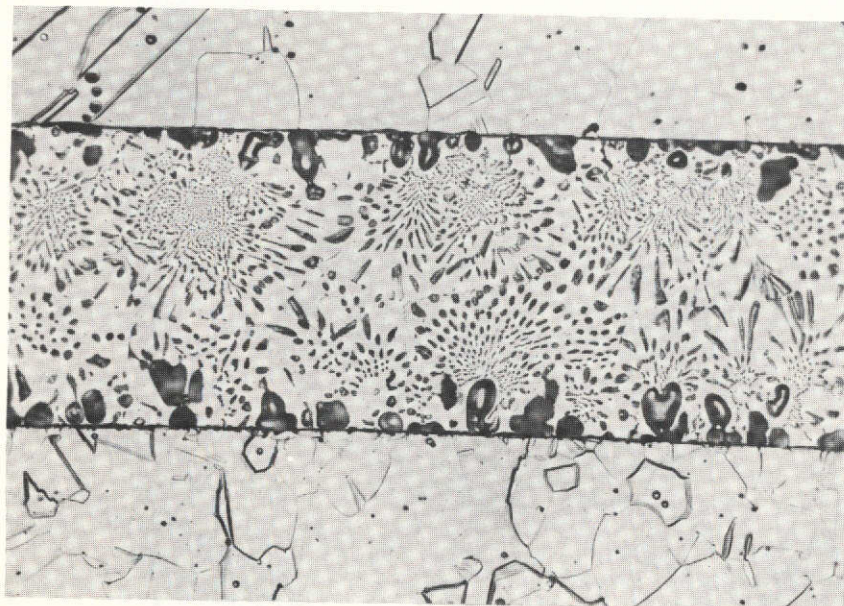
The lower half of this section is shown at 20X in Figure II-18b. The ring groove is essentially void except for some filler metal remaining in one corner. This section of joint between the tube and sleeve is completely void; however, the joint in the upper half of this section was well filled with filler metal. The presence of



250X

As Polished

5G491



250X

Etched

5G637

FIGURE II-14. MICROSTRUCTURE IN SECTION MCS-2.4 (15 mm)

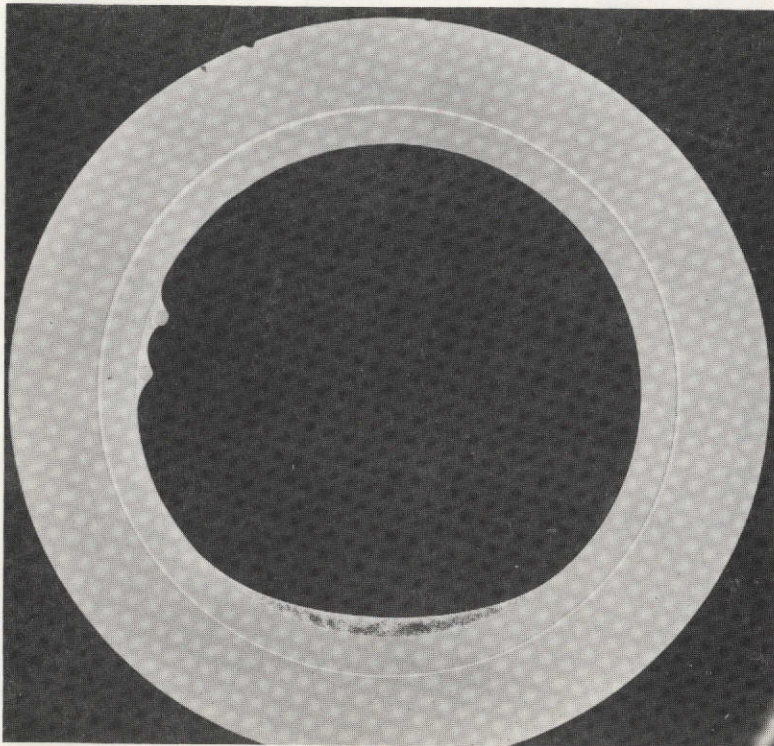


250X

As Polished

5G490

FIGURE II-15. MICROSTRUCTURE OF BULK FILLER METAL IN SECTION MCS-2.4 (15 mm)

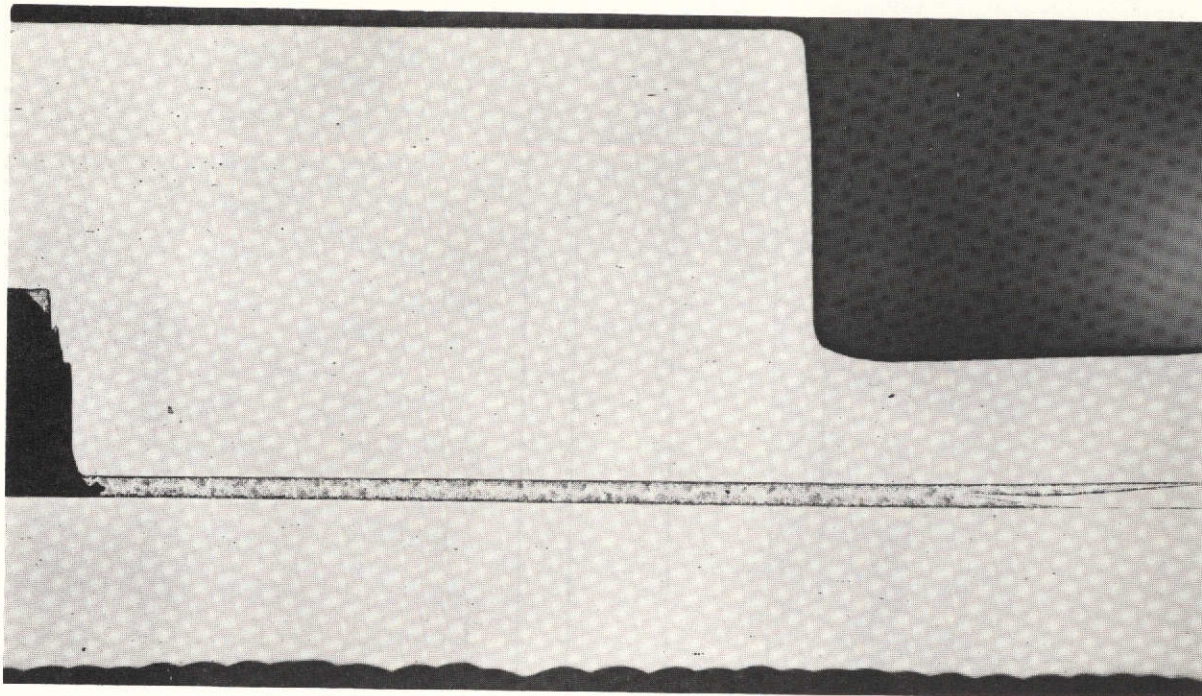


4X

As Polished

5G510

FIGURE II-16. CROSS SECTION MCS-2.7 (26 mm)



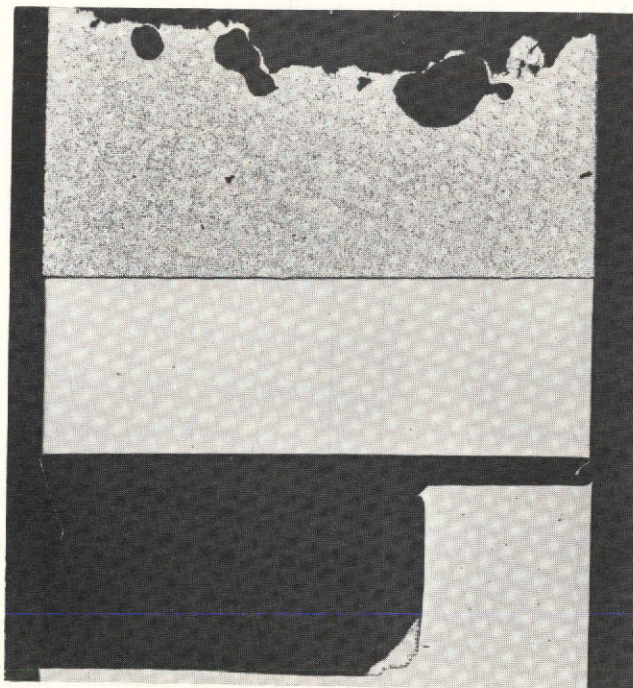
4X

5G503

FIGURE II-17. RADIAL SECTION MCS-2.9 AT 180° (30 to 35 mm)

6 mm

2 mm



20X

As Polished

5G500

Tube

Gap

Sleeve

FIGURE II-18b. RADIAL SECTION MCS-3.2 (2 to 6 mm)

→ Denotes surface perpendicular to axis of sample

+ Denotes surface parallel to axis of sample

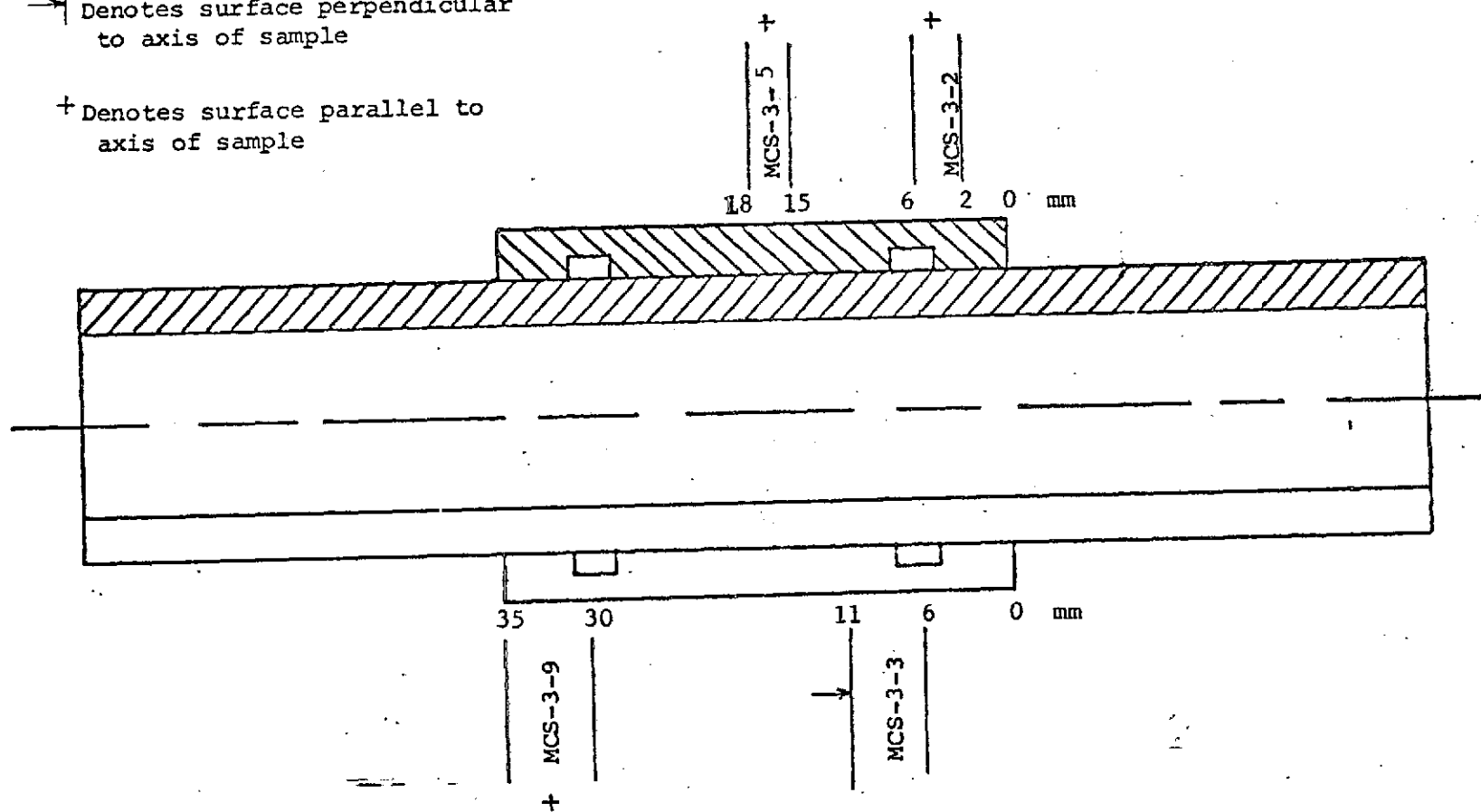


FIGURE II-18a. SURFACES EXAMINED DURING METALLOGRAPHIC EVALUATION (MCS-3)

voids in this area was indicated by radiography. As observed previously with Samples MCS-1 and MCS-2, filler metal accumulated on the bottom inside of the tube during brazing. However, the surface of the accumulated filler metal was extremely rough and there were numerous indications of voids or porosity. In contrast, the surface of the accumulated filler metal in the other two samples (MCS-1 and MCS-2) was very smooth. Due to an equipment malfunction, the maximum temperature to which Sample MCS-3 was heated during brazing was about 100 F (37.8 C) lower than the temperature to which the other samples were heated. Apparently, the surface roughness is associated with the manner in which the filler metal flowed and solidified.

Section MCS-3-3

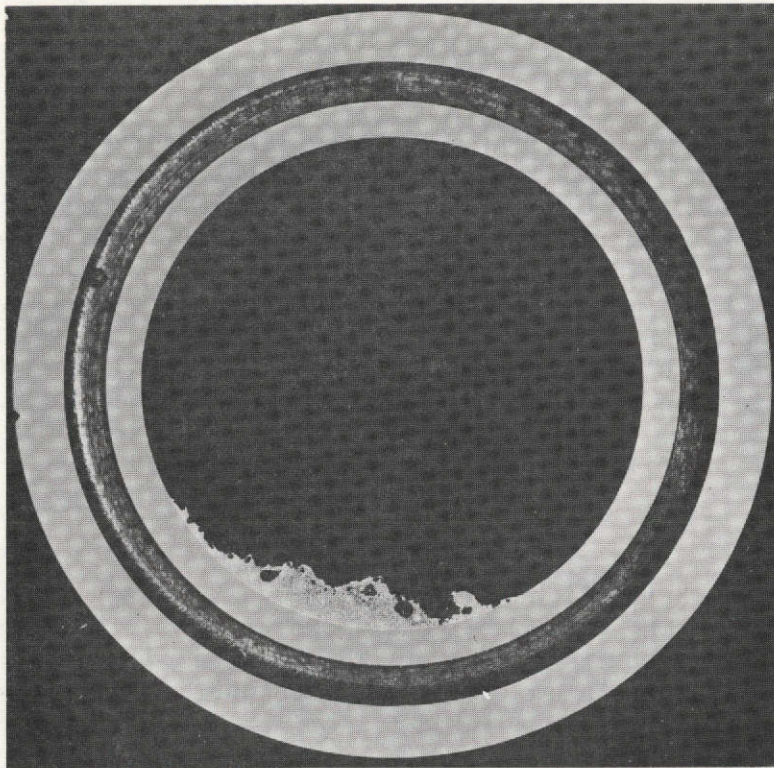
A section through the right-hand ring groove is shown at 4X in Figure II-19a. The ring groove is void; however, a thin film of filler metal was present on its surfaces. The surface roughness of the filler metal that accumulated inside the tube during brazing is clearly evident. An area of accumulated filler metal is shown at 100X in Figure II-19b. Voids or pores are present in this area. The microstructure of this area is somewhat different from that observed in similar sections from Samples MCS-1 and MCS-2. Although the maximum brazing temperature for Sample MCS-3 was less than it was for the other two samples, the products of the reaction between the base metal and the molten filler metal appear to be dispersed in larger amounts throughout the microstructure.

Section MCS-3-5

The upper and lower portions of the section adjacent to the slits in the center of the tube are shown at 20X in Figures II-20a and II-20b. In Figure II-20a, there is a more or less continuous void in the joint between the tube and sleeve. However, it appears that filler metal was present in this area, and that it drained away during the solidification process. The bottom joint, i.e., the area at the 6 o'clock position during brazing, was completely filled with filler metal (Figure II-20b). Filler metal has also accumulated inside the tube and along the wall of the slit; the slit is not visible in Figure II-20a because it is not continuous around the circumference of the tube.

Section MCS-3-9

The upper and lower sections of this joint are shown at 20X in Figures II-21a and II-21b; this section is located at the far left-hand side of the sample and it includes a portion of the filler metal ring groove. The joint between the tube and the sleeve is well brazed; there were a few isolated voids of no significance. The ring groove is essentially void. The surface roughness of the filler metal accumulated inside the tube is evident in Figure II-21b; numerous voids are present also.

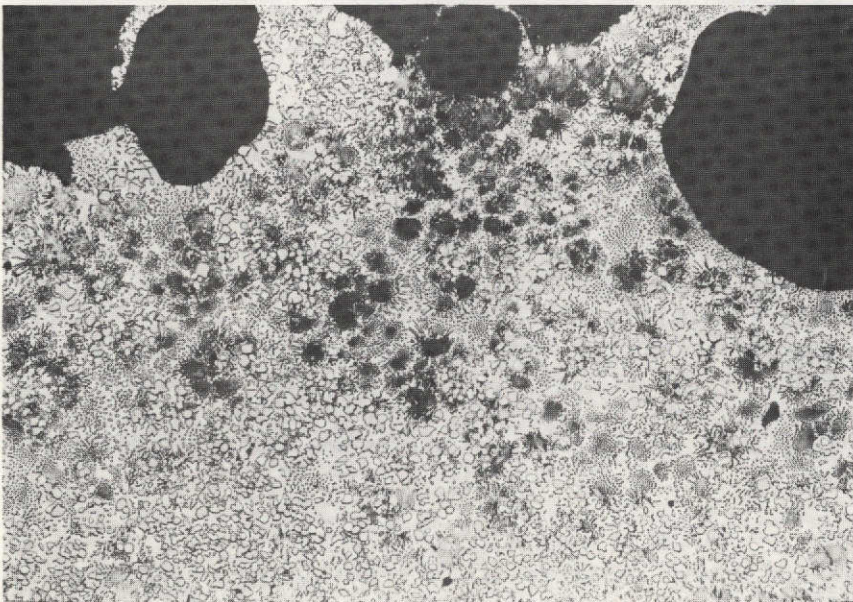


4X

As Polished

5G511

FIGURE II-19a. CROSS SECTION MCS-3.3 (11 mm)



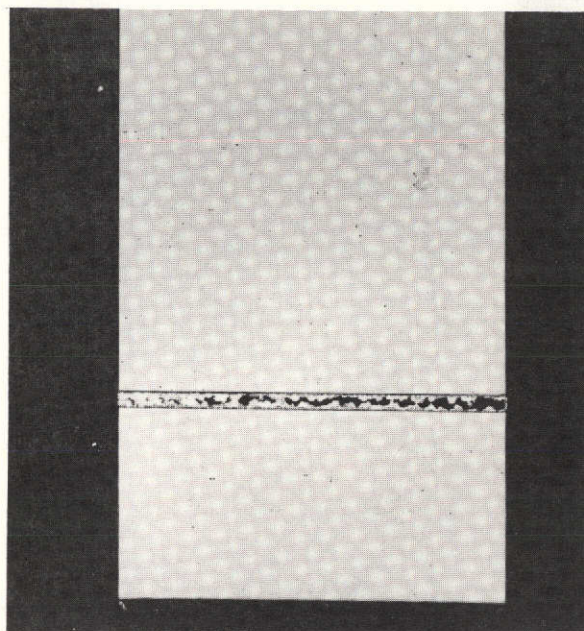
100X

As Polished

5G494

FIGURE II-19b. MICROSTRUCTURE OF BULK FILLER
METAL IN SECTION MCS-3.3 (11 mm)

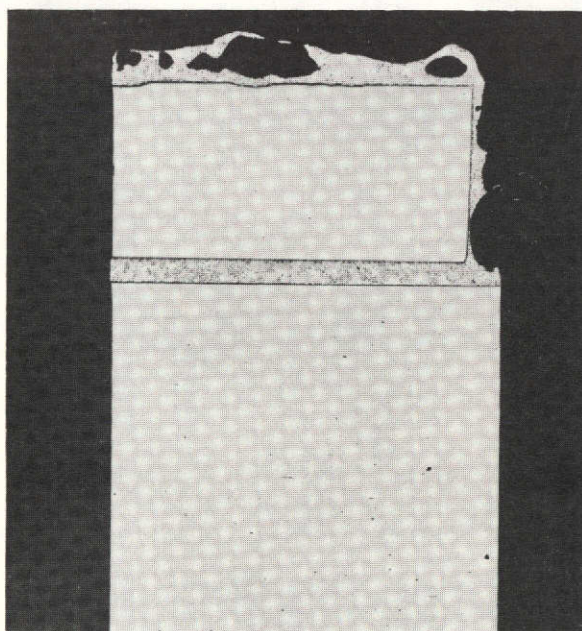
0°



18 mm

15 mm

180°

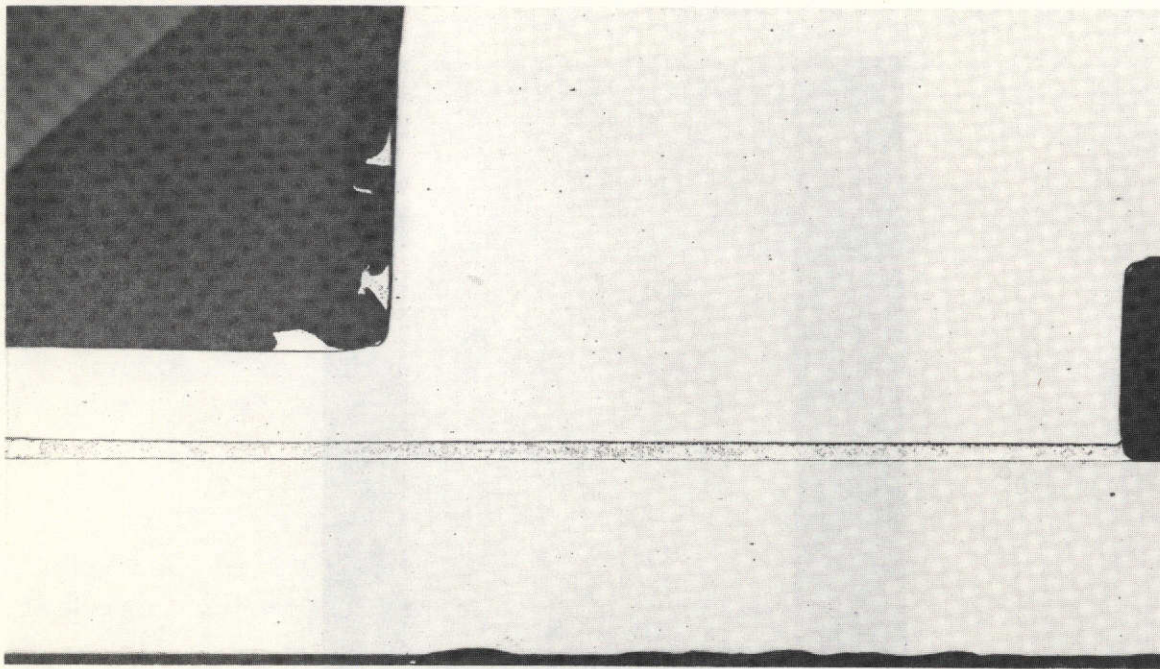


20X

As Polished

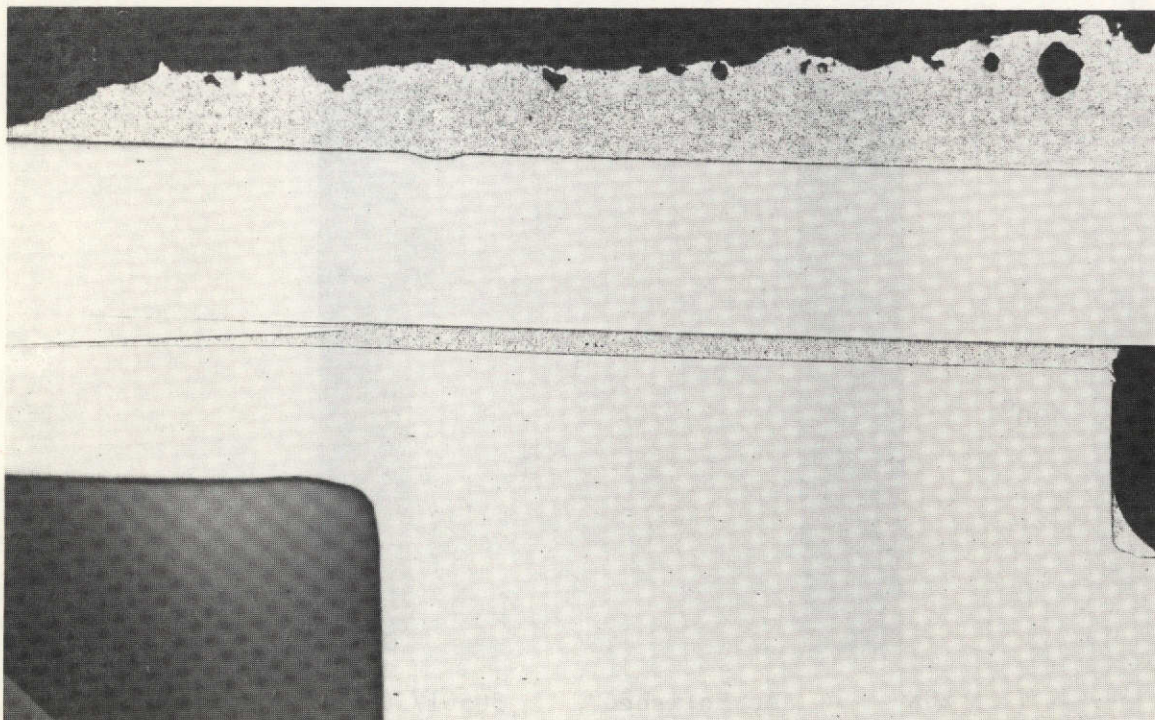
5G501/502

FIGURE II-20. RADIAL SECTION MCS-3.5 (15-18 mm)



35mm

30 mm



20X

As Polished

5G506/505

FIGURE II-21. RADIAL SECTIONS MCS-3.9 (30-35 mm)

MICROSTRUCTURAL STUDIES

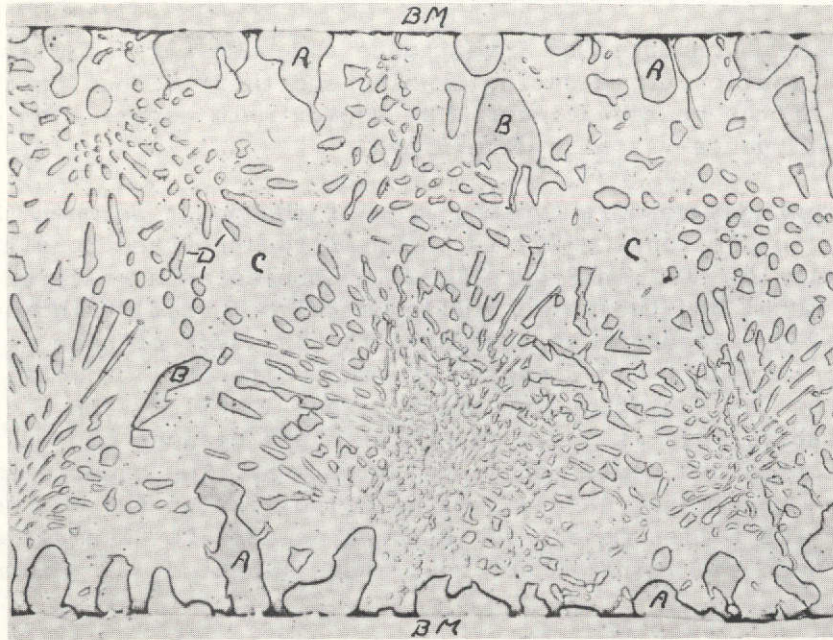
Studies were conducted to investigate the base metal-filler metal reactions that occurred during brazing and their effect on the microstructure of the brazed joints. The approximate composition of some phase constituents was also determined.

The microstructure of a typical area of the joint between the tube and sleeve in Section MCS-2-4 is shown in the unetched condition at a magnification of 500X in Figure II-22. Considerable reaction between the base metal and the molten filler metal occurred during brazing. In Section MCS-2-4, measurements indicated that a layer of base metal (about 0.0005 inch thick) was dissolved by the molten filler metal to form another phase at the joint interface (areas labelled A in Figure II-22). Presumably, this is a copper-nickel phase because copper and nickel form a continuous series of solid solutions. The other elements contained in the base metal have a limited solubility in the molten constituents of the filler metal. This phase appears to disperse also in the area between the joint interfaces (areas labelled B in Figure II-22).

The microstructure of the brazed joint was studied by electron microprobe analysis. An area* similar to that shown in Figure II-22 was scanned with the electron microprobe to determine the distribution of the elements in the filler metal (silver and copper) and the major elements in the 304L stainless steel base metal (nickel, chromium, and iron). The resulting X-ray images for these elements are shown in Figures II-23a through II-23e. By examining the variations in intensity that indicate the approximate concentration distribution of each element in the area being scanned, it was possible to estimate the approximate composition of phase constituents in the areas of interest. The results of these studies are discussed below.

- (1) The phase (A in Figure II-22) along the joint interface that was produced by dissolution of the base metal by the molten filler metal contained 73 percent (or more) copper, some silver (about 6 percent), and a small amount of nickel. Chromium and iron were not detected in this area.
- (2) The composition of the phases labelled B and D in Figure II-22 was almost identical to that of the phase labelled A. These particles resulted from the base metal-filler metal reaction and became detached as dissolution of the base metal progressed.
- (3) The light areas (C in Figure II-22) are composed of essentially pure silver.
- (4) The presence of nickel, chromium, and iron in the base metal (E in Figure II-22) is indicated by the X-ray images for these elements.

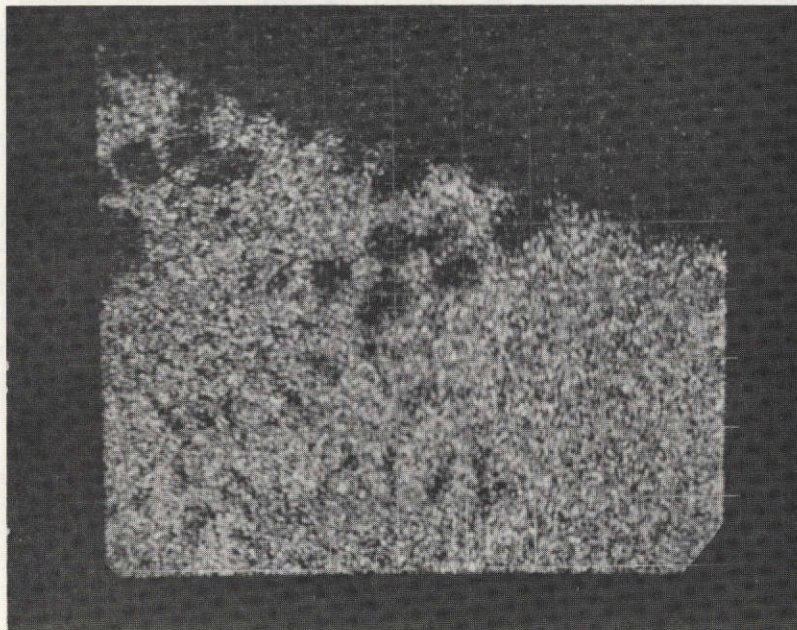
* The area scanned by the electron microprobe differed slightly from that shown in Figure II-22, because the specimen was repolished before study. However, the area scanned contained the features indicated in this figure.



500X

5G492

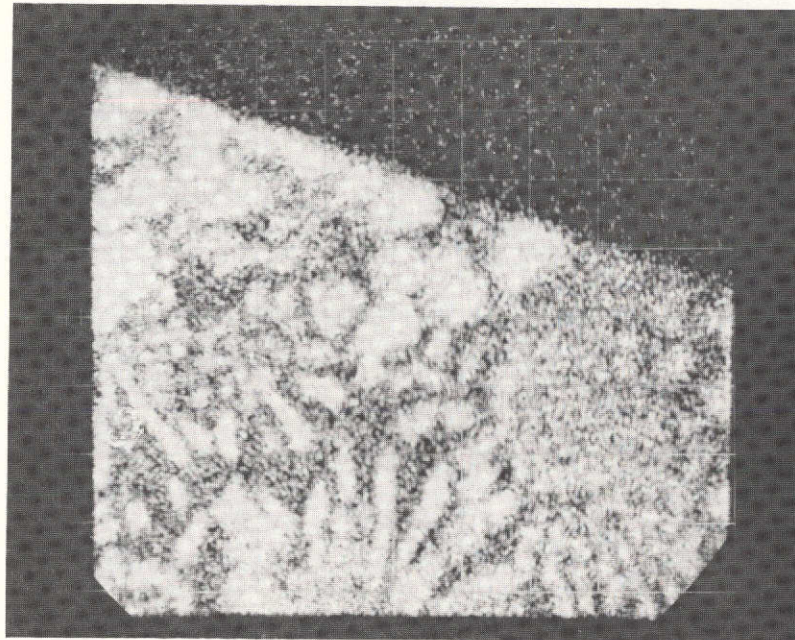
FIGURE II-22. PHASES PRESENT IN SECTION MCS-2.4



300X

11476

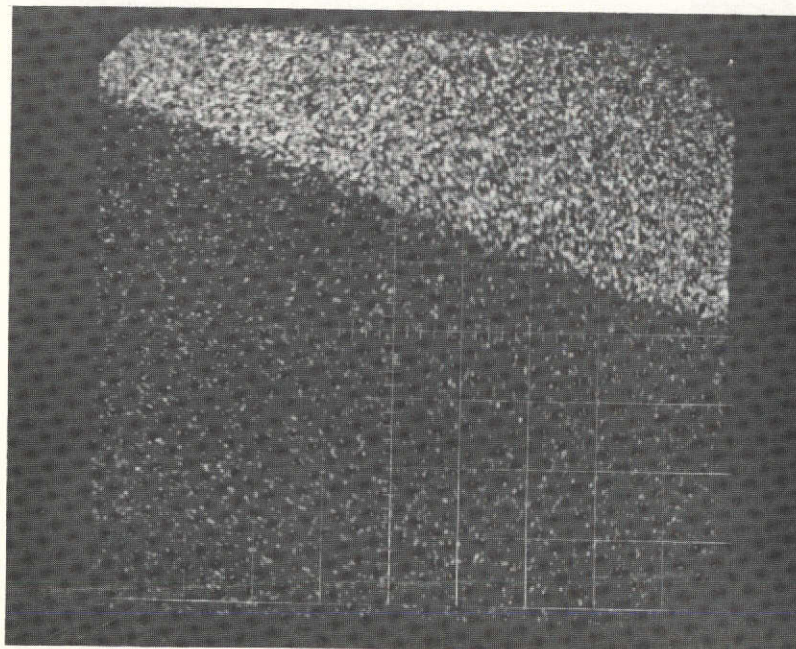
FIGURE II-23a. SECTION MCS-2.4 - SILVER X-RAY IMAGE



~ 300X

11478

FIGURE II-23b. SECTION MCS-2.4 - COPPER X-RAY IMAGE

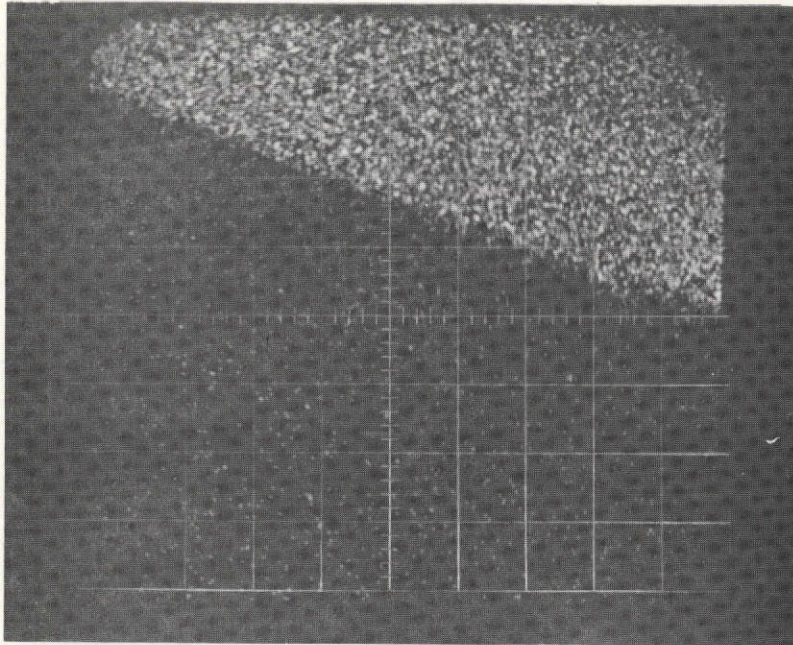


~ 300X

11479

FIGURE II-23b. SECTION MCS-2.4 - NICKEL X-RAY IMAGE

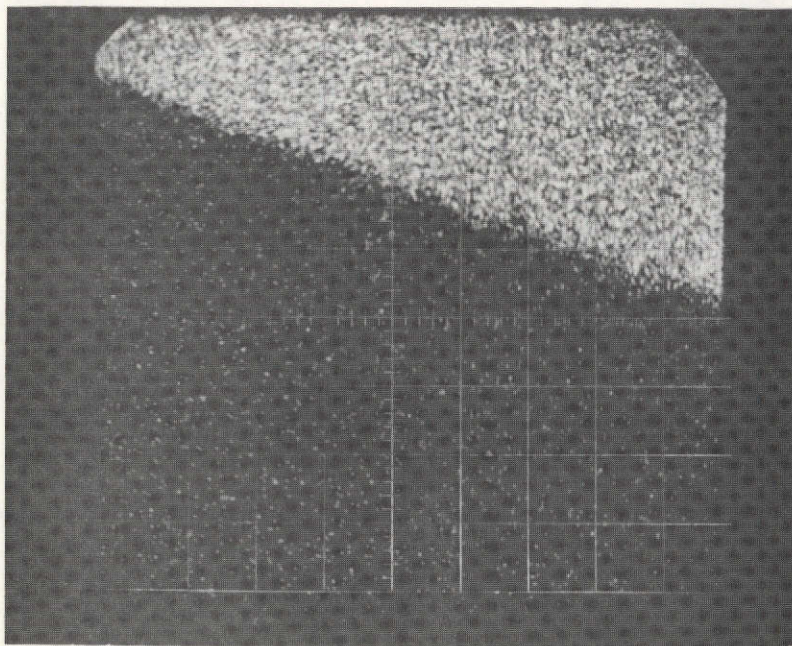
REPRODUCIBILITY OF THE
ORIGINAL PAGE IS POOR



~ 300X

11477

FIGURE II-23d. SECTION MCS-2.4 - CHROMIUM X-RAY IMAGE



~ 300X

11475

FIGURE II-23e. SECTION MCS-2.4 - IRON X-RAY IMAGE

SECTION III

EVALUATION OF SKYLAB SAMPLES

A detailed examination of two of the brazed specimens processed on Skylab was conducted. Specimen SLS-1 was a stainless steel assembly similar to the ground characterization samples described in Section II. Specimen SLN-2 was a nickel assembly similar to the ground characterization samples described in Section I. Specimens SLS-2 and SLN-4 were examined at the University of Wisconsin after some processing at Battelle and ORNL.

MATERIAL TRANSFER

Specimens SLS-1 and SLS-3 were hand carried to Battelle following a meeting at MSFC on July 18. Specimens SLN-2 and SLN-4 (after sectioning) were picked up at ORNL on August 20. Specimen SLN-4 was delivered to the University of Wisconsin on August 21. Specimen SLS-3, after sectioning at Battelle, was given to the University of Wisconsin on August 2.

SPECIMEN PROCESSING

Processing of the specimens followed the procedures previously developed and demonstrated in processing ground characterization samples. Examination of the radiographs taken at MSFC did not provide definite proof of the braze extent in Specimen SLS-1. A leak test was required to establish if brazing had occurred. Specimens SLS-1 and SLS-3 were attached to a helium mass spectrometer at one end of the tube. A rubber stopper was inserted in the opposite end of the tube. Tests were then run for leakage through the annular braze joint. The mass spectrometer used had previously been calibrated to 1.08×10^{-11} atm sec. No leak was detected in SLS-1. Leakage occurred in SLS-3 as expected based on the radiographic appearance. The leak tests showed that the apparent lack of voids shown in the radiograph of Specimen SLS-1 was a proper interpretation.

Both specimens were then centered in a lathe for marking of sectioning planes. Centering was with a tapered rod on the ID of the tube. SLS-3 was marked routinely. However, complete circumferential scribe marks could not be made on SLS-1. A few measurements were then made to determine the extent of offset or out of roundness. The tube showed 0.003-in. TIR at the igniter end and 0.005-in. TIR at the opposite end. TIR on the sleeve ranged from 0.010 to 0.013 in. An

additional longitudinal scribe line was added to the sleeve to assist in subsequent orientation. This line is at an angle to the original groove, being closest at the igniter end.

Radial cuts were then made to section the specimens into thin washer-like pieces. The locations of these cuts is tabulated in Table 1. Also indicated are longitudinal cuts made to expose ring groove areas.

Cut sections of Specimens SLS-1 and SLS-2 were mounted and polished for detailed examination.

All sections were examined at low and high power magnification to determine (1) visual appearance of the braze, (2) confirm radiographic findings, and (3) select sections for metallographic examination. Results are discussed below.

Specimen SLS-1

The tube-sleeve assembly was almost a perfectly void-free braze from end to end. Braze filler metal was evident around the entire joint circumference in each section. The only void area apparent in the radiograph (just below the top ring groove at Position F) was exposed in Section 1.7.1. Excess filler metal flowed through the center slits and collected inside the tube between about 80 degrees and 235 degrees, and 270 degrees and 10 degrees. The ring grooves were generally empty of filler metal except for a small bridge in the igniter end groove at Position B.

The most notable observation was wide variations in the braze gap of all sections between the ring grooves. This is discussed in more detail later.

Figure III-1 shows the appearance at 3 mm (1.2). This section is between the igniter end of the sleeve and the adjacent ring groove. Sections at 0, 31, and 35 mm were similar in appearance. Some idea of the gap variations is evident: compare the thickness at 45 degrees and 235 degrees. A very small void is present at 235 degrees.

Figure III-2 shows the section at 14 mm and was generally typical of other sections between the ring grooves at 19 and 23 mm. Both the variation in gap width and braze alloy inside the tube are seen readily.

The longitudinal sections of the igniter end ring groove are shown in Figure III-3. Excellent fill of the gap area has occurred. Also, fillets have been retained both at the ends of the gap and in the remote corners of the ring groove. Portions of the excess filler metal inside the tube are also seen. Some narrowing of the joint gap at the 10-mm plane is apparent.

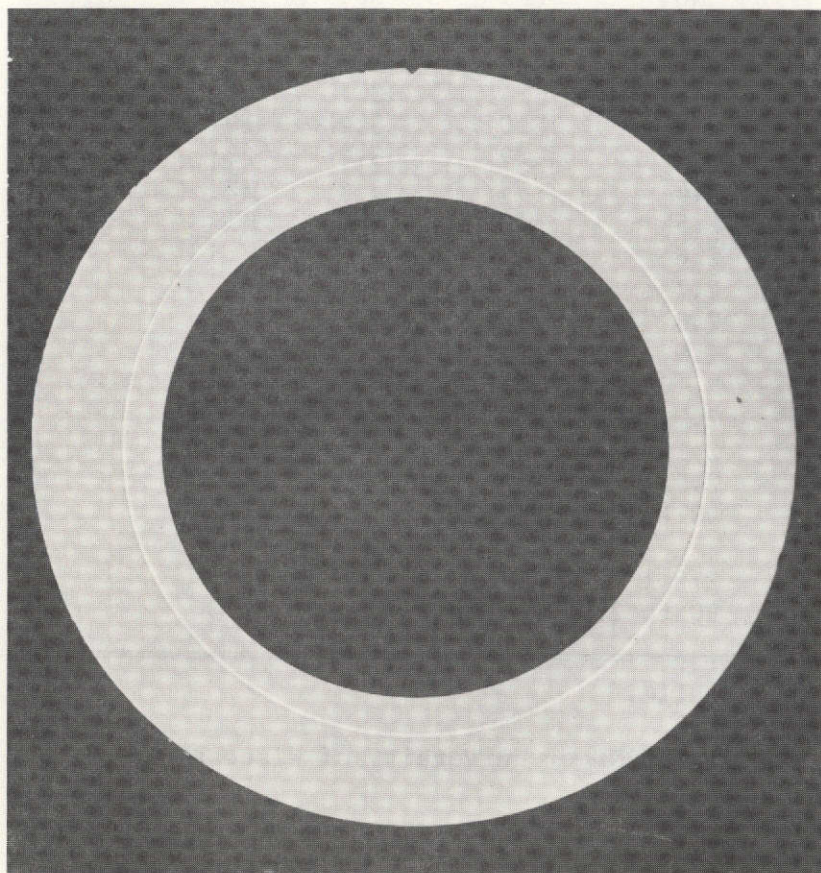
TABLE III-1. LOCATION OF SECTIONING PLANES - SKYLAB SPECIMENS-M552

Specimen SLS-1(a)		Specimen SLN-2(b)		Specimen SLS-3(a)		Specimen SLN-4(b,c)	
<u>No.</u>	<u>MM.</u>	<u>No.</u>	<u>MM.</u>	<u>No.</u>	<u>MM.</u>	<u>No.</u>	<u>MM.</u>
	-4		-8		0		
1.1	0	2.1	-4	3.1	3		
1.2	3	2.2	0	3.2	10		
1.3	10	2.3	2	3.3	24		
1.4	14	2.4	5	3.4	32		
1.5	19	2.5	10	3.5	35		
1.6	23	2.6	15				
1.7	31	2.7	20				
1.8	35	2.8	25				
1.9	39	2.9	31				
1.10	43	2.10	35				
		2.11	38				
		2.12	42				
1.3.1	3.5/10	2.5.1	5.5/10				
0 to 180 degrees		90 to 270 degrees					
1.7.1	23.5/31	2.9.1	25.5/31				
30 to 210 degrees		90 to 270 degrees					

(a) Sectioned at Battelle.

(b) Sectioned at ORNL.

(c) Data available from ORNL or University of Wisconsin.

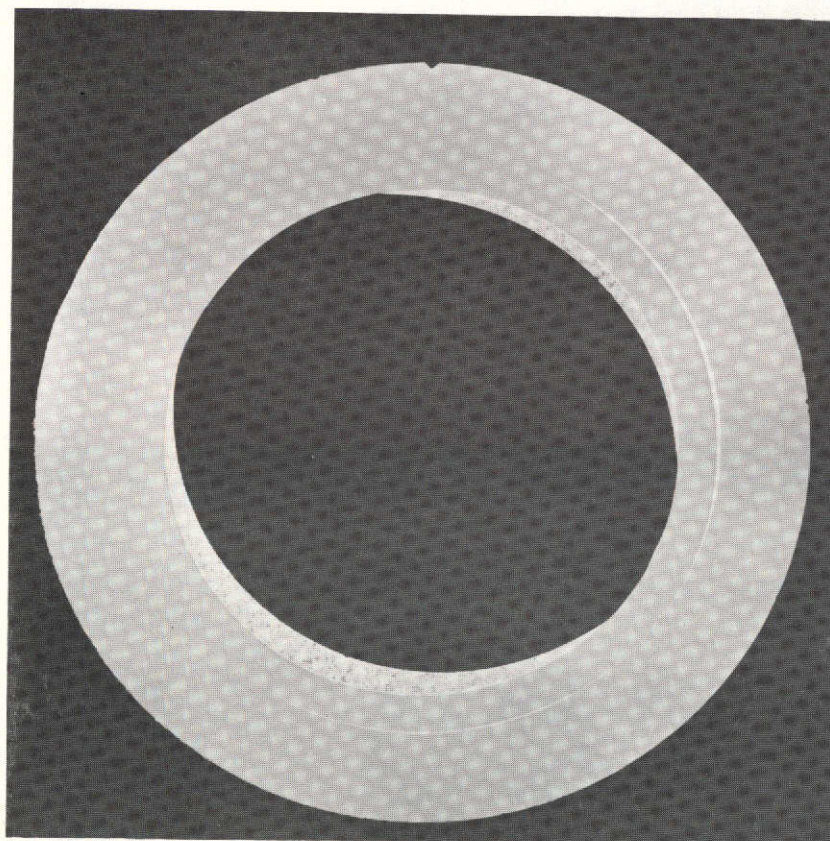


4X

As Polished

7G867

FIGURE III-1. CROSS SECTION SLS-1.2 (3 mm)

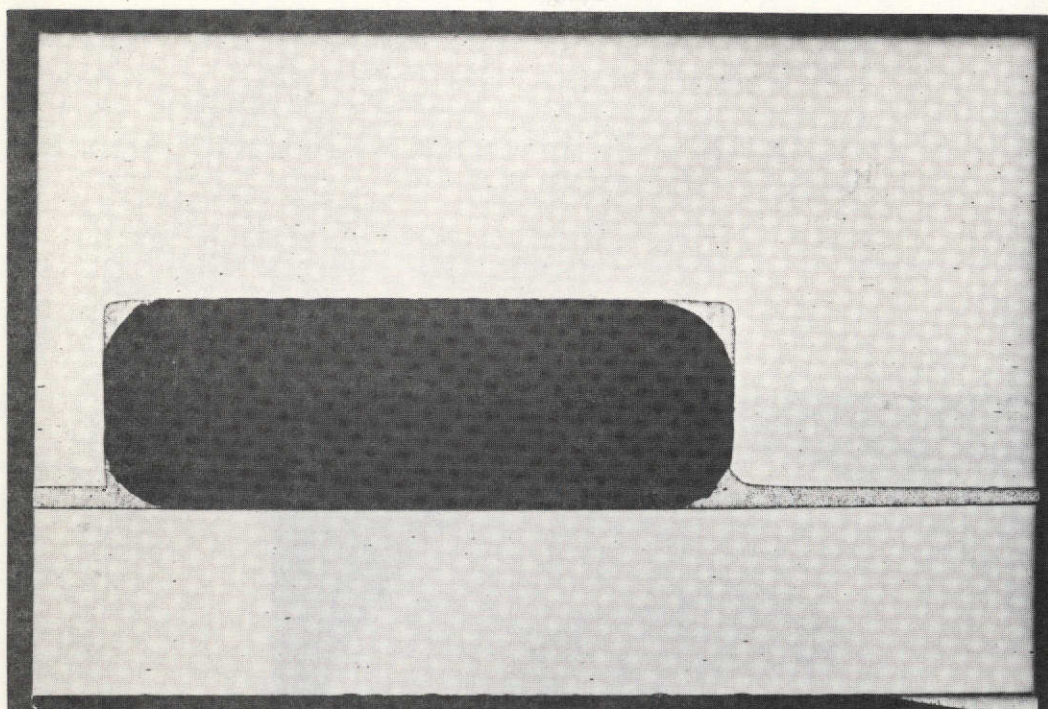


4X

As Polished

7G868

FIGURE III-2. CROSS SECTION SLS-1.4 (14 mm)

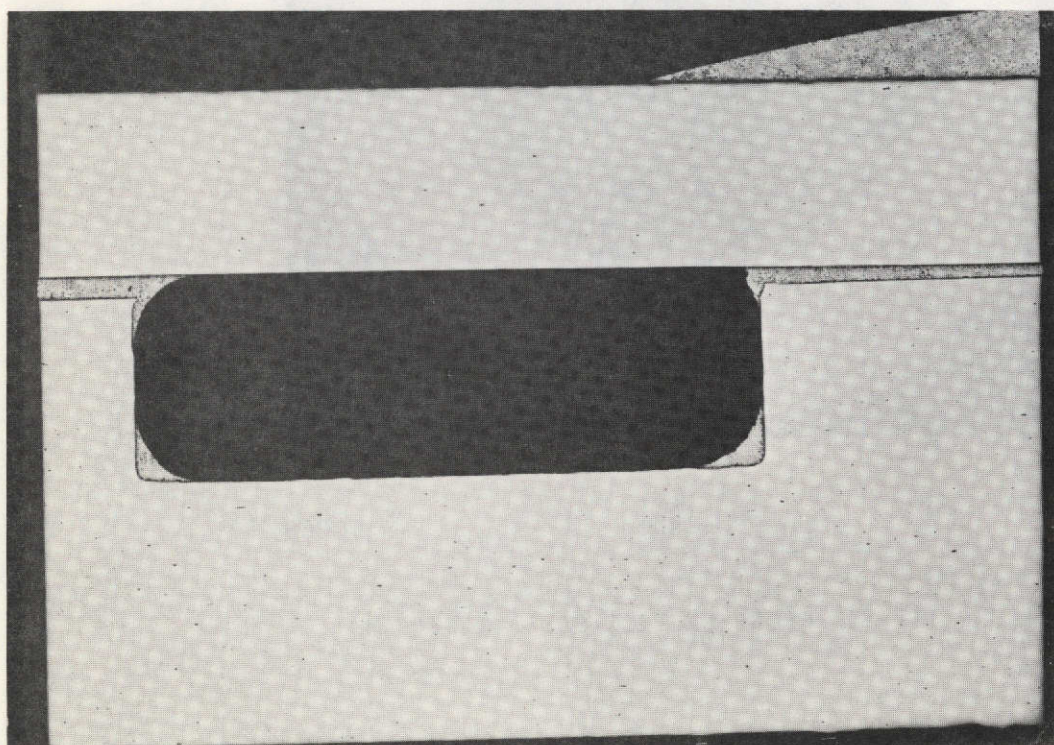


0°

3.5 mm

Tube Inner Surface

10 mm



180°

20X

As Polished

7G869

7G870

FIGURE III-3. RADIAL SECTIONS THROUGH IGNITER RING GROOVE
SLS-1.3 (3.5 to 10 mm)

The longitudinal section at 30 degrees between 23.5 and 31 mm is shown in Figure III-4. This section was taken through the only area containing an apparent void on the radiograph. The void area is confirmed. Again, good fillets were retained in the ring groove except where insufficient alloy was available next to the void. Higher magnification views of the void region show the typical appearance of a shrinkage void caused by draining of some of the final liquid to other regions during final solidification.

Microstructures

The braze region microstructure is shown in Figure III-5 at 250 and 500X. The phases present are essentially identical to those observed in the ground characterization specimens. The discrete particle phases are very high copper with some silver present. The matrix phase is essentially pure silver. A small amount of nickel from the stainless steel has reacted with the braze alloy and is present in the larger second phase particles.

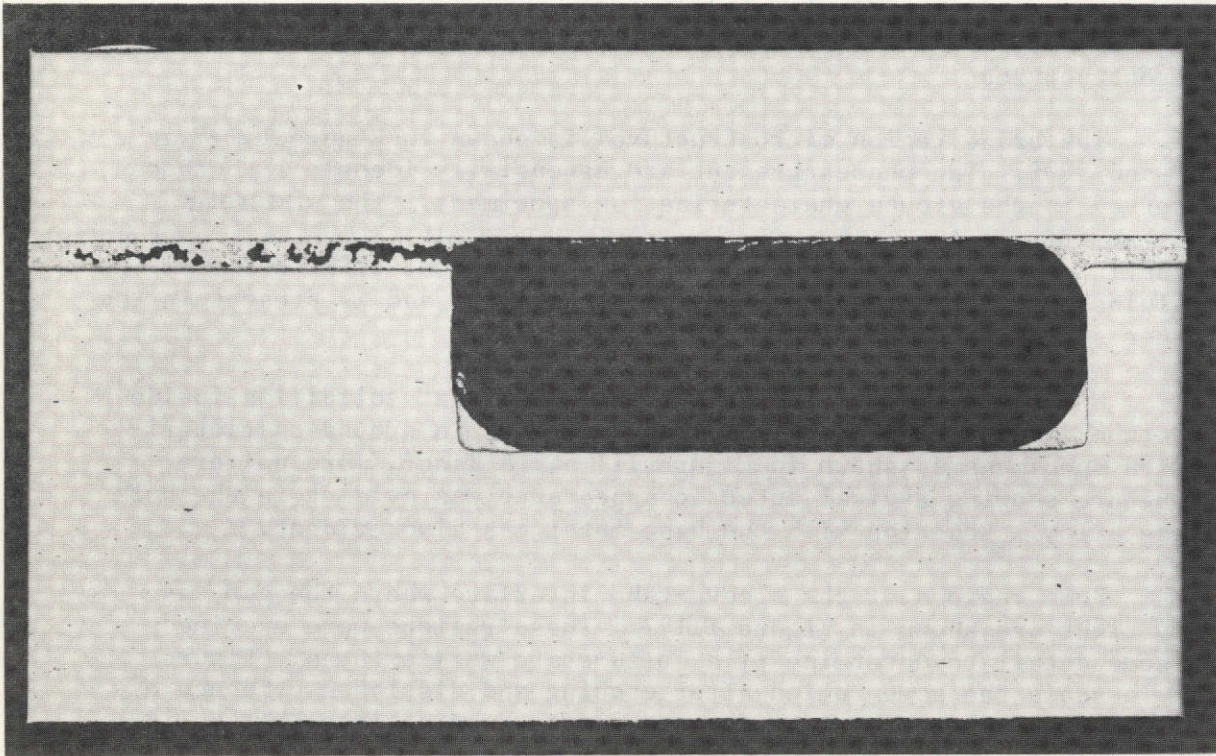
Microstructure of the bulk braze alloy that solidified inside the tube is also similar to comparable regions in ground characterization specimens as shown in Figure III-6. A finer, more uniform structure showing typical eutectic appearance was evident in the bulk braze alloy. Reaction with the base metal was also evident.

Some regions of the sleeve-tube interface where the gap was very tight are shown in Figure III-7. These regions were examined in some detail to determine if a solid-state weld existed. Figure III-7b shows the same region after etching and discloses evidence of grain growth across the interface needed to substantiate that solid-state welding (diffusion bonding) did indeed occur.

Microstructures in the area containing a void are shown in Figure III-8. The void shape is similar to that of comparable regions examined in ground characterization specimens. The voids are a result of draining of the area during the last stages of solidification.

Gap Variation Studies

Measurements of both the joint gap and diameters at various points were made in attempts to resolve the gap variations observed. The joint gap measurements are shown in Table III-2. The measured gap ranged from 0 to a maximum of 0.007 in., with most measurements being less than the intended 0.005-in. gap. Average gaps at each sectioning plane are plotted in Figure III-9, to better illustrate this variation. Diameter measurements of individual sections indicated some minor out of round conditions, but were not helpful in establishing the basic cause of the gap variations.

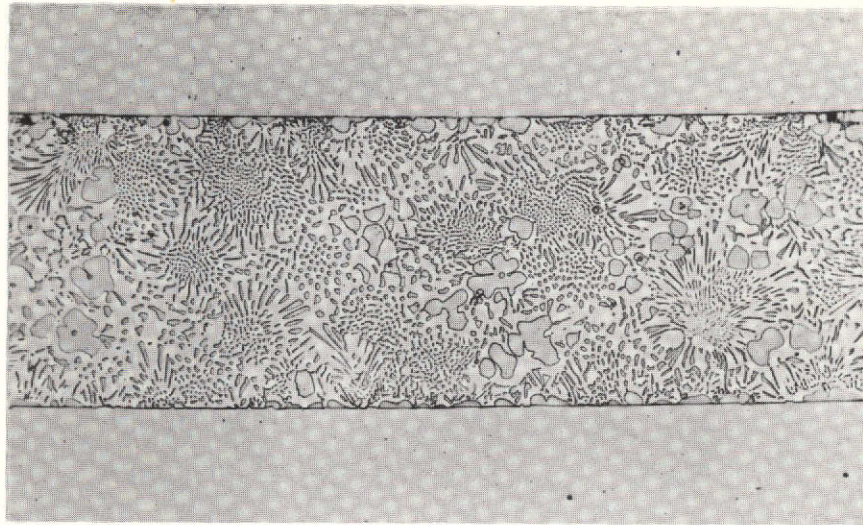


20X

As Polished

7G871

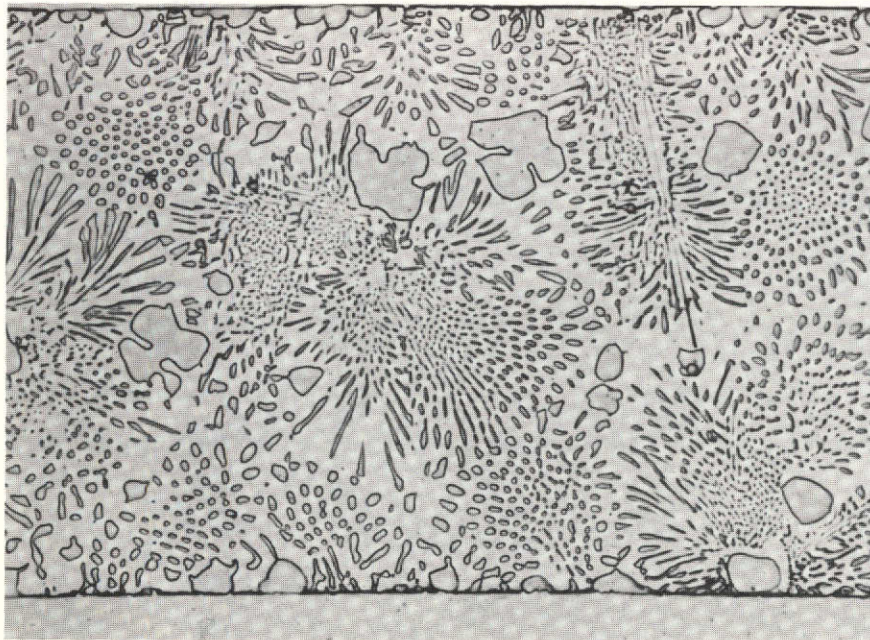
FIGURE III-4. RADIAL SECTION OF RING GROOVE AREA -
SLS-1.7.1 (23.5 to 31 mm and 210°)



250X

As Polished

7G853

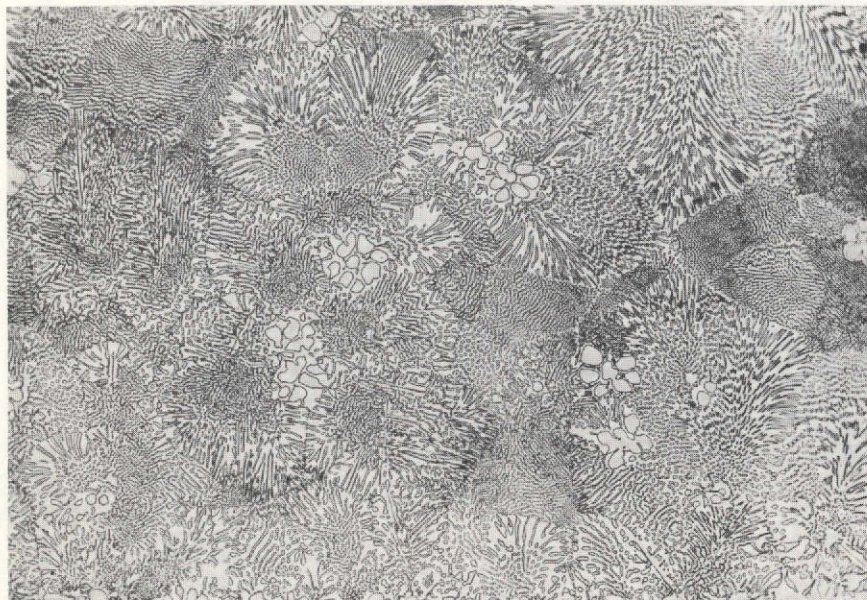


250X

As Polished

7G856

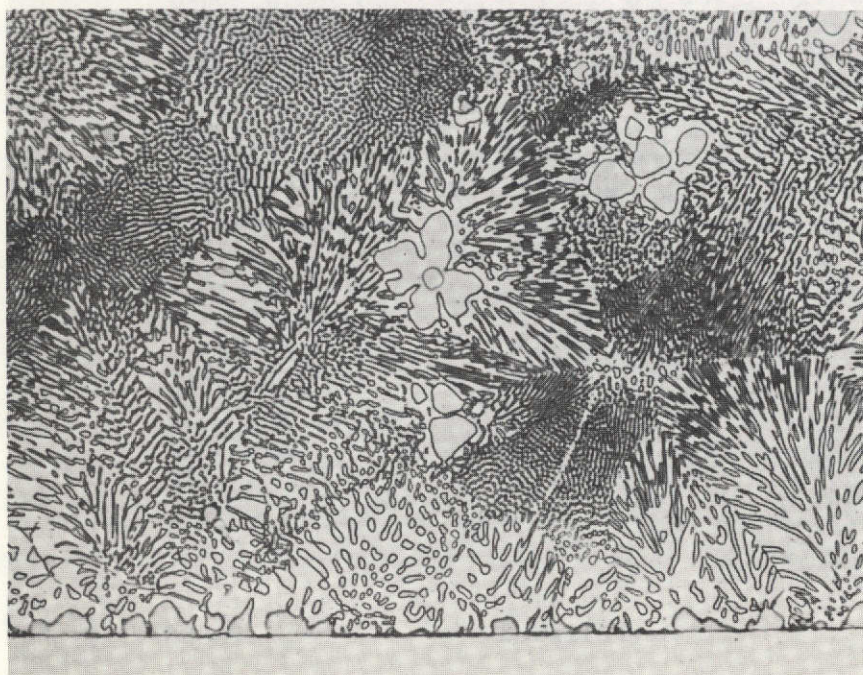
FIGURE III-5. TYPICAL MICROSTRUCTURE IN
SLS-1.4 (14 mm and 300°)



250X

As Polished

7G860



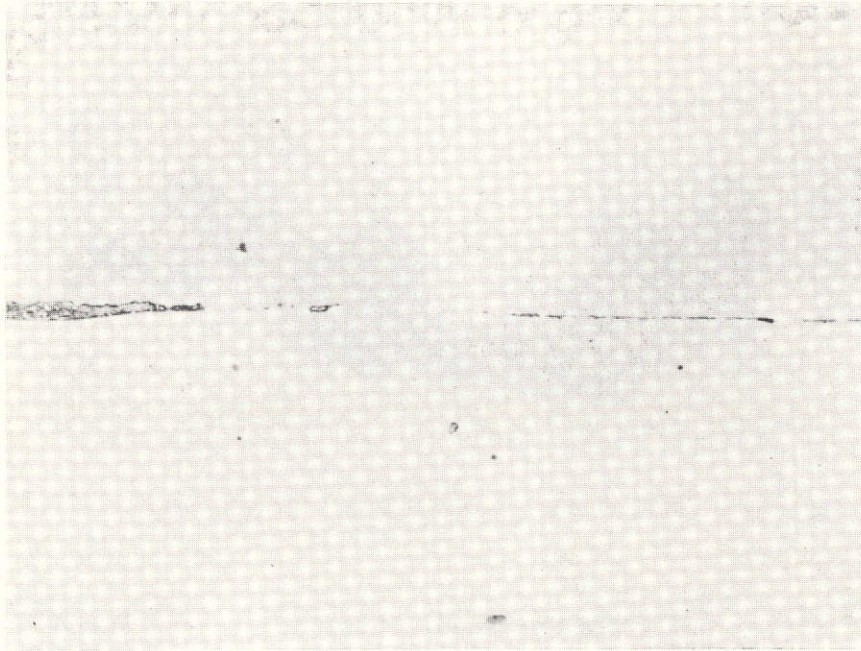
500X

As Polished

7G862

FIGURE III-6. MICROSTRUCTURE OF BULK BRAZE ALLOY -
SECTION SLS-1.4 (14 mm and 300°)

a.



500X

As Polished

7G851

b.

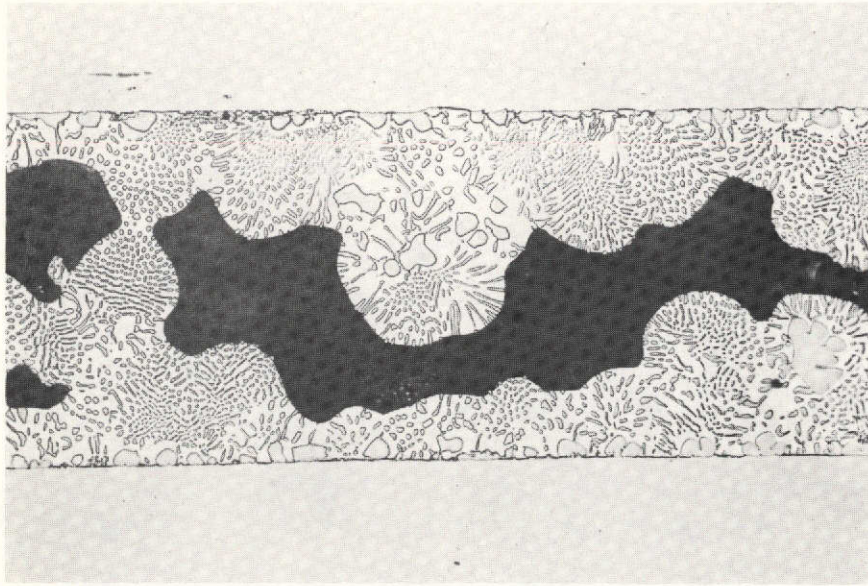


500X

Etched

7G852

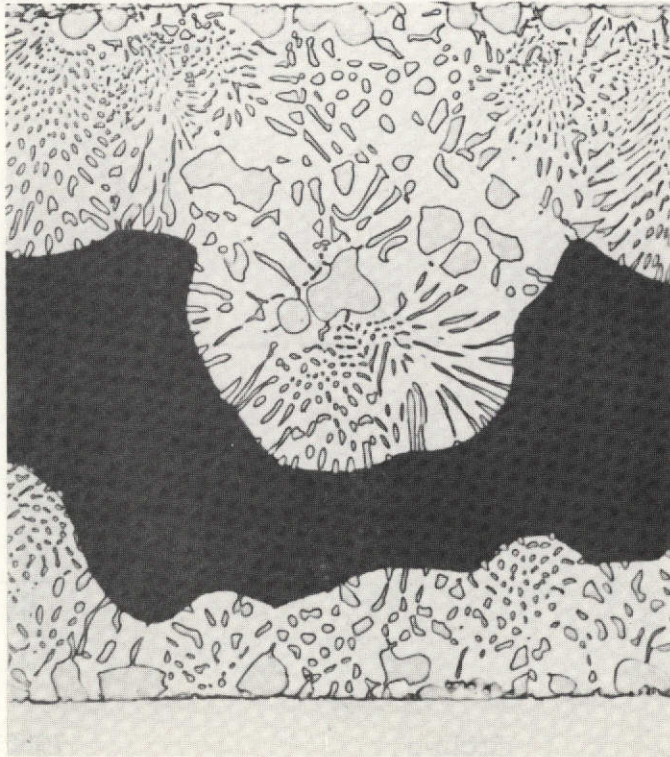
FIGURE III-7. SOLID-STATE BOND AREA -
SECTION SLS-1.4 (14 mm and 0°)



250X

As Polished

7G864



500X

As Polished

7G866

FIGURE III-8. SHRINKAGE VOIDS IN SECTION SLS-1.7.1 (24 mm and 210)

TABLE III-2. MEASUREMENTS OF JOINT GAP - SPECIMEN SLS-1

Sample No.	MM. (a)	Gap thickness, inch x 10 ⁻⁴ , at position shown in degrees												Average
		30	60	90	120	150	180	210	240	270	300	330		
1.1 inner	0	33	6	5	8	3	3	4	2	3	4	4	9	5
	outer	0	12	15	14	32	27	23	27	23	11	21	4	19
1.2	3	42	34	30	36	48	50	52	57	58	55	55	50	47
1.3(c)	3.5	49						48						49
	10	38						28						33
1.4	14	0	6	8	0	0	11	25	18	9	50	54	19	17
1.5	19	1	0	2	0	1	9	12	9	19	47	38	11	12
1.6	23	25	8	4	23	29	11	9	36	64	51	31	25	26
1.7(c)	23.5		9						68					38
	31		33						70					52
1.8	35	38	39	42	47	53	45	47	54	57	54	48	44	47
1.9	39	0	0	4	5	5	4	5	3	6	11	9	13	5

(a) Location along length.

(b) This contains the wedge except at 0°, hence there are two gaps.

(c) Longitudinal section.

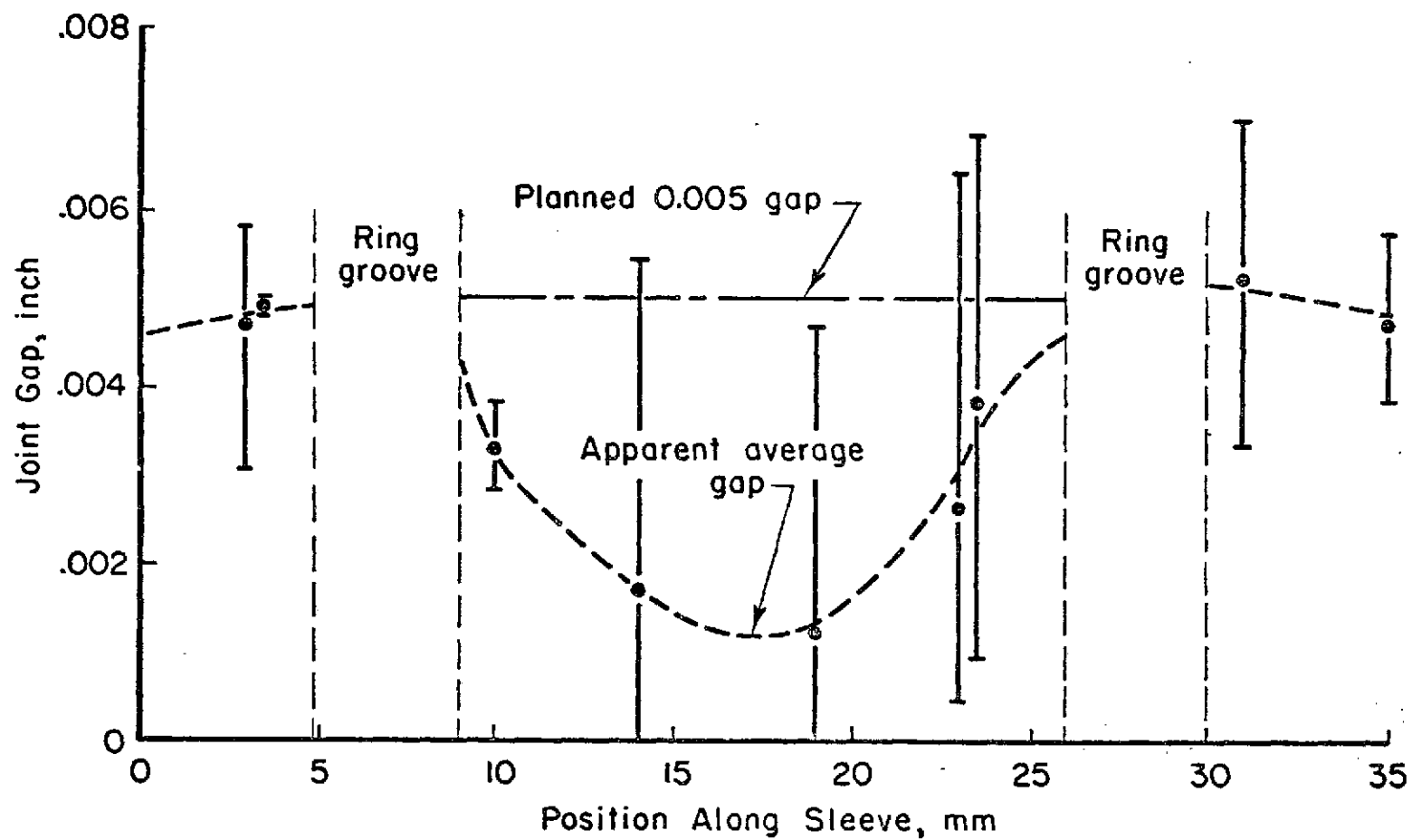


FIGURE III-9. PLOT OF JOINT GAP MEASUREMENTS

Discussion with other investigators, and dimensional checks made at MSFC, suggest that the ends of the tube may have been restrained by the container used to hold the specimens. Such restraint would prevent free thermal expansion of the tube axially and would produce some radial upset.

Specimen SLN-2

This tube-sleeve assemble contained a moderate amount of void area as reflected in the radiograph. Both ring grooves contained areas where excess braze alloy collected.

Figure III-10 shows the appearance in the ring groove area at 5 mm and in the nominal 0.010-inch gap region at 20 mm. The excess braze alloy collected in the ring groove is apparent, as well as the fact that it has not collected in a small area. All other sections were examined visually at low and high magnification and were similar in appearance to the section at 20 mm. Some voids are seen in this section near 0 and 315 degrees. Variation in the joint gap is also apparent.

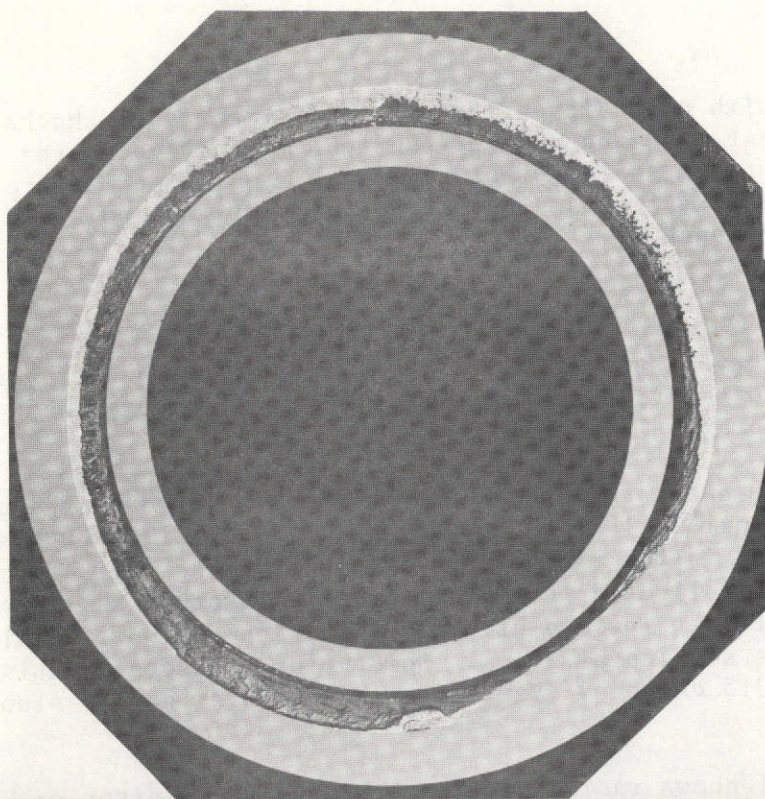
Figure III-11 shows radial sections through the igniter end ring groove. The rough surfaces of the meniscus regions is similar to the surface found in shrinkage voids. A number of these voids also are contained in this region. Figure III-12 shows similar sections through the opposite ring groove. All figures of the ring grooves show good braze alloy retention in the corner areas and well formed fillets.

Microstructures and Composition

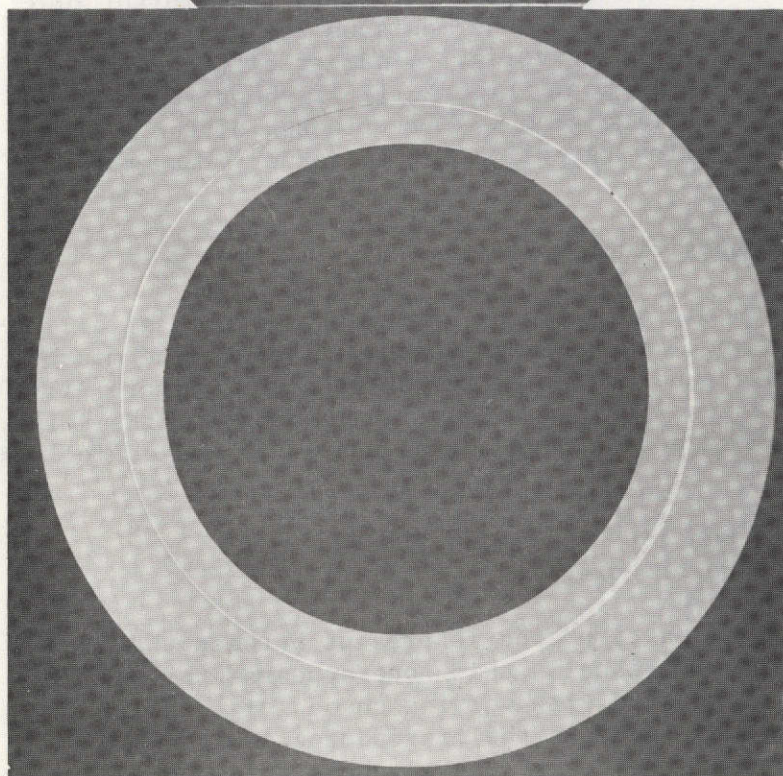
The braze region microstructures varied appreciably at different locations in this specimen and also in comparison to the microstructure observed in ground characterization studies. Figure III-13 illustrates this variation within a single radial plane of the joint. The morphology of the braze structure can be characterized as follows:

1. Coarse - See 0° , 50° , 90° in Figure III-13
2. Fine - See 180° in Figure III-13
3. Very fine - See Figure I-4

In all microstructures a reaction zone is present between the nickel parts and the braze alloy. Visually this zone appears gray next to the nickel, then copper colored with varying shades of intensity. The second phase particles (gray in the microphotographs) exhibit similar color shadings; in the coarse second phase evidence of coring is shown by a grayish hue in the interior.



2.4 Igniter End
Ring Groove



2.7 Nominal
0.010 inch-gap

4X

As Polished

9G167/168

FIGURE III-10. SECTION SLN 2.4 (5 mm) and 2.7 (20 mm)

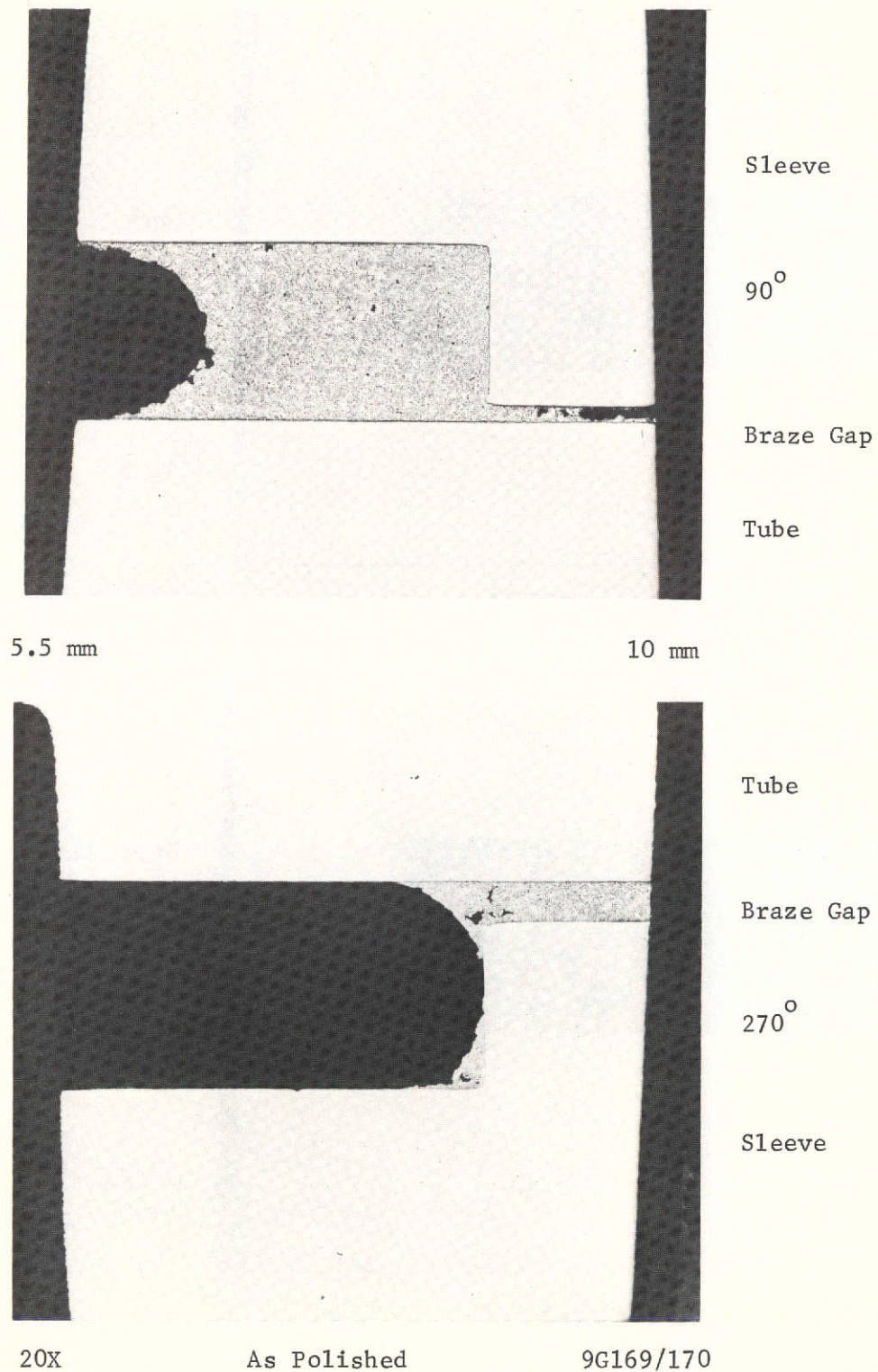
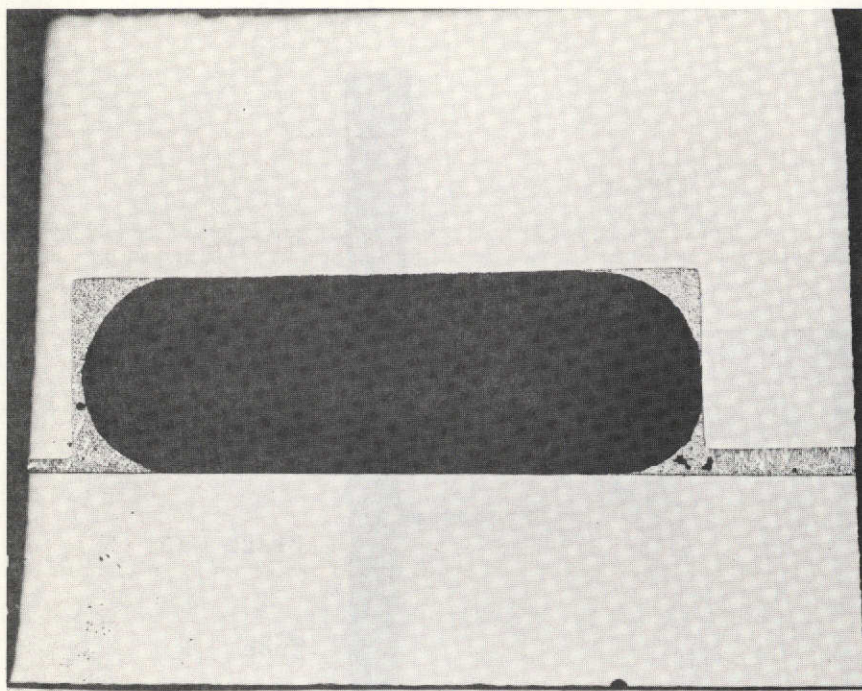


FIGURE III-11. SECTION SLN-2.5.1 (5.5 to 10 mm and 90 and 270°) SHOWING MENISCUS SHAPE AND VOID AREAS AROUND IGNITER END RING GROOVE



Sleeve

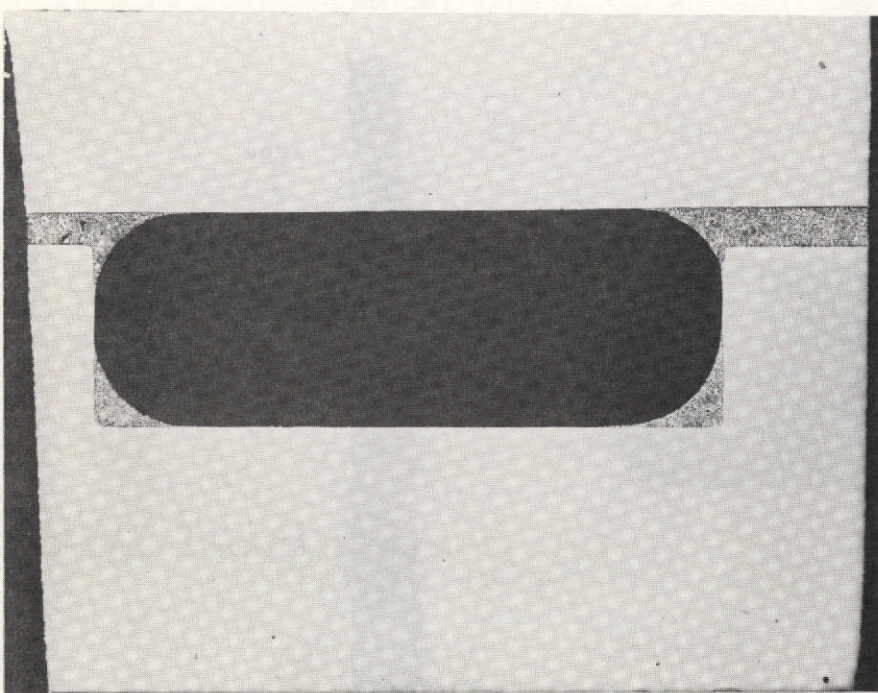
90°

Braze Gap

Tube

25.5 mm

31 mm



Tube

Braze Gap

270°

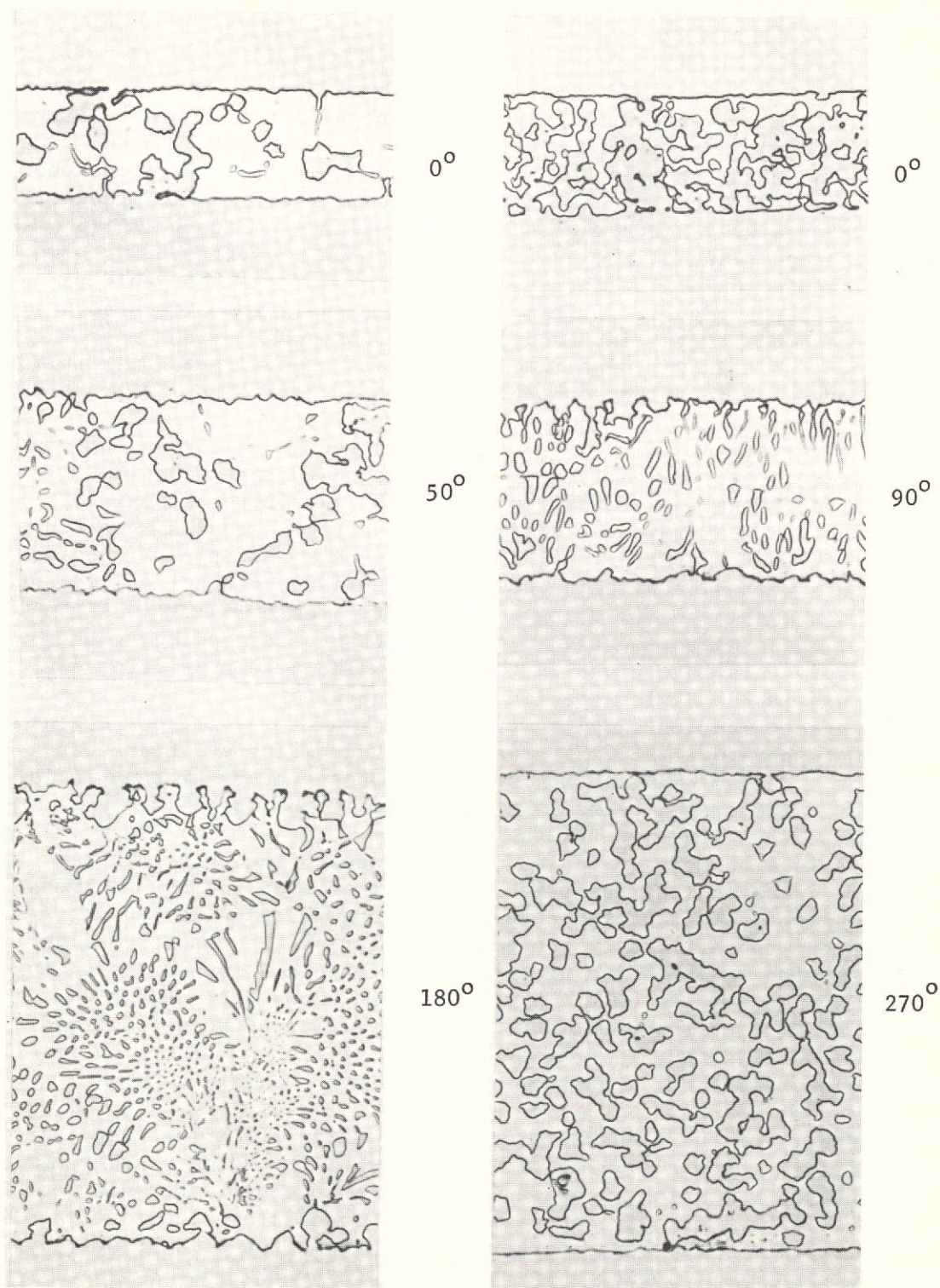
Sleeve

20X

As Polished

9G172/171

FIGURE III-12. SECTION SLN-2.9.1 (25.5 to 31 mm and 90 and 270°)
SHOWING FILLETS IN RING GROOVE OPPOSITE IGNITED END



500X

As Polished

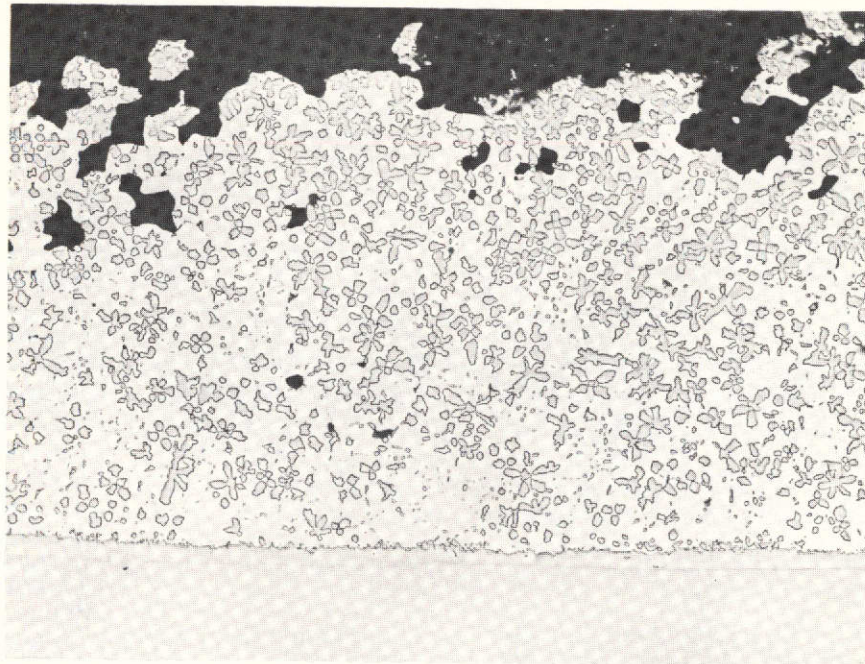
9G176/181

FIGURE III-13. VARIATION IN MICROSTRUCTURE IN SECTION SLN-2.7 (20 mm)

Figure III-14 shows the microstructure of the bulk braze alloy-interface region in a ring groove. All of the braze alloy in the ring groove areas exhibited this coarse-type structure. The reaction zone was noticeably heavier in this area and at some locations had the appearance of a heavy copper plate on the surfaces. Figure III-15 showing the end plane of the braze exhibited the microstructure shown entirely around the braze annulus. Two braze gaps exist on this plane since the spacer wedge is positioned in this area. The wider gap, which corresponds to the intended gap locations, was a fine dendritic structure. The thin gap contained a few coarse second phase particles, but was very high in silver content.

The variations in the structures observed in the Skylab specimen precluded direct comparison with the ground characterization specimens for phase identification. Electron microprobe scanning, volume fraction measurements, and magnetic particle studies were conducted to further characterize these structures. The volume fraction measurements were done by point counting techniques since insufficient contrast was available for using a Quantimet. Table III-3 gives the results of these measurements. Figure numbers corresponding to the field measured also are given in the table. The volume fraction of second phase in the Skylab specimen ranged between 15 and 58 percent. Ground characterization samples were in the range of 20 to 26 percent and a low temperature (1500 F) slow cooled vacuum furnace braze was 29 percent. The volume fraction of second phase (or β) present in low temperature-slow cooled braze is almost exactly that predicted by reference to the silver-copper phase diagram. The thermal cycle of this braze is also most suitable for reference to the phase diagram. The volume fraction results for the ground characterization specimens indicate slightly less of the copper-rich beta phase being present. This apparent copper loss can be accounted for by the copper tied up in the reaction zones on the nickel interface. The wide variation in volume fraction results on the Skylab samples shows both copper enrichment and copper loss. Effects of the relation between joint width and reaction zones and higher silver losses at the end planes by vaporization only partially explain the observed variation.

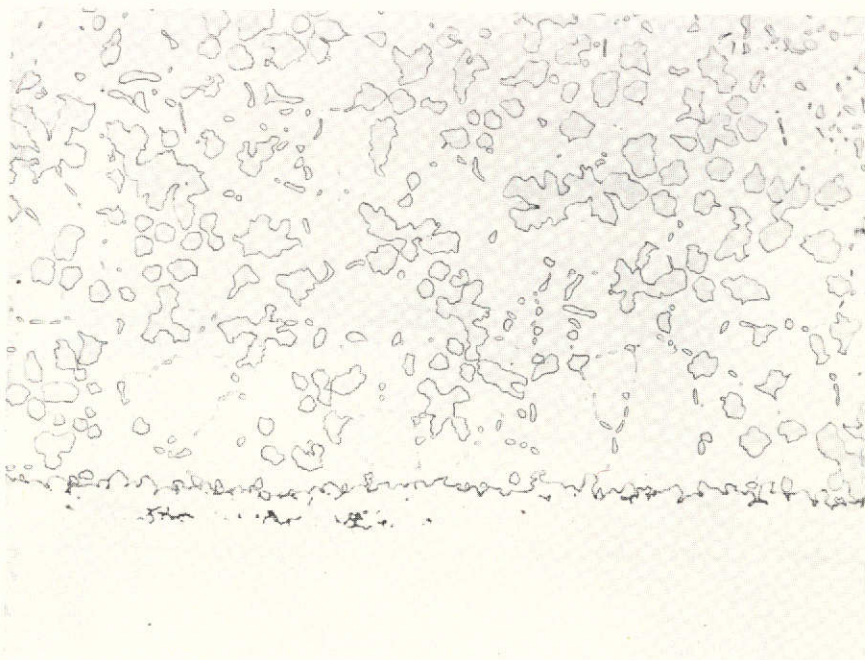
Results of the electron microprobe studies are illustrated in Figures III-16 through III-19. Four regions of the 20 mm plane showing pronounced variation in braze width and morphology were selected for study. A high copper concentration was found along the interface at each location. The copper distribution within the braze proper matched its apparent location in the second phase (β) particles. Nickel was associated with the copper (as a cored solid solution) in the coarse second phase particles but not in the fine particles. The silver concentration reflected its presence as the matrix phase (α) and its absence in any area containing nickel.



100X

As Polished

9G174

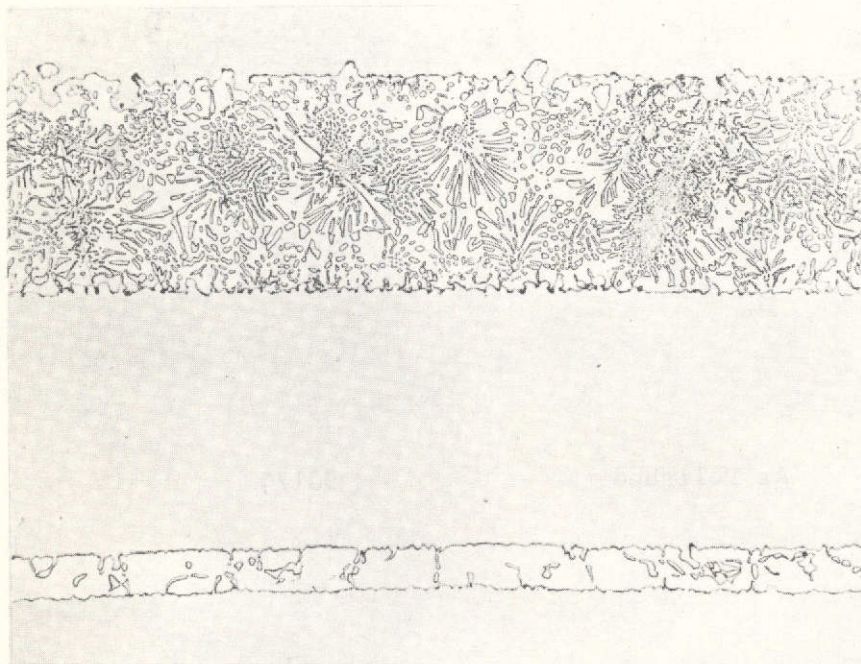


250X

As Polished

9G175

FIGURE III-14. MICROSTRUCTURE OF BRAZE IN RING GROOVE SHOWING COARSE COPPER-NICKEL PHASE AND WIDE DIFFUSION ZONE (SLN-2.4 - 5 mm)



Tube

Braze Gap

Wedge

Braze

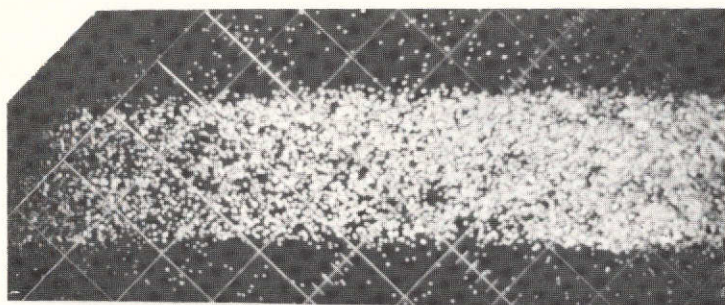
Sleeve

250X

As Polished

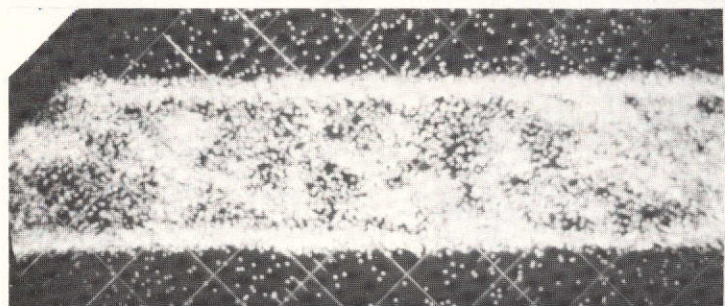
9G173

FIGURE III-15. SECTION SLN-2.10 (35 mm) SHOWING VARIATION IN BRAZE MICROSTRUCTURES



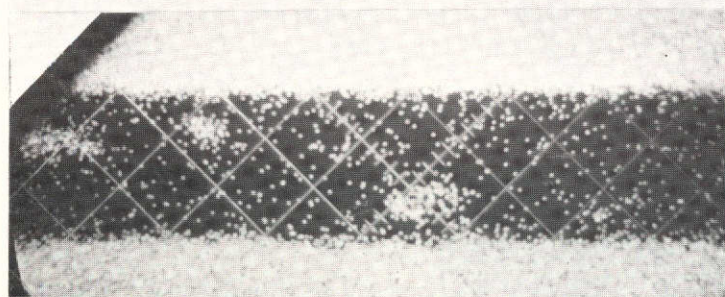
Ag Concentration

625X



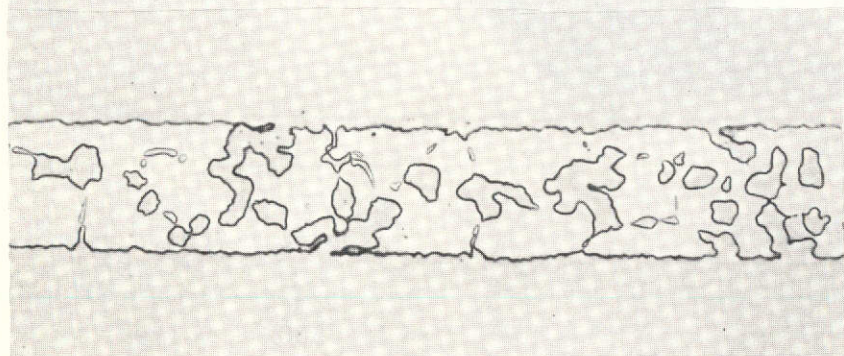
Cu Concentration

625X



Ni Concentration

625X



Optical Structure

500X - 9G176

FIGURE III-16. COMPARISON OF OPTICAL AND ELECTRON MICROPROBE IMAGES - SECTION SLN-2.7 (20 mm - 0°)

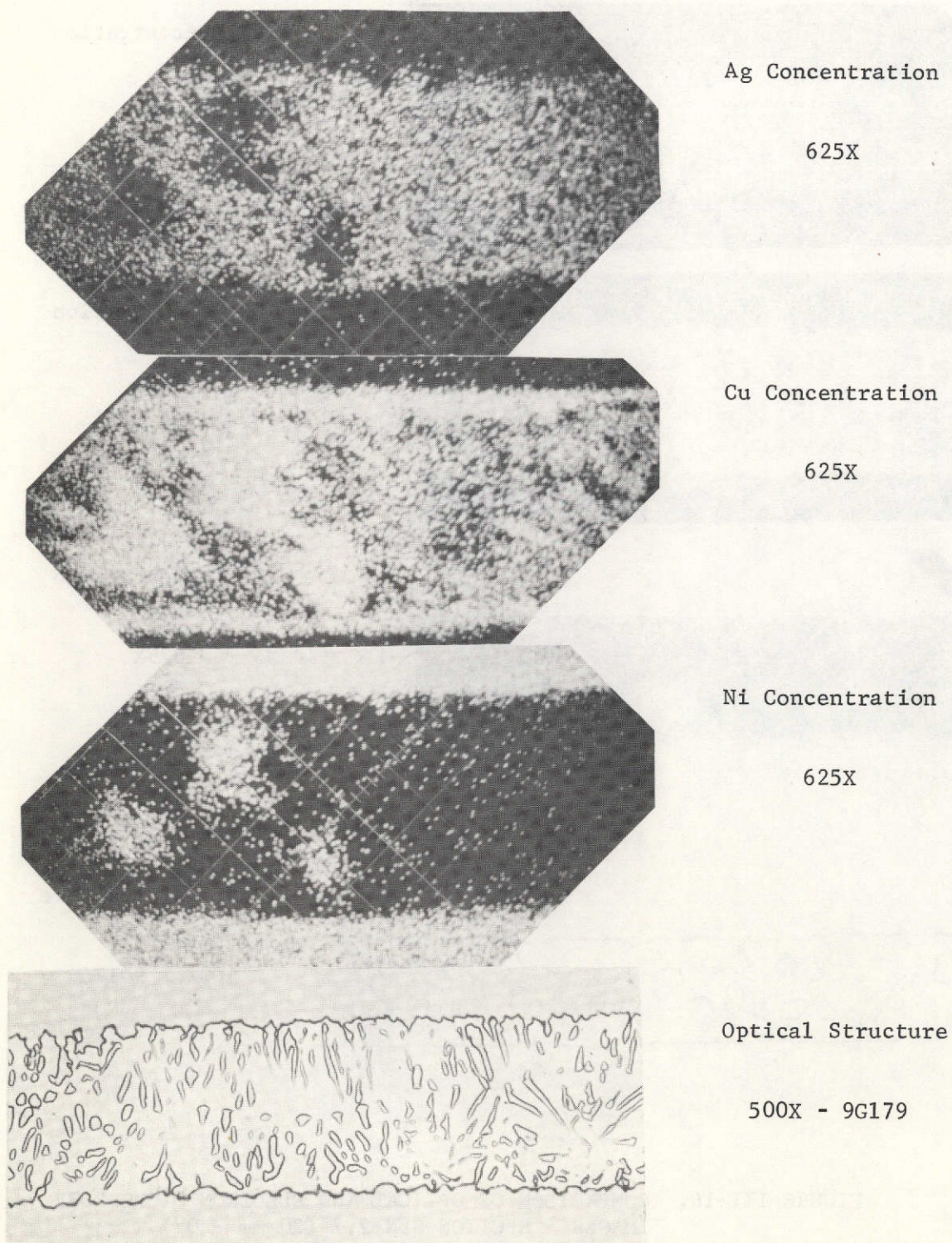


FIGURE III-17. COMPARISON OF OPTICAL AND ELECTRON MICROPROBE IMAGES - SECTION SLN-2.7 (20 mm - 90°)

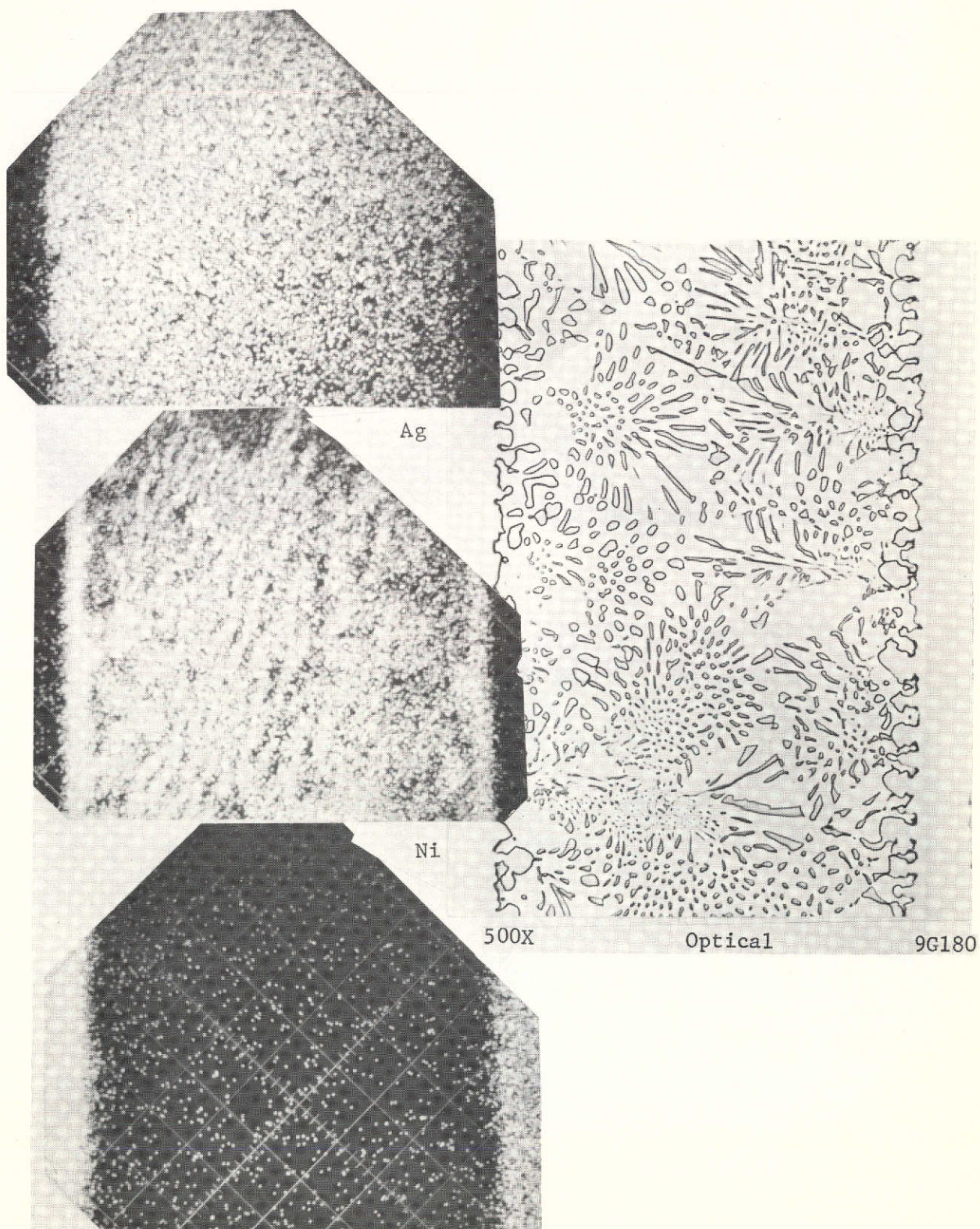


FIGURE III-18. COMPARISON OF OPTICAL AND ELECTRON MICROPROBE IMAGES
SECTION SLN-2.7 (20 mm - 180°)

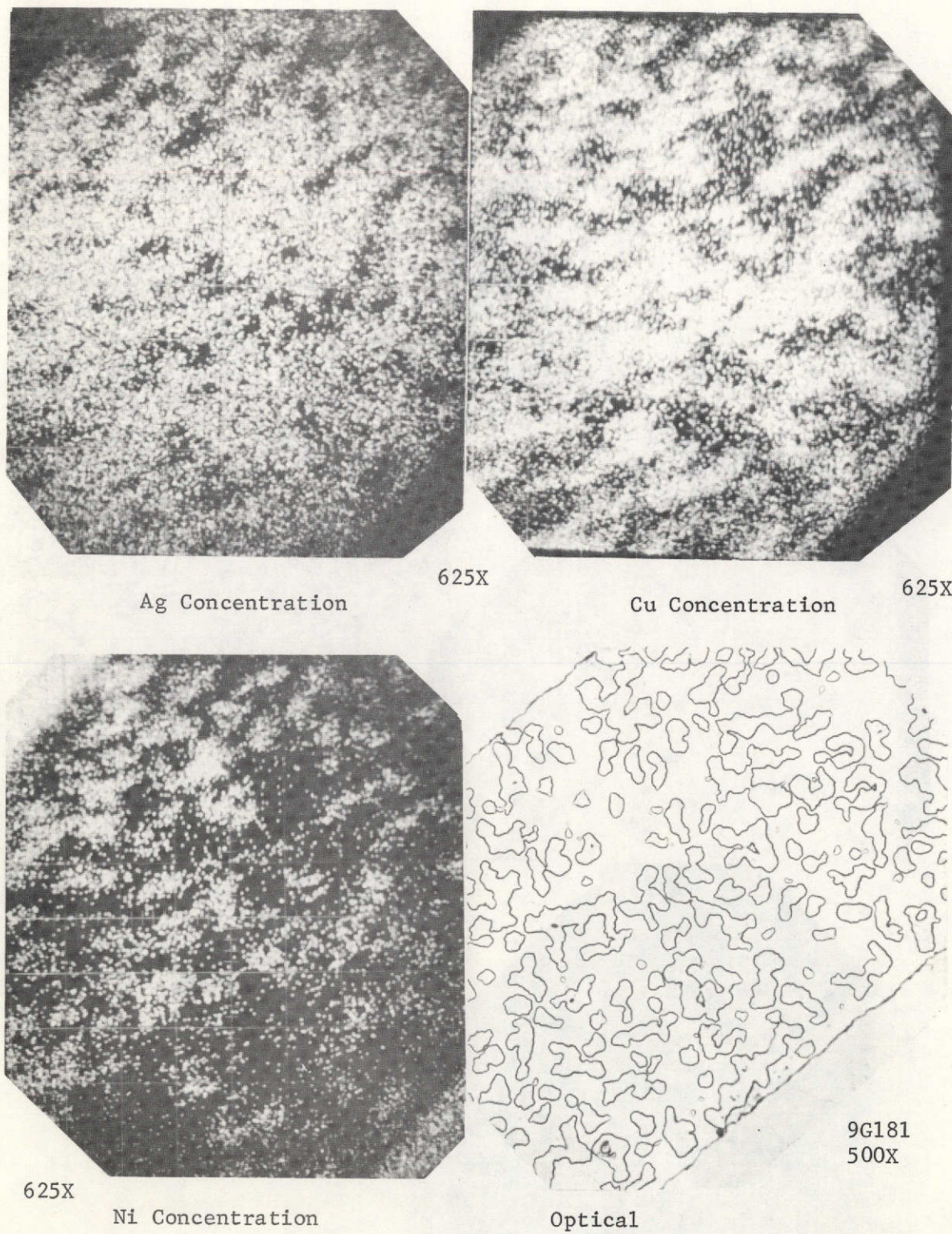


FIGURE III-19. COMPARISON OF OPTICAL AND ELECTRON MICROPROBE IMAGES - SECTION SLN 2.7 (20 mm - 270°)

TABLE III-3. VOLUME FRACTION OF SECOND PHASE IN BRAZE GAP

Section	Location	Structure	Figure	Volume Fraction, %
SLN-2.7	0	Coarse	III-13	24
SLN-2.7	0	Continuous Coarse	"	58
SLN-2.7	50	Coarse	"	15
SLN-2.7	90	Fine	"	19
SLN-2.7	180	Fine	"	19
SLN-2.7	270	Coarse	"	31
SLN-2.4	Ring Groove	Coarse	III-14	22/29
SLN-2.10	End	Fine	III-15	43
MCN-2.1	--	Fine	I-4 & 5	20/26
MCN-3.4	--	Fine	I-17	26
BCL-1500	Fillet	Mixed	I-21a	29

Visual studies using a solution of magnetic particles were used to further define regions of high nickel content. At ambient temperature, the nickel-copper solid solution is only magnetic at nickel levels above 70 percent. By magnetizing a specimen SLN-2.7 and observing the distribution of small particles on the surface, the limits of this level of nickel were established. No nickel at this level was observed within the braze alloy itself or in the protrusions extending from the reaction zone. The magnetic/nonmagnetic demarcation line was very distinct and followed the base of the protrusions as shown in Figure III-20.

An extended, detailed study employing statistical analysis of the data would be required to more fully characterize the exact composition of the phases in the Skylab specimens. Limitations inherent in quantitative metallography of samples containing the variation in microstructure present in this specimen would make such studies of little value in explaining the structures observed.

Gap Variation

Specimen SLN-2 also contained joint gap variations that were to some similar to those found in SLS-1. The joint gap measurements made are tabulated below.



Magnetic

Non Magnetic

Magnetic

500X

9G180

FIGURE **iii-20** LIMITS OF MAGNETIC REGION
INDICATING HIGH NICKEL CONTENT

		Gap thickness, inch x 10 ⁻³ , at position shown in degrees												
Section	MM	0	30	60	90	120	150	180	210	240	270	300	330	Avg
2.3	2	8			6			10			10			9
2.6	15	3	2	2	3	4	4	4	6	9	8	6	4	4
2.7	20	1	1	2	2	1	2	5	8	9	6	6	3	4
2.8	25	3			3			6			8			5
2.10*	35	4			5			4			5			5

* Gap is quite uniform since this section contains a portion of the wedge.

The joint gap appears to be almost as expected at either end of the sleeve. The smaller gap between the ring grooves appears to be related to tube-sleeve offset with the gap tending to be thin between 180 and 330 degrees, and wide between 330 and 180 degrees.

SECTION IV

CONCLUSIONS

Results of the examinations conducted on both the ground-based characterization and Skylab braze specimens are useful in evaluating a number of braze properties. In addition, comparisons of the data obtained at 1 g versus 0 g show some of the expected differences. A few variations observed in the Skylab specimens cannot be fully explained. It was not possible to record the time-temperature cycle on the Skylab processed specimens so the exact thermal cycle is not known. However, all inferential evidence indicates that the exothermic units worked properly and supplied a heat input similar to that supplied to the ground characterization specimens. The observed variations in the joint gap spacing and some microstructure variations probably resulted from axial restraint and a different cooling rate in the Skylab specimens examined.

The experimental conditions were representative of common production brazing operations and also were compatible with scientific study.

Wetting and flow of the molten braze alloy in the systems studied was expected to be excellent, as it was. All of the surface available for contact with the braze alloy was wet at some time during the brazing cycle. Void areas in the assemblies were all the result of shrinkage of the molten braze during solidification. No instances of poor surface wetting or flow due to surface oxides, dirt, or other causes were observed. The general excellence of wetting and flow characteristics precluded any indication of variation of these characteristics with the gravitational field.

The insignificant gravity forces in the Skylab noticeably increased the effects of surface tension forces on the braze alloy. The size of the fillet areas retained in the ring grooves of the Skylab specimens were several times larger than on ground characterization samples. Excess braze alloy in the ring grooves or on the inner tube surface always collected at the lowest point on the ground characterization specimens but was randomly distributed in the Skylab specimens.

Comparisons of the microstructures and chemical composition in the braze region did not disclose any pronounced gravitational effect. The variations that were observed appear to be largely a result of differences in the local cooling rates and alloy element segregation. A local area that was joined by diffusion bonding rather than brazing was identified in the Skylab stainless steel specimen.

The experimental results clearly show that exothermic brazing is a useful joining method for use in space. The procedures and process controls required in space would in fact be less restrictive than on earth.